ISTANBUL TECHNICAL UNIVERSITY ★ INSTITUTE OF SCIENCE AND TECHNOLOGY

THREE DIMENSIONAL SHAPE OPTIMIZATION OF BODIES SUBJECTED TO AIR FLOW BY HEURISTIC ALGORITHMS

Ph.D. Thesis by

Ergüven VATANDAŞ, M.Sc.

Department: Aeronautical Engineering

Programme: Aeronautical Engineering

APRIL 2006

İSTANBUL TECHNICAL UNIVERSITY ★ INSTITUTE OF SCIENCE AND TECHNOLOGY

THREE DIMENSIONAL SHAPE OPTIMIZATION OF BODIES SUBJECTED TO AIR FLOW BY HEURISTIC ALGORITHMS

Ph.D. Thesis by

Ergüven VATANDAŞ, M.Sc.

(511992004)

Date of submission : 09 November 2005

Date of defense examination : 12 April 2006

Supervisor (Chairman) : **Prof. Dr. İbrahim ÖZKOL**

Members of the Examining Committee **Prof. Dr. Hasan HEPERKAN (Y.T.Ü.)**

Prof. Dr. Zahit MECİTOĞLU (İ.T.Ü.)

Assoc.Prof.Dr. Metin O. KAYA (İ.T.Ü.)

Assis.Prof.Dr. Erol UZAL (İ.Ü.)

APRIL 2006

İSTANBUL TEKNİK ÜNİVERSİTESİ ★ FEN BİLİMLERİ ENSTİTÜSÜ

HAVA AKIMINA MARUZ ÜÇ BOYUTLU CİSİMLERİN SEZGİSEL YÖNTEMLERLE ŞEKİL OPTİMİZASYONU

DOKTORA TEZİ

Y. Müh. Ergüven VATANDAŞ

(511992004)

Tezin Enstitüye Verildiği Tarih : 09 Kasım 2005
Tezin Savunulduğu Tarih : 12 Nisan 2006

Tez Danışmanı : Prof. Dr. İbrahim ÖZKOL

Diğer Jüri Üyeleri Prof.Dr. Hasan HEPERKAN (Y.T.Ü.)

Prof. Dr. Zahit MECİTOĞLU (İ.T.Ü.)

Doç. Dr. Metin O. KAYA (İ.T.Ü.)

Y.Doç.Dr. Erol UZAL (İ.Ü.)

NİSAN 2006

ACKNOWLEDGEMENTS

I am grateful to my supervisor, Professor Dr. İbrahim ÖZKOL for his zealous guidance throughout this study. He has been very patient in working with me.

I would like to thank Professor Dr. Zahit MECİTOĞLU, Assoc.Prof.Dr. Metin O. KAYA, Assis.Prof.Dr. Selman NAS, Dr. Erdal YILMAZ, Colonel Cemal ÖKSÜZ and Assoc.Prof.Dr. Maj. Abdurrahman HACIOĞLU for their support and encouragement.

I am grateful to Turkish Air Force and Istanbul Technical University for this research opportunity.

I would also like to thank Informatics Institute for its support in a part of the computations.

Finally, I would like to thank my wife, Yeşim, and my daughters, Rana and Reyhan, for their patience during my study.

April 2006 Ergüven VATANDAŞ

TABLE OF CONTENTS

LIST OF ABBREVIATIONS

ASOP3D : Aerodynamic Shape Optimization Program for 3-D Geometries
CFD : Computational Fluid Dynamics
VGA : Vibrational Genetic Algorithm
PVM : Parallel Virtual Machine

LIST OF FIGURES

Page No

LIST OF SYMBOLS

a : Constant parameter to define the weight of the lift coefficient
α : Angle of Attack
b : Wing length or constant parameter to define the weight of the thickness ratio in the fitness function
$\mathbf{C_D}$: Drag coefficient calculated
$\mathbf{C_L}$: Lift coefficient calculated
$\mathbf{C_{Ld}}$: Design lift coefficient
cr : Root chord
ct : Tip chord
D : Drag force
$\overline{\delta}$: Initial displacement in dynamic mesh
δ : Displacement in the coordinates of each node in dynamic mesh
$\mathbf{e_x, e_y, e_z}$: Unit vectors in the local coordinate system
$\mathbf{e_1, e_2, e_3}$: Unit vectors in the global coordinate system
E : Total energy per unit mass
Є : Criterion for convergence
F : Flux vector
f,g,h : Component of the flux F in Cartesian coordinates
H : Total enthalpy
γ : Ratio of specific heats
$\mathbf{k_m}$: Spring stiffness of each side of the cells in dynamic mesh
kmax : Maximum number of iterations
kn : Number of control points (total gene number of a chromosome)
MA : The main amplitude
n : The total number of individuals in a population
μ : Viscosity
$\mathbf{P_{avr}}$: Average pressure in a wall boundary element
P : Pressure
ρ : Air density
S : Wing area
sw : Leading edge sweep angle
Th : Thickness ratio of the produced wings
$\mathbf{Th_d}$: Design thickness ratio
$\mathbf{U_\infty}$: Free stream velocity
U : Solution vector in the Euler flow solver
u : A random real number between [1,0],
u, v, w : Cartesian velocity components
V : Air velocity
***w*1** : A user defined real number between [0, 2]
y_i^m : y coordinate of the control points (genes)

THREE DIMENSIONAL SHAPE OPTIMIZATION OF BODIES SUBJECTED TO AIR FLOW BY HEURISTIC ALGORITHMS

SUMMARY

Today, evolutionary type of algorithms is entering in many engineering fields. This design and optimization technique is required to create a population; once the population is created new members are obtained by processing the previous ones. Recent developments in computer technology and numerical algorithms let the researchers develop fast and powerful ways plugging the evolutionary type algorithms by which several parameters can be determined considering and satisfying many requirements simultaneously to find an optimum solution, i.e. a design fulfilling all requirements including in the fitness function in the design of aerodynamic-shaped objects such as wing sections, airfoils, turbine blades or other lift producing surfaces.

The time-consuming flow solvers and gradient type optimization techniques have not been preferred recently. Instead, flow solvers are carried into parallel computing type machines and optimizations are carried out by evolutionary techniques.

This study combines the Vibrational Genetic Algorithm with Dynamic Mesh technique and Euler flow solver; and then optimizes 3-D wing model (Onera M6 wing) by using them. Onera M6 wing has been optimized by two parameters, the wing section and the taper ratio by combining recent preferable approach i.e. parallel computing and evolutionary techniques. For the 3-D models obtained during the optimization stages, the mesh required is generated by dynamic mesh technique. The code developed for this aim is robust and faster than the codes, which are only producing mesh by classical techniques. The Euler flow solver has been used to obtain the flow parameters for each member. Because the operating time of the program is very long, on account of our low capacity computer resources, parallel processing has been used. Obviously the strategy applied here can be used for any slowly deforming complex geometries, as long as an effective combination of the genetic algorithm and dynamic mesh be succeeded.

The Vibrational Genetic Algorithm (VGA) is a GA, which uses the vibration concept, in that, by applying a vibrational mutation periodically to all individuals in a population; they are spread out over the design space. Therefore, it becomes possible to escape from local optimums and thus to obtain a global optimum quickly. This vibration strategy in mutation is used after a recombination.

The unstructured tetrahedral mesh is modified according to the change in wing shape by using dynamic mesh technique and for all members of a generation; new mesh structures have been calculated.

Aerodynamic force, lift and drag, calculations have been done by using a finite element method. The pressure value for each triangular wall boundary face is taken as the average of the pressures on the corner nodes. Then the total forces are calculated by using a numerical integration.

In the optimization process, there are 14 members in each generation. These are 14 Onera M6 wing planforms that have different wing sections and taper ratios. The best member is kept in each generation and carried into the next generation. So the best member found in each generation cannot be worse than the best member of the previous generations.

The CPU time of the first step in dynamic mesh method is approximately the same as mesh generation time. However, later steps of dynamic mesh technique need much less time than the first step. Therefore, especially, if a lot of similar configurations are to be considered, the dynamic mesh method offers more advantage.

From the results, it is observed that the optimization process is working as expected. The drag coefficient was reduced by about 25 percent. While this has been done, its lift coefficient and thickness ratio are tried to be close to the design value determined at the beginning. This is done by arranging the fitness function. At the 30^{th} generation the discrepancy between the lift coefficient of the best member and the design lift coefficient value is about 1 percent and the difference between thickness ratios is 3 percent.

The taper ratio is getting smaller while the code is trying to minimize the drag force. But it cannot be reduced to very small values and is kept almost the same at later steps, because the program should not only reduce the drag force but also hold the lift force close to the design value.

The outline of the thesis is as follows:

- In Chapter 1, the general research is introduced. The design and optimization stage of the present engineers and researchers is outlined and expressed. The drag case which has attracted the most of the aerodynamicists interest is explained.

- In Chapter 2, the theoretical basis of Dynamic Mesh, Vibrational Genetic Algorithm (VGA), Euler flow solver is explained. In this chapter, some of the developed techniques to overcome the difficulties of 3-D problems such as parallelization and purified genetic algorithm for taper ratio optimization are introduced. Some explanations of the verification of the techniques used in this research are also included in this chapter.

- In Chapter 3, the detailed structure and outline of this research is illustrated. The structure of the algorithm used, flow charts of the programs, model and the grid type employed for the applications are explained in this chapter. It can be called as the outline of this work.

- In Chapter 4, all applications are shown. All results of all applications are illustrated mostly by using figures. They are compared and discussed. Applications have been made basically in three sections: without a thickness ratio constraint, with a thickness ratio constraint and with a thickness ratio constraint together with a taper ratio design variable. The last one is also applied to a finer mesh structure.

- In Chapter 5, all research plan, applications and results are evaluated. Comments on the whole work are included in this chapter. It contains also some concluding remarks and suggested works for the future.

The originality of this study is that:

- The dynamic mesh technique has been applied for the first time to determine the mesh structures of genetically obtained new members in genetic algorithms.

- Vibrational Genetic Algorithm is applied to 3-D wing optimization problems.

- To overcome some problems encountered in 3-D applications, such as large calculation time, flow solution difficulties, force calculations; some techniques like parallelization, purification and finite element numeric integration are employed, developed and adapted to this research.

HAVA AKIMINA MARUZ ÜÇ BOYUTLU CİSİMLERİN SEZGİSEL YÖNTEMLERLE ŞEKİL OPTİMİZASYONU

ÖZET

Günümüzde evrimsel algoritmalar mühendislik uygulamalarında gittikçe daha fazla yaygınlaşmaktadır. Bu yöntemde önce bir başlangıç popülasyonu oluşturulur; daha sonra yeni bireyler öncekilerin üzerinde bir takım işlemler yapılmasıyla elde edilir. Bilgisayar teknolojilerindeki son gelişmeler araştırmacıların bir çok parametreyi aynı anda hesaplayıp dikkate alabilen ve optimum bir sonuç arayan evrimsel algoritmalar gibi hızlı ve etkin yöntemler geliştirmelerine imkan sağlamıştır. Örneğin bir kanat yada türbin kanadı kesitine ait bir çok parametreyi içeren bir uygunluk fonksiyonunu sağlayan çözümün aranması gibi.

Özellikle üç boyutlu problemlerde çok uzun zaman gerektiren akış çözücü programlar ve gradyen esaslı yöntemler artık pek fazla tercih edilmemektedir. Bunların yerine paralel hesaplama yöntemleri ve evrimsel algoritmalar daha fazla tercih edilmektedir.

Bu çalışma titreşimli genetik algoritma yöntemini, dinamik ağ ve bir Euler akış çözücüsü ile birleştirerek üç boyutlu kanat modellerinin (Onera M6 kanadı) optimizasyonuna uygulamaktadır. Onera M6 kanadı özellikle iki parametresi, kanat kesiti ve sivrilik oranı üzerinde, evrimsel algoritmalar ve paralel hesaplama yöntemleriyle optimize edilmiştir. Optimizasyon işlemleri sırasında elde edilen 3 boyutlu modeller için yeni ağ yapıları dinamik ağ yöntemi kullanılarak hesaplanmıştır. Bunun için geliştirilen yazılım sıfırdan ağ üreterek çözüm yapanlara göre daha etkin ve hızlıdır. Akış alanlarını çözmek için bir Euler akış çözücü program kullanılmıştır. Toplam işlem zamanı oldukça uzun olduğundan ve bilgisayar alt yapısının yeterli olmayışı nedeniyle paralel hesaplama yöntemi kullanılmıştır. Burada genetik algoritma ve dinamik ağın birleştirilmesiyle geliştirilen strateji küçük değişim gösteren herhangi bir geometri için kullanılabilir.

Titreşimli Genetik Algoritma (TGA) dizayn alanına yayılmış bütün bireylere periyodik olarak titreşimli mutasyon uygulayan bir konsep kullanmaktadır. Bu sayede yerel optimumlardan kurtulup, global optimuma daha hızlı ulaşabilmektedir. Mutasyona uygulanan bu titreşim stratejisi yeniden birleştirme işleminden sonra uygulanmaktadır.

Yapısal olmayan "tetrahedral" çözüm ağı kanat geometrisindeki değişime uygun olarak dinamik ağ yöntemiyle modifiye edilmekte ve yeni modellere ait ağ yapıları hesaplanmaktadır.

Taşıma ve sürükleme gibi aerodinamik kuvvetler bir sonlu eleman yöntemiyle hesaplanmaktadır. Kanat üzerindeki her bir üçgen ağ elemanı için basınç değeri köşe noktalarındaki basınç değerlerinin ortalaması olarak alınmıştır. Bundan sonra toplam kuvvetler nümerik bir integrasyonla bulunmaktadır.

Optimizasyon işlemi sırasında her bir nesilde 14 birey bulunmaktadır. Bu bireyler farklı kesitlere ve sivrilik oranlarına sahip 14 değişik Onera M6 kanadıdır.

Her nesilde bulunan en iyi birey bir sonraki aşamada aynen korunmaktadır. Dolayısıyla her bir nesilde bulunan en iyi birey en kötü ihtimalle bir öncekinin aynısı olacaktır.

Dinamik ağ yönteminde ilk hesaplama yeniden ağ üretilmesi kadar zaman alabilmektedir. Ancak sonraki hesaplamalar çok daha kısa sürmektedir. Dolayısıyla özellikle çok sayıda birbirine yakın model üzerinde hesaplama yapılacaksa dinamik ağ yöntemi daha avantajlı olabilmektedir.

Sonuçlar analiz edildiğinde, optimizasyon işleminin beklendiği şekilde geliştiği gözlemlenmektedir. Sürükleme kuvvetinin yaklaşık yüzde 25 azaldığı görülmüştür. Ayrıca bu yapılırken taşıma kuvvetinin ve kalınlık oranının başta belirlenmiş dizayn taşıma kuvveti ve orijinal kalınlık oranına yakın kalması sağlanmıştır. Bu işlem uygunluk fonksiyonu ile ayarlanmaktadır. Örneğin 30ncu nesilde taşıma kuvvetindeki değişim yüzde 1, kalınlık oranında değişim ise yüzde 3 mertebesindedir.

Program sürükleme kuvvetini minimize etmeye çalışırken sivrilik oranının azaldığı gözlemlenmiştir. Ancak bu azalma çok düşük seviyelere inememekte, belli bir aşamadan sonra hemen hemen sabit kalmaktadır, çünkü programın amacı sadece sürüklemeyi azaltmak değil aynı zamanda taşıma kuvvetini sabit tutmaktır.

Tezin ana bölümleri:

- Bölüm 1: Genel olarak araştırma konusu tanıtılmaktadır. Günümüz dizayn ve optimizasyon çalışmalarının geldiği aşama kapsamlı bir örneklemeyle izah edilmektedir. Aerodinamik ile uğraşan araştırmacıların en çok ilgisini çeken konulardan biri olan sürükleme kuvveti detaylı bir şekilde açıklanmaktadır.

- Bölüm 2: Euler akış çözücü program, dinamik ağ yöntemi ve titreşimli genetik algoritma yöntemlerinin teorik temelleri anlatılmaktadır. Özellikle üç boyutlu problemlerde karşılaşılan bazı sorunları aşabilmek için geliştirilen paralelleştirme stratejisi ve sivrilik oranı optimizasyonunda kullanılmış saflaştırılmış genetik algoritma olarak isimlendirilen yöntemler ve gerekçeleri anlatılmaktadır. Ayrıca bu bölümde Euler akış çözücü ve titreşimli genetik algoritma yöntemlerini doğrulama amacıyla bazı uygulamalara ve karşılaştırmalı sonuçlarına yer verilmiştir.

- Bölüm 3: Bu bölümde bu çalışmada kullanılan ve geliştirilen yöntemlerin detaylı yapısı açıklanmaktadır. Programların yapısı ve akış şemaları, kullanılan model ve ağ yapısı izah edilmiştir. Yapılan çalışmaların ana hatları bu bölümdedir.

- Bölüm 4: Bütün uygulamalar bu bölümde gösterilmiştir. Elde edilen bütün sonuçlar çoğunlukla şekiller kullanılarak izah edilmiş, kıyaslanmış ve yorumlanmıştır. Uygulamalar üç grupta yapılmıştır: kalınlık oranı şartı olmadan, kalınlık oranı şartı ile birlikte ve hem kalınlık oranı şartı, hem de ilave dizayn değişkeni olarak sivrilik oranı kullanılarak. Sonuncusu ayrıca daha yoğun bir ağ yapısı için de uygulanmıştır.

- Bölüm 5: Bütün çalışma planı, uygulamalar ve sonuçlar bu bölümde değerlendirilmiştir. Tezin tamamını kapsayan yorumlara da yer verilmiştir. Ayrıca bu bölümde ulaşılan bazı yargılar ve bu tezin devamı niteliğinde ileride yapılması önerilen çalışmalar da bulunmaktadır.

Bu çalışmanın orijinalliği:

- Dinamik ağ yöntemi ilk kez genetik algoritmada elde edilen yeni bireylerin ağ yapısının bulunmasında kullanılmıştır.

- Titreşimli Genetik Algoritma (TGA) üç boyutlu kanat optimizasyonu için uygulanmıştır.

- Özellikle problemin üç boyutlu olması nedeniyle ortaya çıkan problemleri aşabilmek için paralelleştirme, saflaştırma ve sonlu eleman nümerik integrasyon gibi yöntemler kısmen geliştirilerek bu probleme uyarlanmıştır.

1. INTRODUCTION

Aircraft design presents a grand challenge to numerical optimization. It is in nature multidisciplinary among aerodynamics, structure, control and propulsion. Especially, aerodynamic calculation requires more computer resources and the resulting aerodynamic performance is very sensitive to the geometry. **(Obayashi 1998a)**

In the aircraft design, one of the most important parts is wing design and optimization. Among the wing design parameters, aerodynamic forces are usually aimed to be calculated and optimized. Wing forces are of great contribution to aircraft capabilities and essential role in aircraft performance.

There are mainly three aerodynamic forces (lift, drag and side forces) and three aerodynamic moments (pitch, roll and yaw). Especially lift and drag forces have had the top role.

Lift is the aerodynamic force resolved in the direction normal to the free stream due to the integrated effect of the static pressures acting normal to the surfaces.

Before proceeding further in any study of computational aerodynamics the issue of drag must be addressed. There are many sources of drag. In three-dimensional flow, and in two dimensions when compressibility becomes important, drag occurs even when the flow is assumed inviscid. Before discussing the aerodynamics of lifting systems, the fundamental aspects of aerodynamic drag will be examined.

Drag is the aerodynamic force resolved in the direction parallel to the free stream due to (1) viscous shearing stresses, (2) integrated effect of the static pressures acting normal to the surfaces and (3) the influence of the trailing vortices on the aerodynamic center of the body. **(Nicolai, 2002)**

There are many factors related to moving body in fluid media. These can be grouped into three different categories:

- Associated with the object

- Associated with the motion of the object
- Associated with the fluid itself

The Object: Geometry has an essential effect on the magnitude of drag. The drag force depends linearly on the size of the object moving through the fluid. The cross-sectional shape of an object determines the form drag created by the pressure variation over the object. Aerodynamic friction part of drag depends on the surface roughness of the object; a roughened surface produces more drag than a smooth, waxed surface. This effect is called skin friction and is usually included in the measured drag coefficient of the object.

Motion of the Fluid: Drag is related to the movement of the aircraft through the fluid, therefore drag depends on the velocity of the fluid. As in lift, drag actually varies with the square of the relative velocity between the object and the fluid. The inclination of the object to the flow also affects the drag generated by a given geometry. If the object moves through the air at speeds close to the speed of sound, shock waves are formed over the object which creates an additional drag called wave drag. The motion of the object through the fluid also causes boundary layers on the object. A boundary layer is a region of low flow speed near the surface which contributes to the skin friction.

Properties of the Fluid: Drag depends directly on the density, viscosity and compressibility of the flow moving over the aircraft. These factors affect the wave drag and skin friction.

All of this information can be gathered as the factors that affect drag into a single mathematical equation called the Drag Equation. With the drag equation, we can predict how much drag force is generated by a given body moving at a given speed through a specified fluid. **(Benson 2004)**

$$D = C_D \frac{\rho V^2}{2} S \tag{1.1}$$

Inviscid Drag Due to Lift: This is usually called induced drag. The drag that results due to the influence of trailing vortices (shed downstream of a lifting surface of finite aspect ratio) on the wing aerodynamic center. The influence is

an impressed downwash at the wing aerodynamic center which induces a downward incline to the local flow. (It is present in the absence of viscosity)

Viscous Drag Due to Lift: The drag that results from the integrated effect of the static pressure acting normal to a surface resolved in the drag direction when an airfoil angle of attack is increased to generate lift. (it is present without vortices)

Skin Friction Drag: The drag on a body resulting due to the viscous shearing stress over its wetted surface.

Pressure Drag: Sometimes called form drag. The drag on a body resulting from the integrated effect of the static pressure acting normal to the surface resolved in the drag direction.

Interference Drag: The increment in drag from the proximity of two bodies to each other. For example, the total drag of a wing-fuselage combination will usually be greater than the sum of the wing drag and fuselage drag separate from another.

Profile Drag: Generally taken to mean the sum of the skin friction drag and the pressure drag for a two-dimensional airfoil.

Trim Drag: The increment in drag resulting due to the aerodynamic forces required to trim the aircraft about its center of gravity. Usually this takes the form of added drag-due-to-lift on the horizontal tail.

Base Drag: The contribution to the pressure drag attributed to a separated boundary layer acting on an aft facing surface.

Cooling Drag: The drag resulting from the momentum lost by the air moving through the power plant installation (i.e. heat exchanger) for purposes of cooling the engine, oil and etc.

Ram Drag: The drag resulting due to the momentum lost by the air as it slows down to enter an inlet.

Wave Drag: Limited to supersonic flow. This is a pressure drag resulting from noncancelling static pressure components on either side of a shock wave acting on the surface of the body from which the wave is emanating. **(Nicolai, 2002)**

At transonic speeds there exist local buckets of supersonic flow delimited by shock waves. Shock-induced boundary layer separation and shock waves are consistent source of drag at these speeds. At a certain Mach number that depends on the airfoil and the angle of attack, a wave drag starts to build up due to the increasing effect of the shock wave. Once the flow is fully supersonic, the drag coefficient falls.

In general the total drag consists of the skin friction (viscous) drag; the induced drag (as in subsonic flows), the (supersonic) drag due to volume, and the (supersonic) wave drag due to lift.

Supersonic flows are considered well behaved and more stable, as compared with transonic flows, because the problem of the shock at the wall is eliminated. **(Filippone, 2004)** In 2-D transonic flows wave drag can reach up to 60 percent of total drag. **(Hacıoğlu, 2003b)**

Drag is at the heart of aerodynamic design. The subject is fascinatingly complex. All aerodynamicists secretly hope for negative drag. It's also terribly important. Even minor changes in drag can be critical. For instance, on the Concorde, a one count drag increase ($\Delta C_D = .0001$) requires two passengers, out of the 90 ~ 100 passenger capacity, be taken off the North Atlantic run. In design studies a drag decrease is equated to the decrease in aircraft weight required to carry a specified payload the required distance. General drag structure is illustrated in Figure 1.1 **(Hendrickson, et al., 1997)**

Owing to the recent developments in computer sciences, Computational Fluid Dynamics (CFD) and computational optimization methods have become more important. Through this way experimental works can be decreased significantly in both time and cost.

In this sense, for the computational fluid dynamics, optimization problems can be classified into the following major considerations (Mali et al.):

- Objective or fitness function to be minimized or maximized.
- Design variables which affect the fitness value
- A set of constrains that allow the variables to take on certain values but exclude others.

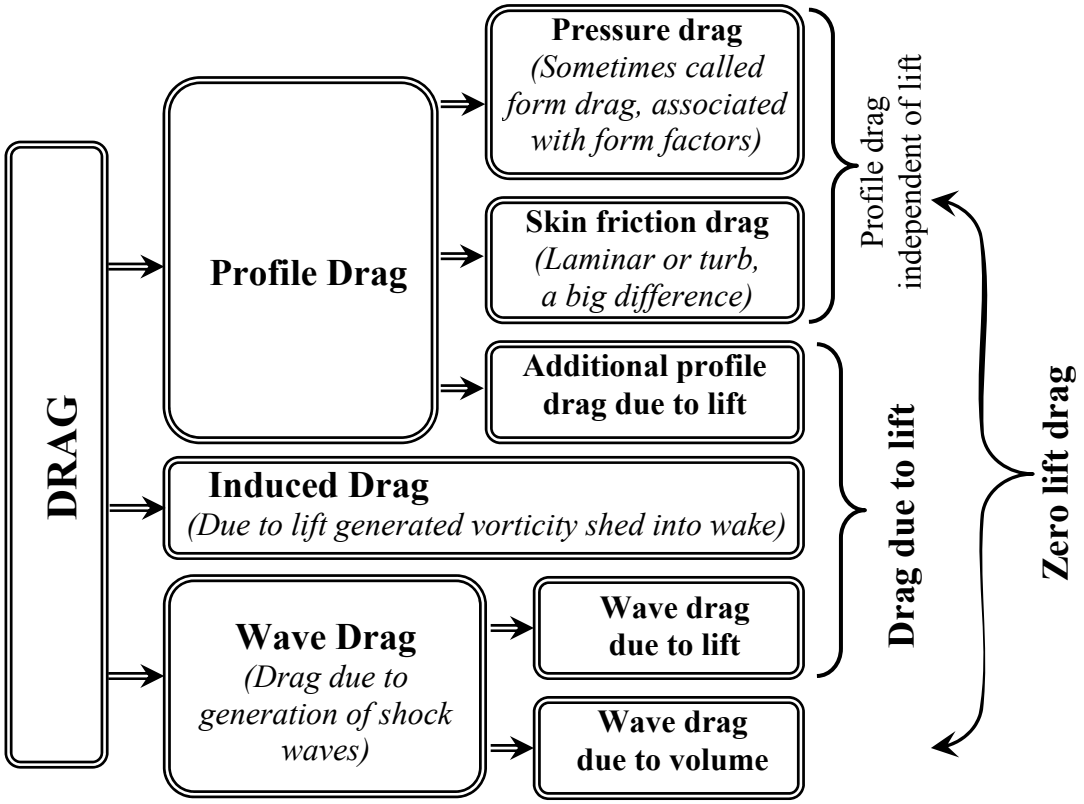

Figure 1.1 : General drag structure

There are two common strategies in engineering optimizations, gradient-based and gradient-free. Genetic Algorithm (GA) and Search Algorithm (SA) are non-gradient methods. However they require large number of function evaluation. On the other hand, gradient-based methods require far fewer function evaluations as long as provided accurate gradient information is available. In the most general sense, optimization is a process of achieving a best outcome of a given operation while satisfying a set of given constraints. The cost (or objective) function is the term applied to this outcome that needs to be improved (or optimized) **(Foster and Dulikravich, 1997)**

Evolutionary algorithms, for example Genetic Algorithms, are known to be robust **(Golberg, 1989)** and have been enjoying increasing popularity in the field of numerical optimization in recent years. GAs are search algorithms based on the theory of natural selection and natural genetics. One of the key features of GAs is that they search from a population of points and not from a single point. **(Obayashi et al. 1998b)**

Evolutionary algorithms (EAs) represent a powerful search and optimization paradigm, in comparison to the other methods. In some cases, they have advantages over existing computerized techniques. However, the efficiencies and reliability of EAs for solving the complex and multimodal optimization problems should be investigated for satisfying the practical requirements at present. Currently, it is an important research area for EAs. **(Liang, 2003)**

However, in CFD applications, especially for 3-D geometries, one of the most important problems in application of Genetic Algorithms is CPU time usage and the main time consuming part of this application is flow solver. In comparison to the genetic processes, flow solver is highly weighted.

Continuous changing or deforming of the bodies during these design processes let the researchers develop different methodologies which can be classified into the following four different groups,

- Mass – spring – damper (MSD) systems
- Boundary element method (BEM)
- Finite difference method (FDM)
- Finite element method (FEM)

The MSD model, which is applied in this study, is the simplest computationally, but does not allow accurate modeling of material properties, which are not needed for the general shape optimization.

Therefore, in this study, dynamic mesh method **(Batina, 1990-1991)** is implemented on a real coded genetic algorithm to demonstrate gain in computational time as well as in higher performance for optimized parameters. **(Vatandaş et al. 2003)**

In this work, at first, the airfoil section of Onera M6 wing has been improved. Airfoil sections are represented by control points as design variables. In the optimization process, as a constraint, the lift force is held fixed and as an objective, the drag force has been tried to be minimized. Later in addition to the lift force, the thickness ratio is held fixed. After this, the taper ratio is added to the design variables. Because the operating time of the program is very long, on

account of our low capacity computer resources, to overcome such difficulties, Parallel Processing has been used.

1.1 Previous works

In recent years, GA has been used for aerodynamic optimization, airfoil and wing design. **Obayashi and Takanashi (1995)** have applied GA based method to the inverse design problem of an airfoil by using a Navier-Stokes solver. **Quagliarella and Della Cioppa (1994)** have developed a method of transonic airfoil design by using a full potential flow solver. These works have shown that GA based methods can be successfully used for aerodynamic optimization and design. **(De Falco, 1997)**

Various techniques have been developed on aerodynamic applications of GA. **De Falco et al. (1996)** have developed a method called "Breeder Genetic Algorithms" which converges more rapidly and contains a way of selecting best individuals of population. They also used a binary code and developed a mutation operator called M_{ijn} and a more rapid GA. **(De Falco et al. 1998)**

Vicini and Quagliarella (1999) have developed an efficient and fast hybrid method which combines RKGA with gradient based techniques. **Klein and Sobieczky (2001)** have developed a GA which provides a flexible data input system for high speed wing and airfoils. **Jones et al. (2000)** have developed a GA for aerodynamic and aero-acustic wing sections and they improved efficiency of airfoil while reducing the noise level.

For high lift, multi-element airfoils **Quagliarella and Vicini (1999)** have presented a multi-objective genetic optimization method. Besides, a new coding techniques called "Taguchi" was introduced by **Oyama et al. (1998)**

Two hybrid optimization methods used for preliminary design of three dimensional shapes were introduced by **Foster and Dulikravich (1997)**. In a comparison to the gradient based method, the hybrid genetic algorithm has been shown to be able to achieve impressive convergence on highly constrained problems while avoiding local optimums.

Quiet Supersonic Platform (QSP) program **(Chung, 2004)** is an example problem requiring Multidisciplinary Design Optimization (MDO) in which the noise level

of the ground boom signature of a supersonic business jet is expected to be significantly reduced while challenging aerodynamic performance requirements must be met at the same time. An efficient and robust design methodology using approximation techniques such as response surface and Kriging methods, augmented by gradient information, has been developed and tested on simple analytic functions for this problem. A multiobjective optimization to simultaneously minimize boom and drag at fixed lift has been performed to search for the Pareto design front by using a genetic algorithm based on different kinds of approximation models.

Multidisciplinary Design Optimization (MDO) techniques have been successfully applied in sizing the wing boxes of the newly developed Fairchild Dornier regional jet family. A common finite element model for the whole aircraft was used for the static and aero-elastic optimization and analysis purposes. **(Schuhmacher, 2001)**

Fanjoy (2001) has combined the aerodynamic shape and structural topology into a single problem statement, with the intent of discovering non-traditional rotor blade cross-section forms. A GA method has been used to generate solutions to this problem.

A robust aircraft design methodology has been developed by **(Gundlach, 2004)** for analysis and optimization of the Air Vehicle (AV) segment of Unmanned Aerial Vehicle (UAV) systems. The developed optimizer seeks to minimize AV design gross weight for a given mission requirement and technology set all three UAV families show significant design gross weight reductions as technology improves.

Some new approaches to genetic algorithms used for aerodynamic design and optimization, called Vibration concept and Distribution Strategies (DS) are proposed by **Hacıoğlu (2003b)**. Vibrational Mutation and Vibrational Crossover techniques resulted from Vibration concept, and the method of Vibrational Genetic Algorithm (VGA), which uses these techniques, are detailed. Besides, the Distribution of Objective Function (DOF) and the Distribution of Elitism (DE) techniques, come from DS, is given. Some applications of these new techniques to the aerodynamic design and optimization are performed.

Vibration concept is based on that the population is spread out over the design space periodically to make exploration/exploitation of the genetic algorithm effective. DS aims to decrease total function evaluation by distributing genetic operations. Effectiveness of these methods is shown by making their applications to inverse airfoil design and transonic airfoil optimization, and the number of Computational Fluid Dynamics calculations are decreased considerably **(Hacıoğlu, 2003b)**.

The genetic algorithm has been also used for the determination of the optimum geometry of heat exchanger body. **(Ozkol, Komurgoz, 2005)**

1.2 Developed and Applied Methods in Wing Aerodynamic Design

Genetic algorithms resemble evolution theory by Darwin which claims that a biological population adapts to its environment by selection, crossover and mutation. **(Hacıoğlu, 2003a)**

A target pressure optimization code with GA has been developed for transonic wing design problems by **Kim and Rho (1998).** The inverse design of transonic wings has been performed by the hybrid inverse optimization method with the optimized target pressures.

Multi-Objective Genetic Algorithm (MOGA) based on the Pareto ranking has been applied to the multidisciplinary optimization of a transonic wing planform by **Obayashi, et al. (1997)**. The MOGA has been applied to multidisciplinary design optimization problems of transonic and supersonic wing planform shapes by **Obayashi et al. (1998a)**.

Gradient-based optimization methods require derivatives of the objectives and constraint functions. Often these functions are evaluated by using computationally intensive analysis. Mali et al. have used automatic differentiation for 3-D Euler CFD code written in FORTRAN 77 programming language. The calculated gradients are compared with those obtained through forward difference. The generated derivative code is used for an optimization study to maximize L/D of ONERA-M6 wing with angle of attack as a parameter.

Gundlach (1999) has developed an alternative configuration that is the strut-braced wing, which uses a strut for wing bending load alleviation, allowing

increased aspect ratio and reduced wing thickness to increase the lift to drag ratio. High aerodynamic efficiency means reduced fuel consumption and smaller, quieter, less expensive engines with lower noise pollution. The developed configuration is lighter, burns less fuel, requires smaller engines and costs less than equivalent cantilever wing aircraft. **(Gundlach 1999)**

Two major aircraft optimal design projects have been illustrated by **Hu (2003)**. The first is the application of material optimization of aligned fiber laminate composites in the presence of stress concentrations. The second project is the application of piezoelectric actuator placement on a generic tail skins to reduce the 2 mode vibration caused by buffet.

In general, for aerodynamic design problems, stream function based methods **(Dulikravich, 1991)**, numerical optimization **(Vanderplaats, 1984)** or control theory **(Jameson, 1988)** are used. Besides expert systems based methods **(Tong, 1985)** have been also developed.

1.3 Recent Studies and Present Status of the Wing Design

Scientists are researching on 3-D design problems by using parallel processing and hybrid methods in today's world. The improved computer capability has given the opportunities to work on more complex geometries and 3-D mesh structures that have millions of elements.

For instance, a parachute shape optimization has been achieved by using space-time finite element techniques developed for computation of fluid – structure interaction problems. **(Tezduyar et al., 2005)**

The wing design researchers generally concentrate on reducing the drag force while holding the lift force at a pre-determined design value. For structural analysis constraints, keeping the thickness ratio is also important, besides, in the aspect of stability, location of mean aerodynamic chord or moment around the leading edge must be conserved.

In recent years, researchers have mostly worked on 3-D wing shape optimizations **(Obayashi et al., 1998b)**, aircraft fuselage shape optimizations or submarine shape optimizations **(Liu et al., 2005)**.

These works require complex mesh structures that have large number of elements, higher computer resources (capabilities) and some additional and supportive methods that can make the process faster and efficient.

2. THEORETICAL BASIS: DYNAMIC MESH AND GENETIC ALGORITHM

2.1 What is Dynamic Mesh

Mesh modification can be needed in case of a geometry change (i.e. change in airfoil section, twist angle or taper ratio) or in case of a change in angle of attack. In these cases, mesh structures should be modified with no deformation and no change in general shapes of cells.

In dynamic mesh algorithm the original mesh corresponding to the initial geometry is moved to conform to the shape of a member by modeling each edge of each tetrahedron by a spring. **(Batina, 1990-1991)** The stiffness of the spring for a certain edge i-j is taken to be inversely proportional to the length of the edge as

$$k_m = 1/[(x_j-x_i)^2+(y_j-y_i)^2+(z_j-z_i)^2]^{1/2} \qquad (2.1)$$

The grid points on the outer boundary of the mesh are held fixed and the instantaneous location of the points of the inner boundary (geometry of a member in a generation) are given by the prescribed surface motion. At each time step, the static equilibrium equations in the x, y and z directions, which result from a summation of forces, are solved by an iterative calculation at each interior node i of the grid for the displacements δ_{xi}, δ_{yi}, and δ_{zi}. This is accomplished by using "predictor – corrector" procedure, through which the displacements of the nodes is first predicted by extrapolation from grids at previous time levels according to

$$\overline{\delta_{xi}} = 2\delta_{xi}^{n} - \delta_{xi}^{n-1} \qquad \overline{\delta_{yi}} = 2\delta_{yi}^{n} - \delta_{yi}^{n-1} \qquad \overline{\delta_{zi}} = 2\delta_{zi}^{n} - \delta_{zi}^{n-1} \qquad (2.2)$$

and then these displacements are corrected using several Jacobi iterations of the static equilibrium equations using:

$$\delta_{x_i}^{n+1} = \frac{\sum k_m \bar{\delta}_{x_m}}{\sum k_m} \qquad \delta_{y_i}^{n+1} = \frac{\sum k_m \bar{\delta}_{y_m}}{\sum k_m} \qquad \delta_{z_i}^{n+1} = \frac{\sum k_m \bar{\delta}_{z_m}}{\sum k_m} \tag{2.3}$$

In these equations, the summations are performed over all of the edges of tetrahedra that make up the control volume of node i (i.e. neighboring points of node i). The new locations of the interior nodes are then calculated by

$$x_i^{n+1} = x_i^n + \delta_{x_i}^{n+1} \qquad y_i^{n+1} = y_i^n + \delta_{y_i}^{n+1} \qquad z_i^{n+1} = z_i^n + \delta_{z_i}^{n+1} \tag{2.4}$$

By using the equation (2.4), new x, y and z coordinate values of each interior node are calculated. These changes in coordinate values depend on the boundary conditions explained before on the free stream (outer) boundary, symmetry plane and the wing surface (wall) boundary.

2.2 Genetic Algorithm and Vibrational Genetic Algorithm as an Evolutionary Type Algorithms

Genetic Algorithms (GA) are developing procedures. They resemble Darwin's theory of evolution which claims that a biological population adapts to its environment by selection, crossover and mutation.

GA is nongradient method **(Haftka and Gürdal, 1992)** that offers a promising answer to complex optimization problems. In general, a GA is broken into three major steps: evaluation, crossover, and mutation. An initial population of complete design variable sets is analyzed according to some cost function. Then this population is merged using a crossover and mutation methodology to create a new population. This process continues until a global minimum is found. **(Foster and Dulikravich, 1997)**

Hacioglu **(Hacıoğlu and Özkol, 2002)** has been developed its procedures on especially 2-D airfoils and called it as Vibrational Genetic Algorithm (VGA). The Vibrational Genetic Algorithm (VGA) is a GA, which uses the vibration concept. In that, by applying a vibrational mutation periodically to all individuals in a population, they are spread out over the design space. Therefore, it becomes possible to escape local optimums and thus to obtain a global optimum faster. **(Vatandaş et al., 2005a)**

Vibration strategy in mutation is used after a recombination. Entire genes in all the chromosomes are mutated based on the vibration wave as follows,

$$\begin{aligned} & y_i^m = y_i^m \cdot [1 + MA \cdot u \cdot Sin(2 \cdot \pi \cdot fr)] \\ & m = 1,....,n \\ & i = 1,....,kn \end{aligned} \tag{2.5}$$

or

$$\begin{aligned} & y_i^m = y_i^m \cdot [1 + w1 \cdot MA \cdot (0.5 - u)] \\ & m = 1,....,n \\ & i = 1,....,kn \end{aligned} \tag{2.6}$$

Where y_i^m are the control points (genes), kn is the chromosome length (total gene number of a chromosome), n is the total number of individual in the population, MA is the main amplitude, u is a random real number between [1,0], and $w1$ is a user defined real number between [0, 2] and controls MA.

The vibrational mutation is implemented starting from a certain gene position at the first chromosome, and throughout the genes at the same positions in the other chromosomes. This process is applied to all the individuals in the population every IP period. The mutation rate P_m is equal to $1/IP$ where IP is an integer number. Since a random distribution in a narrow band helps reaching the global maximum as close as possible, the main amplitude MA is evaluated during the genetic process as follows:

$$MA = \left[\frac{\log(1 + AF_0)}{\log(1 + AF_k)} \right]^r \tag{2.7}$$

where AF_0 and AF_k are average fitness values at the initial and current steps of the genetic process respectively, and r is a real number.

The Vibrational Genetic Algorithm (VGA) has also been used for solving continuous covering location problems by **Ermiş et al. (2002)**

2.3 Dynamic Mesh and Genetic Algorithm

In many engineering fields, Realistic behavior of deformable objects is essential, numerical solutions of flow problems with complex moving or deforming

boundaries generally require the solution of the corresponding fluid equations of motion on unstructured dynamic meshes. In the field of aerodynamics, the inviscid type of modeling, the dynamic mesh technique has been applied to unsteady Euler airfoil solutions **(Batina, 1990)** and unsteady Euler algorithm for complex aircraft aerodynamic analysis by **John T. Batina (1991)**. In these works, the dynamic mesh technique has been used for modifying the existing mesh to conform to the body which was changing its orientation or shape.

By using the dynamic mesh technique, the original mesh can be modified to fit the change in angle of attack which results in any geometrical change in the body of aircraft or for instance the change in the shape of an aircraft fuselage.

As an example of applications in genetic algorithm, the dynamic mesh method has been used to modify the mesh to fit the change in twist angle of a wing. **(Obayashi, S. et al. 1998b)**

Especially for 3-D domains an integrated grid generation as a part of the flow solver may not be available or each grid generation for the newly produced members by modification in genetic algorithm may not be as successful as desired. Even an integrated and successful mesh generation may be possible, this process is time consuming. Especially in case of slightly deformed or modified, lots of bodies, grid modification can be more beneficial.

2.4 Dynamic Mesh in This Work

Since the differences developed at each step in geometries of new members are not much, therefore, it is possible to use dynamic mesh methods to determine the mesh structures of new members. In this work, because the population members are obtained by modifying the previous ones, each member is considered as one step of geometry-change of a deforming body, for example a wing inflating, deflating or cambering. **(Vatandaş, et al., 2003)** Because of small differences between the shapes of genetically obtained wing structures, the dynamic mesh technique can be implemented to modify the mesh. **(Vatandaş, et al., 2004a)**

The dynamic mesh technique has been applied to obtaining the mesh structures of newly produced population members. These members are different wing geometries that have different wing sections and taper ratios.

Normally generating a mesh for a wing, takes approximately 8-10 minutes, of course, which linearly depending on computer capability **(Van der Burg, 2005)**. Using the dynamic mesh technique takes approximately the same amount of time for the first step, as any mesh generating technique requires.

However, for the following steps this time can be reduced up to 10 times and this gives the opportunity for several computational experiments to be carried out.

At first the members of populations are ordered in accordance with their chamber and then the dynamic mesh method is applied in this order **(Vatandaş and Özkol, 2004d)**. In the taper ratio together with wing section optimization, because the geometry changes due to the taper ratios are much higher than the changes in wing sections, the population members are ordered in accordance with their taper ratios. Dynamic mesh calculations have been performed through this order.

2.5 Flow Solving Method

'Acer3D' is a flow solver program, which solves inviscid compressible Euler flow equations on unstructured tetrahedral grids. It is sequential version of parallel flow solver known as 'Pacer3D'. Serial and parallel versions together with parallel adaptive sensor program are developed in a Ph. D. thesis study by Erdal Yılmaz **(Yılmaz, 2000)**

U is a vector quantity per unit volume, acting in an arbitrary volume Ω, fixed in space and bounded by a closed surface S. The local U intensity changes depending on the effect of fluxes and sources. F, the flux vector has two parts: the diffusive and the convective parts. According to the conservation law, the variation per unit time of the quantity U within the volume D, should be equal to the net contribution from the incoming fluxes through the surface S with the surface element vector dS pointing outward plus the contributions from the sources of the quantity U.

The sources contain volume and surface sources. Hence the general form of the conservation equation for U can be written as the following **(Hirsch, 1988)**:

$$\frac{\partial}{\partial t}\iiint_{\Omega} U d\Omega + \iint_{S} \vec{F}.\vec{n}\, dS = \iiint_{\Omega} Q_O d\Omega + \iint_{S} Q_S.\vec{n}\, dS \tag{2.8}$$

If there are no surface and volume sources, the right hand side of the Equation (2.8) vanishes. For compressible Euler equations, Equation (2.8) becomes:

$$\frac{\partial}{\partial t}\iiint_{\Omega} U d\Omega + \iint_{S} \vec{F}.\vec{n}\, dS = 0 \tag{2.9}$$

Here U is the solution vector and represents the conserved quantities and F is the flux vector with

$$U = \begin{pmatrix} \rho \\ \rho u \\ \rho v \\ \rho w \\ \rho E \end{pmatrix} \quad f = \begin{pmatrix} \rho u \\ \rho u^2 + p \\ \rho uv \\ \rho uw \\ \rho uH \end{pmatrix} \quad g = \begin{pmatrix} \rho v \\ \rho vu \\ \rho v^2 + p \\ \rho vw \\ \rho vH \end{pmatrix} \quad h = \begin{pmatrix} \rho w \\ \rho wu \\ \rho wv \\ \rho w^2 + p \\ \rho wH \end{pmatrix} \tag{2.10}$$

Where, f, g, and h are components of the flux F in Cartesian coordinates, ρ is density, u, v, and w are Cartesian velocity components, p is pressure, H is total enthalpy, and E is total energy per unit mass and

$$E = \frac{p}{(\gamma - 1)\rho} + \frac{u^2 + v^2 + w^2}{2} \qquad H = E + \frac{p}{\rho} \tag{2.11}$$

The Euler equations are discretized in space by using the finite volume formulation **(Hirsch, 1988).** The finite volume method is based on the application of integral form of the balance laws. In numerical solution, each cell or element that defines the physical domain is treated as a finite volume. The conservative discretization is achieved by applying the integral form of the Euler equations at the level of each elementary cell. **(Yılmaz, 2000)**

In the cell-centered approach, each cell is thought as a control volume. The mean values are stored at the gravity center of each cell. The fluxes are obtained through an interpolation process. The flow variables are assigned to grid nodes. All neighbor cells surrounding each node form the control volume for that node. This is called as overlapping cells.

In the node-centered approach, the unknowns are associated with the mesh vertices and a control volume is constructed around each mesh vertex without overlapping neighboring cell. In the flow solver ACER3D **(Yılmaz 2000)** the overlapping cell-vertex algorithm is used **(Slooff and Schmidt, 2000)**.

In order to provide stability and eliminate non-physical solutions, some dissipation terms are needed in the solution of Euler equations. The dissipation can be added explicitly or it can exist in the spatial discretization. In ACER3D, oscillations due to the numerical solution method are damped by using artificial dissipation terms **(Slooff and Schmidt, 2000)**.

In the Euler flow solver ACER3D, an explicit scheme with multi-stage time discretization and local time-stepping are used for advancing in time **(Hirsch, 1988)**. The usage of explicit scheme in time domain is simpler and more efficient especially for vector and parallel computers. However, more numerical calculations per time step is needed in the implicit scheme. **(Yılmaz, 2000)**

As the initial conditions, freestream values are used in the entire flow field of interest. The boundary faces are marked with different indexes corresponding to the different boundary conditions. The following indices are used for the boundary conditions:

3 → inviscid wall

4 → symmetry condition

5 → far field

The boundary condition needed for inviscid flows, at surfaces of object is the flow tangency or zero velocity at the normal direction to the boundary. This is achieved by assigning zero to the convective fluxes along all mesh faces at the surface of object during the initial iterations.

The symmetry surface is thought as inviscid wall boundary condition. Therefore, only the normal velocities are taken as zero at boundary faces.

2.6 General Parallelization Strategy

The Euler flow solver ACER3D **(Yılmaz, 2000)** solves the flow field on a coarse grid of Onera M6 wing in about 10 hours by using a 1.3 GHz. P-IV processor. In

genetic algorithm generally 30-100 generations, each having 12-30 members are needed to achieve a reasonable solution.

This means 150 – 1200 days which is not feasible and applicable. Therefore some both hardware and software conditions must be improved to make this optimization process applicable. These are:

- Restarting the flow solver from the previous solution
- Using dynamic mesh technique to modify the mesh
- Using parallel processing

Parallel processing code distributes a task to available computing resources by using communication network to obtain faster solution for large scale-problems. There are several methods for parallel implementations depending on the type of the problem and the algorithm. Most of the CFD applications involve in domain decomposition approach. However functional decomposition can be better for interdisciplinary problems. In the first one, the solution domain is subdivided into small parts to solve each one or multiple parts at each processing node. In the second method, computation is decomposed and then distributed to each processing node. **(Yılmaz, 2000)**

In parallel processing, both the domain decomposition and the functional decomposition, each part of the problem, needs to exchange information with its neighbors. Most of the applications use two communication libraries for this purpose. The Parallel Virtual Machine (PVM) is the first that was introduced for the communication between computers in 1989 (Al Geist et al., 1994). After PVM, another library was developed for the message passing, the Message Passing Interface (MPI) **(Fostar, 1995)** In the PVM standart, the portability is preferred over performance, whereas the performance has the priority over flexibility in the MPI. However, the usage of the MPI on different platforms is getting more popular and practical. It also provides more functions for controlling the message passing. In the present study MPI was used.

MPI library is used to convert the program ASOP3D into parallel form. Because the flow solution part takes approximately 95 % of the total run time and the other parts are not suitable for parallelization, only the flow solution stage is

made parallel. Therefore due to 14 members to be solved in each generation 14 processors have been used in parallel computing.

MPI is a *specification* for the developers and users of message passing libraries. By itself, it is NOT a library - but rather the specification of what such a library should be. **(Barney, 2005)**

MPI is a library specification for message-passing, proposed as a standard by a broadly based committee of vendors, implementers, and users. **(Ref: MCS)**

- An MPI standard is available for the users.
- MPI was designed for high performance on both massively parallel machines and on workstation clusters.
- MPI is widely available, with both free available and vendor-supplied implementations.
- Test Suites for MPI implementations are available.

2.7 Purified Genetic Algorithm for Taper Ratio Optimization

In the taper ratio optimization, much more changes occur in the wing geometry compared to the wing section optimization. It has been experienced that the geometries of some members in a generation may not be suitable to achieve a good flow solution. These members are eliminated by assigning a lower fitness value to them.

By this method, it has been observed that the code was not kept busy unnecessarily, the solution diverged from those “bad members” and at the later steps these members rarely come out.

In Genetic Algorithm because of genetic operations like crossover, mutation, sometimes it is possible to produce some members in an irregular shape. These members usually are eliminated naturally by having a lower fitness value. However sometimes it is possible not being able to solve the flow domain of these members. In this case the above explained purification process can be applied.

2.8 Verifications

2.8.1 Flow Solver Verification

The flow solver ACER3D was developed by Erdal Yılmaz. **(Yılmaz, 2000)** It was especially applied on Onera M6 wing and verified.

In Figures 2.1-4 the solutions of flow domain over Onera M6 wing are compared for different mesh density and different experimental and numerical methods.

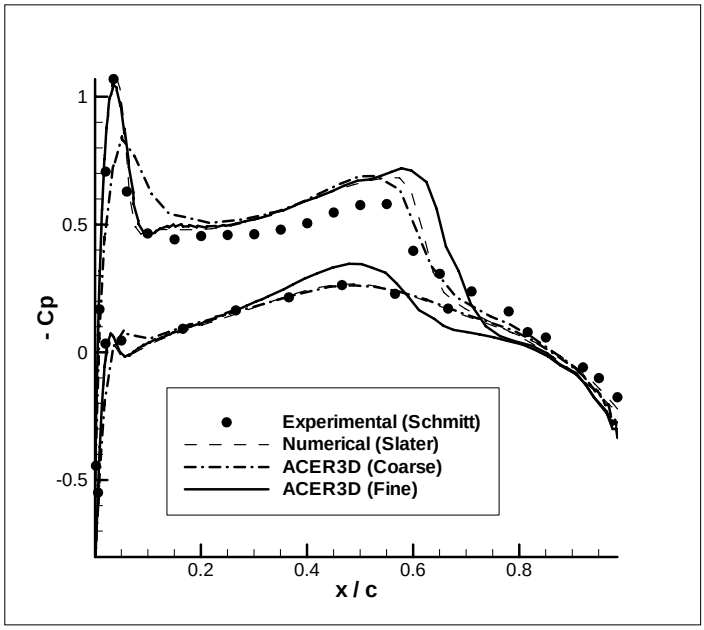

Figure 2.1 : Pressure coefficient distribution over the section at 0.2b

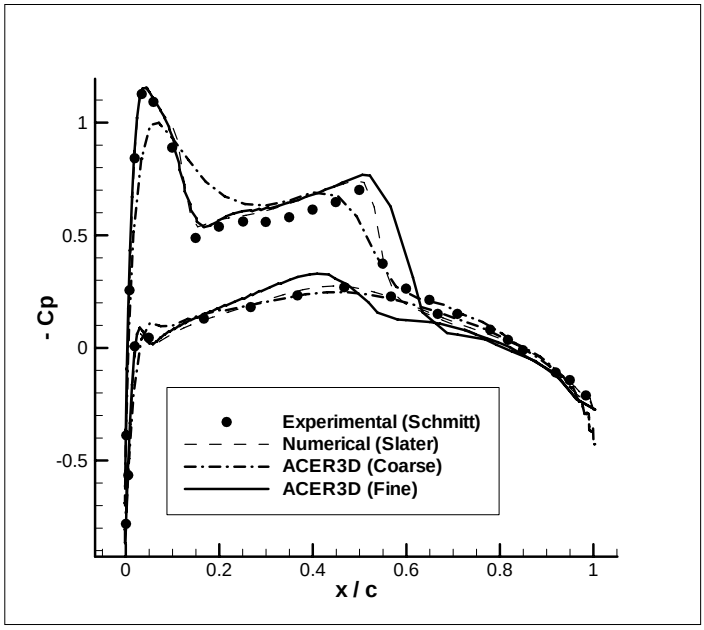

Figure 2.2 : Pressure coefficient distribution over the section at 0.44b

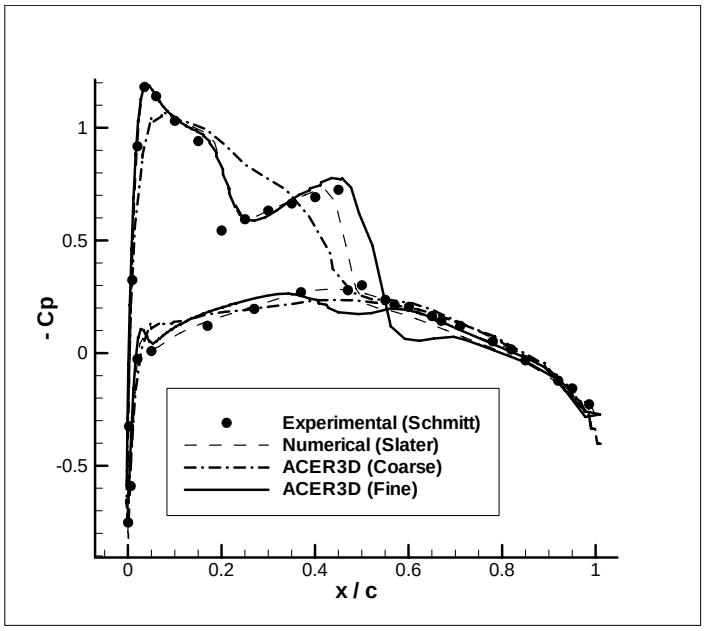

Figure 2.3 : Pressure coefficient distribution over the section at 0.65b

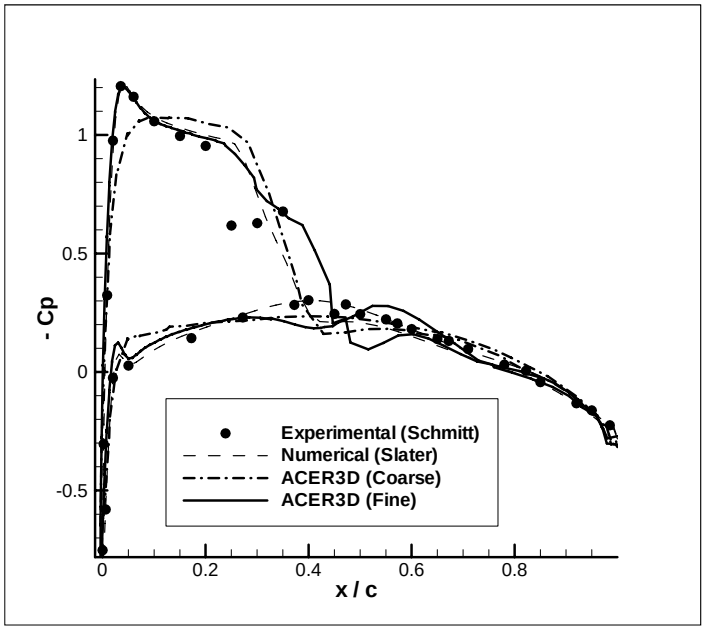

Figure 2.4 : Pressure coefficient distribution over the section at 0.8b

2.8.2 Vibrational Genetic Algorithm Usage and Verification

The Vibrational Genetic Algorithm (VGA) processes have been developed by Abdurrahman Hacıoğlu **(Hacıoğlu, 2003b)** on 2-D airfoils. In his study, all genetic processes are applied to 2-D optimization flow problems and the results obtained are in good agreement with the open literature.

The Vibrational Genetic Algorithm (VGA) is a GA, which uses the vibration concept. Previous works about vibration concept were presented by **Hacıoğlu**

and Özkol (2001-2002). They first introduced *Double Directional Alpha Method* which is named as *vibrational crossover* in their later study. The vibration concept was presented as *vibrational crossover* and *vibrational mutation* in **(Hacıoğlu and Özkol, 2002)**

As noted by **Obayashi et al. (1998b)** the mutation probability for a real coded GA should be set at a higher value than when binary coding is used. Because in binary coding, a change in a single bit can effect significant change in the value of the design variable, but in real number coding a similar change has a lesser effect. Thus a higher mutation probability is justified as a means to enable the algorithm to search the design space thoroughly **(Tse and Chan, 1999)**. This aim can be achieved by *vibrational mutation.* This process is explained and formulated in the following.

Mutation based vibrational concept is based on having samples simultaneously in the various parts of design space by which it is able to catch global optimum as quick as possible. For this purpose, all individuals in a population are mutated in a vibrational manner periodically, so that they spread out over the design space. Thus, it is possible to escape from local optimums more quickly and to find better individuals.

A brief description of the vibrational mutation procedure can be given as the following: At the *IP*th step of genetic process, after the evaluation of fitness values, selection of fitted individuals and recombination, vibration is applied to all new chromosomes. At first, initial genes (j=1) in all chromosomes (i=1 to n) are vibrated; after this, the genes at the second position (j=2) in all chromosomes (i=1 to n) are vibrated. This operation is applied up to when the last genes (j=kn) are vibrated. At next IP-1 step of the genetic process (mutation rate P_m =1/IP), regular genetic operations (evaluations of fitness, selection and recombination) are performed. At the second *IP* th step, vibration is applied just as the first step. The application of vibration process is repeated at every *IP* step while the genetic process goes on.

Experiments were performed for three different cases in Hacıoğlu's thesis **(Hacıoğlu, 2003b)**. One of them is inverse airfoil design in incompressible, inviscid flow; the other is inverse airfoil design in transonic flow; and the other one is airfoil optimization in transonic flow.

Surface pressure coefficient (Cp) distribution, of NACA4412 airfoil at 10° angle of attack is given for inviscid, subsonic, incompressible flow. The flow solution method is vortex panel technique for incompressible, inviscid flow. 120 panels have been used for CFD calculations.

Surface pressure coefficient (Cp) distribution, of NACA64A410 airfoil at 0° angle of attack and M=0.75 (inviscid, transonic flow) is given. A full potential solver with 161x31 O-mesh was used for this transonic, inviscid flow condition.

NACA0012 airfoil has been optimized at Mach 0.75, 2° angle of attack (viscous, transonic flow) and Reynolds number Re_c=9. 10^6. An IBL (Interactive Boundary Layer) solver with full potential solver and 161x31 O-mesh was used for this flow condition. Thickness ratio of the airfoil has been kept at the same level.

The following strategies are used for genetic optimization for the case above:

Strategy I (Regular GA): Crossover technique is BLX-α **(Eshelman and Schaffer, 1993)** with α=0.7 (the best value for this case), P_m =0.015. VGA is not used. Mutation is applied to randomly chosen *i*th gene in *k*th chromosome which is selected randomly in the population, by using this equation:

$$y_i^k = y_i^k \cdot +2 \cdot w \cdot (0.5 - u) \tag{2.12}$$

w was taken as 0.04 for all case. Strategy II (VGA-new): Crossover technique is BLX-α with α=0.7, besides vibrational mutation with new formulations, in equation (2.6), is used. Strategy III: Crossover technique is BLX-α with α=0.7, additionally vibrational mutation with old formulations, in equation (2.5), is used.

As a selection method, Stochastic Universal Sampling **(Baker, 1987)** is used. It is started from the NACA 0012 to reach the target airfoil for inverse design. The thickness ratio of NACA 0012 is changed ±30% uniformly to create the initial population. In the optimization case, it is started from the original airfoil (NACA 0012) exactly to reach the optimized one.

In the inverse design applications, for vibrational mutation, the value of *r* in equation (2.7) was taken as 4. For the applications, 70000 is good enough as the fitness value for the fast convergence. The results presented are the average

value of each 10 different experiments. In Figure 2.5**,** it is shown that how the fitness values developed during the design processes. Horizontal axis shows number of CFD calculations and the vertical axis, fitness values which correspond to each CFD calculations.

In the optimization study, for vibrational mutation, main amplitude *MA* in equation (2.6) is taken as a constant 0.05, since, an optimized shape, which is too close to original one, is searched for.

DISCUSSION: Strategy I (ST-I or RGA) is applied to the population size n=30. In the application of VGA, as in the previous study **(Hacıoğlu and Özkol, 2002)**, small population size is found more convenient. The population size in ST-II application is n=12, for the vibrational mutation IP=3 (P_m=1/3) is chosen. The value of $w1$, in equation (2.5) is 1.0. The Figure 2.5 shows the comparison of best fitness values for two different strategies. The figure reveals out that the both proposed technique, VGA, has comparatively faster convergence than regular GA (ST-I). On the other hand, ST-II (new formulation) with same population size and mutation probability gives better results than ST-III which uses old vibrational mutation formulation in equation (2.5). To obtain target fitness value, in regular GA (ST-I) 1440, in ST-II 732 and in ST-III 1032 CFD calculations are needed. In comparison to the regular case, these CFD calculations indicate that in the ST-II case 49% reduction is observed.

In Figure 2.6 shows how close the target profile geometry to the optimized one by the inverse design. Similarly, Figure 2.7 depicts pressure coefficients for the relating geometries. These two figures clearly indicate the excellence of the implemented method for the inverse airfoil design problem in incompressible and inviscid flow.

The numerical applications show that VGA has a great impact on the number of CFD calculations for the inverse airfoil design and optimization. This method is not only for incompressible subsonic flow condition but for the transonic flow as well. The number of CFD calculations is reduced about more than 45%. For the engineering problems, especially for the inverse airfoil design and optimization, this method seems to be promising.

Finally, VGA applications, either combined or individually, result in a tremendous reduction in CFD calculations and CPU time. It is also possible to use these strategies in many other engineering problems. **(Ermiş et al., 2002)**

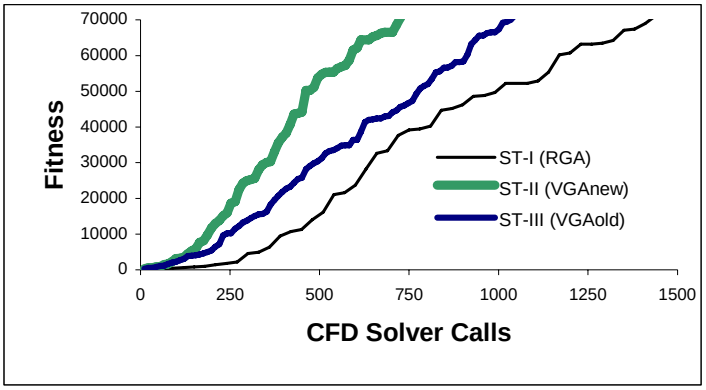

Figure 2.5 : Comparison of best fitness values for strategies I, II and III **(Hacıoğlu, 2003b)**

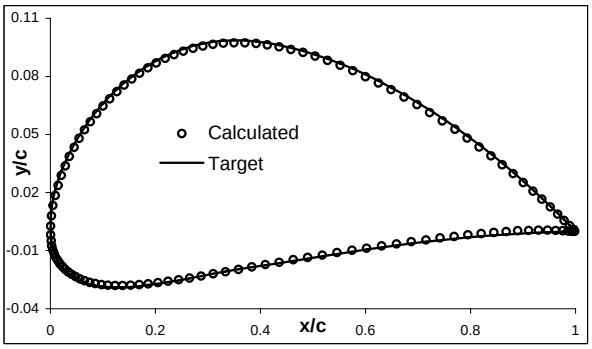

Figure 2.6 : Calculated and target airfoils **(Hacıoğlu, 2003b)**

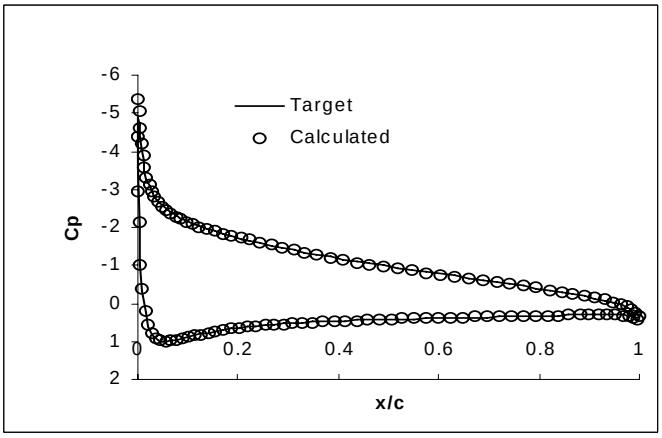

Figure 2.7 : Calculated and target Cp distributions **(Hacıoğlu, 2003b)**

3. MAIN STRUCTURE OF THE DEVELOPED CODE AND APPLICATION STRATEGY

3.1 Basic Concept and Structure of the Optimization Process

In genetic algorithm processes, at first, the initial geometry must be determined. In this work, the initial geometry has been chosen as Onera M6 wing. The control points of the Onera M6 wing section are obtained and used as a starting point.

The mesh structure data of Onera M6 wing is also needed to start the process. Next, the initial population must be determined. The initial population has been produced by altering the thickness ratio of the original Onera M6 wing.

After producing the initial population as control points, the airfoil coordinates of its members are determined by using Bezier Curve method. **(Hacıoğlu, 2003b)**. The mesh structures of the new members are calculated using these airfoil coordinates by modifying the original mesh by simply interpolating and dynamic mesh method **(Batina 1991)**

Later the flow parameters of each individual are calculated by using the flow solver ACER3D **(Yılmaz, 2000)**. ACER3D calculates the pressure distribution over each wing. Next, the lift and drag forces are calculated by integrating these pressure values based on a finite element method as in **(Mecitoğlu and Dökmeci 1990)**. Once the drag and lift forces are calculated, the fitness values are evaluated and the control points of the population members undergo the genetical processes. The program goes back to calculate the mesh structures and flow parameters of these new members.

The main steps of whole project are outlined below in Figure 3.1.

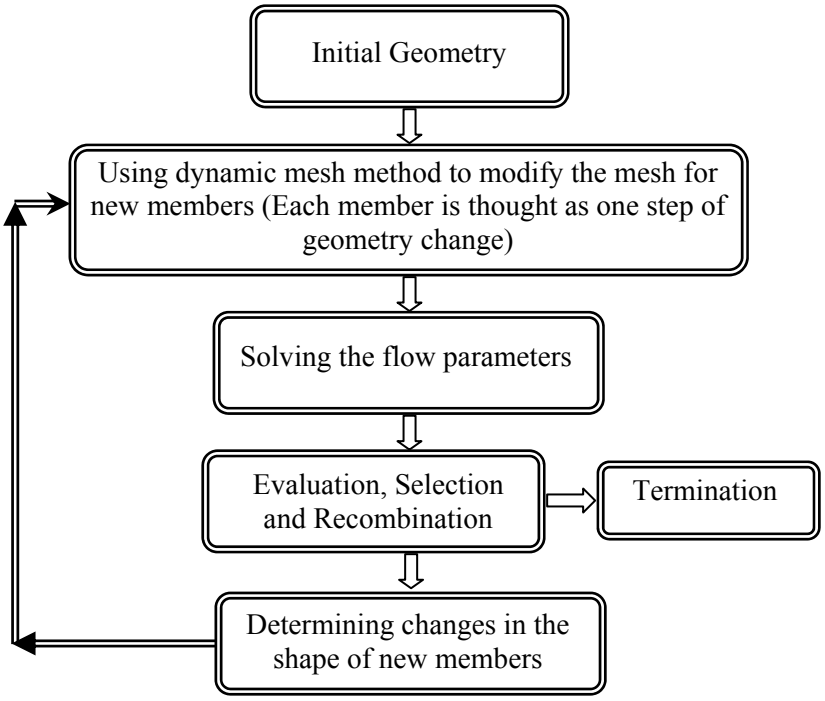

Figure 3.1 : Outlines of the main project

3.2 Airfoil Representation: Using Bezier Curve

Normally in numerical methods, airfoils are represented by about 100 points. However, in GAs much less points are needed for optimized. One of the representing methods by fewer points is using Bezier curve as shown in Figure 3.2. In this method the *x* and *y* coordinate points of an airfoil is obtained through the following equations:

$$y(t) = \sum_{i=0}^{m} C_m^i \, t^i \, (1-t)^{m-i} \, y_i \tag{3.1}$$

$$x(t) = \sum_{i=0}^{m} C_m^i \, t^i \, (1-t)^{m-i} \, x_i \tag{3.2}$$

$$C_m^i = \frac{n!}{i!\,(n-i)!} \tag{3.3}$$

Here x_i, y_i are control points. They have the values in interval [0,1]. *x*, *y* coordinate points of the airfoil are calculated by using the equations (3.1) and (3.2). In 2-D airfoil design problems, while genetic process is using the control points, the flow solver uses the coordinate points.

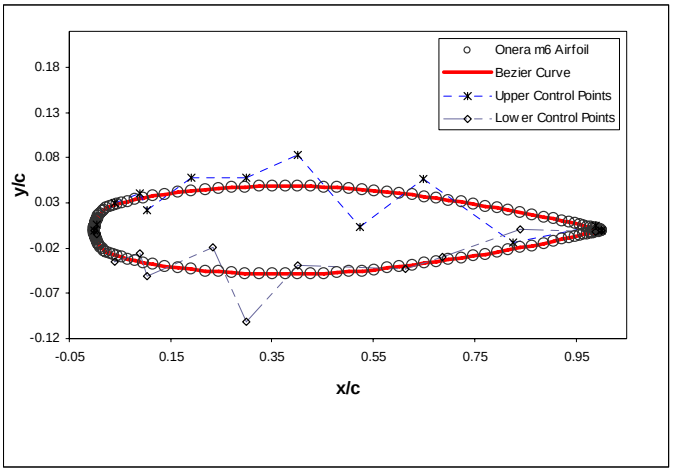

Figure 3.2 : Representing the airfoil with a Bezier Curve

The control points of the airfoil are reproduced and initial population of airfoils is generated as control points. Then using subroutine "Bezier" airfoil coordinates of initial population is obtained.

Next, all nodes on the wing are processed as follows: The chord length is calculated according to *y* coordinate value. Then *x* coordinate value is non-dimensionalized by this chord length. *x* coordinate is compared to *x* values of airfoil and displacements in z coordinate value are calculated by interpolating the differences between y coordinate values of airfoils.

3.3 Program Outline and Flow Charts of ASOP3D

In the Aerodynamic Shape Optimization Program (ASOP3D), there are 14 subroutines, which can be classified into four different phases:

At the first phase, some necessary parameters and input data are collected like initial control points, maximum iteration numbers etc. Then they are reproduced to conform to the initial population. This is achieved by altering the initial wing's thickness ratio.

After producing the initial population as different thickness ratios and/or different taper ratios, their airfoil coordinates are calculated by using Bezier curve method. 143 coordinate points of each airfoil are obtained from 14 control points. Later the subroutine "sequencer" arrange these members of the population. This arrangement is carried out in accordance with their chamber in the wing section optimization. In the taper ratio -together with wing section-

optimization, this arrangement is done based on their taper ratios. Because the geometry changes due to taper ratios are much higher than those due to thickness ratios. **(Vatandaş et al. 2004b)**

At the second phase, the mesh structures of the produced members are determined based on the dynamic mesh technique. In this phase, at first the types (i.e. wall, free stream or symmetry plane) of all nodes and the neighboring nodes of each node are determined and written in a data file. This process is done once and in the other steps, this information can be taken from this data file. **(Vatandaş and Özkol, 2004c)**

After determining the neighbors and the types, initial displacements are assigned and the displacements on the boundaries are determined. The displacements on the wall boundary (i.e. nodes on the wing) are calculated in accordance with the differences in airfoil coordinates calculated before based on Bezier curve method.

On the symmetry plane, the nodes are held fixed in only y axis direction. (i.e. the direction along with the wing from the root to the tip) and they are left to the iteration procedure in the other directions. On the free stream surfaces, all nodes are held fixed in all directions.

The flow chart of the program is illustrated in Figure 3.3 below.

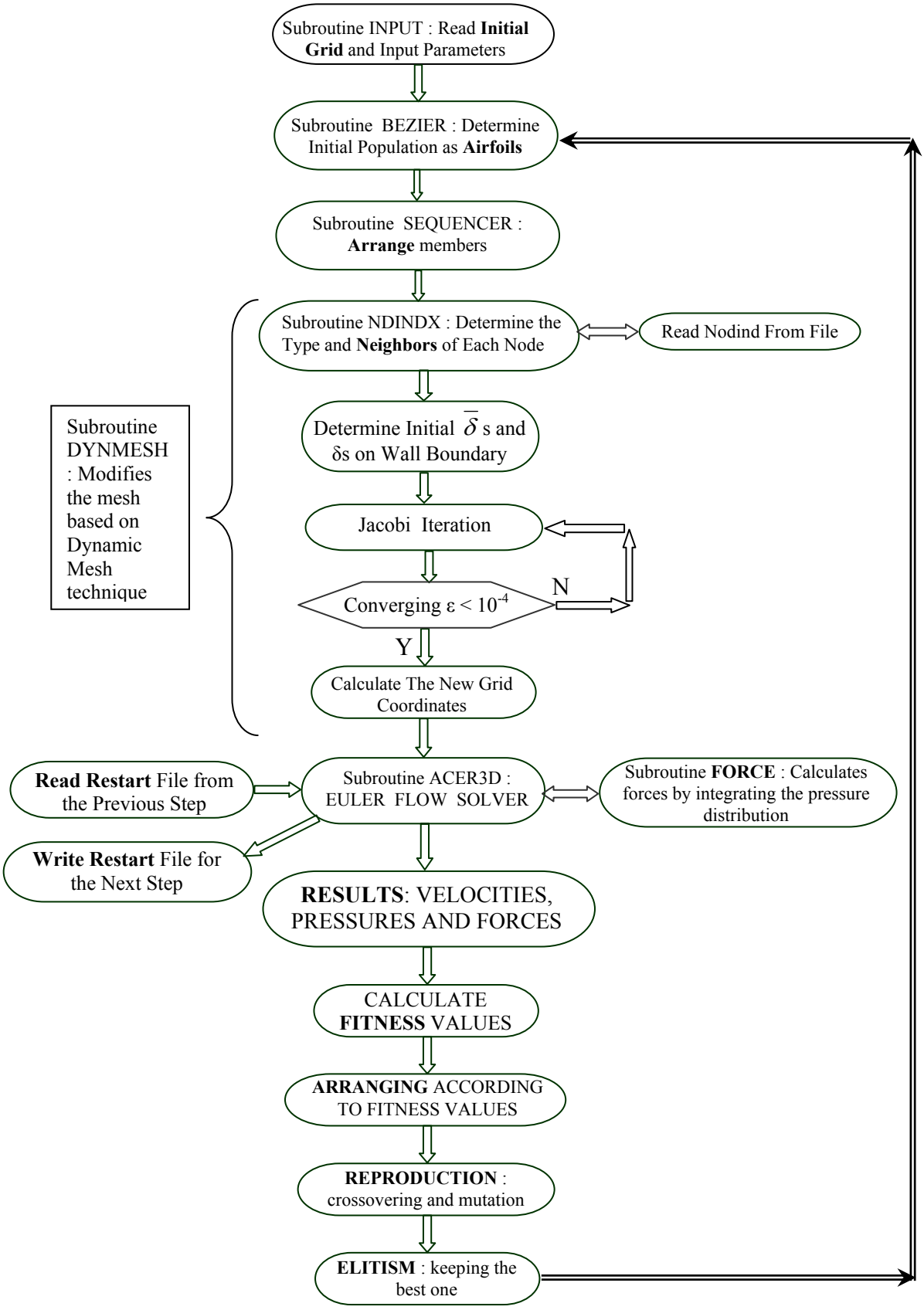

Figure 3.3 : Main outlines of the program

3.3.1 Subroutines, Input – Output Files

1. Input :

a. Reads the parameters like:

kmax : maximum number of iterations in Dynamic Mesh process
ct : tip chord length
cr : root chord length
b : wing length
sw : leading edge sweep angle
epsilon : criterion for convergence in Dynamic Mesh
kn : number of control points representing a wing section

b. Reads the initial airfoil and then reproduces other members of the initial population from this airfoil by altering its thickness ratio.

c. Reads the initial grid file of the wing. (Onera M6)

2. Bezier: Calculates *y* coordinate values of the airfoil by using control points based on Bezier curve method.

3. Dynmesh : Modifies the grid according to the changes in the configuration of population members based on dynamic mesh method.

4. Nodind : This subroutine determines the type and neighbors of each node. Creates an array nodind (i,j) that i (1,npoin) is the node number in the parameter j (1,ndindmax). The first one shows the type of node that is 0,3,4, or 5 Meanings of these numbers are:

0 : the inner node
3 : wall node (nodes on the wing)
4 : nodes on the symmetry plane
5 : nodes on the farfield boundaries

Other j values (i.e. from 2 to "nodinmax") are the neighbor nodes of the node i.

5. Asop_Acer3d: This is an adapted ACER3D Euler flow solver to genetic algorithm optimization. A convergence criterion was added based on the experiences.

6. Fitn : This subroutine calculates the fitness values based on the fitness function (equations (4.1) and (4.3))

7. Sequencer : This code sequences the members of each generation according to mean chamber or taper ratio (if the taper ratio varies).

3.3.1.1 Input Files

Input.dat : Contains the parameters that subroutine input reads.

Om6n.grd : Initial wing grid file

Pop.dat : Contains the control points of the initial airfoil

Orj-xy.dat : Contains the number of points and x coordinates of the initial airfoil.

Casename.dat : Contains the names of grid, restart, output files for all members of a generation

Ndinb.dat : Contains the array "nodind" (If subroutine "nodind" is run once, there is no need to run for each member. It is enough to read from this file.)

3.3.1.2 Output Files :

Airfoils(i).dat : Wing section geometries of all members produced in each generation.

Elit(i).grd : Grid files of all the best members produced in each generation

Elit(i).out : Calculated pressure values and velocities of the best members.

Forces.dat : Calculated force vectors, lift and drag forces.

Hist.dat : Stores some useful parameters like airfoil coordinates, some calculated values to evaluate the process.

3.3.2 Symbols and Some Parameters

npoin : total number of point in the grid

nelem : total number of tetrahedral elements in whole domain

nboun : total number of tetrahedral elements on the boundaries

x, y, z : Cartesian coordinates of each point

p1, p2, p3, p4 : node numbers that form each tetrahedral element as shown in Figure 3.6

bc_index : boundary condition index of a boundary element in the grid data file, typical values are:

3 for inviscid wall

4 for symmetry plane

5 to 8 for far-field, inflow/outflow

3.4 Model

In 1972, the ONERA Aerodynamics Department designed a swept back wing very well instrumented to be used as an experimental support for basic studies of three-dimensional flows at high Reynolds numbers from low to transonic speeds.

In this study, as a test model the Onera M6, a well-known CFD verification wing, shown in Figure 3.4, **(Schmitt and Charpin, 1979)** has been chosen. The Onera M6 is a classic CFD validation wing for external flows because of its simple geometry combined with complexities of transonic flow (i.e. local supersonic flow, shocks, and turbulent boundary layers separation). It has almost been a standard for CFD codes because of its inclusion as a validation case in numerous CFD papers over the years. **(Slater, 2005)**

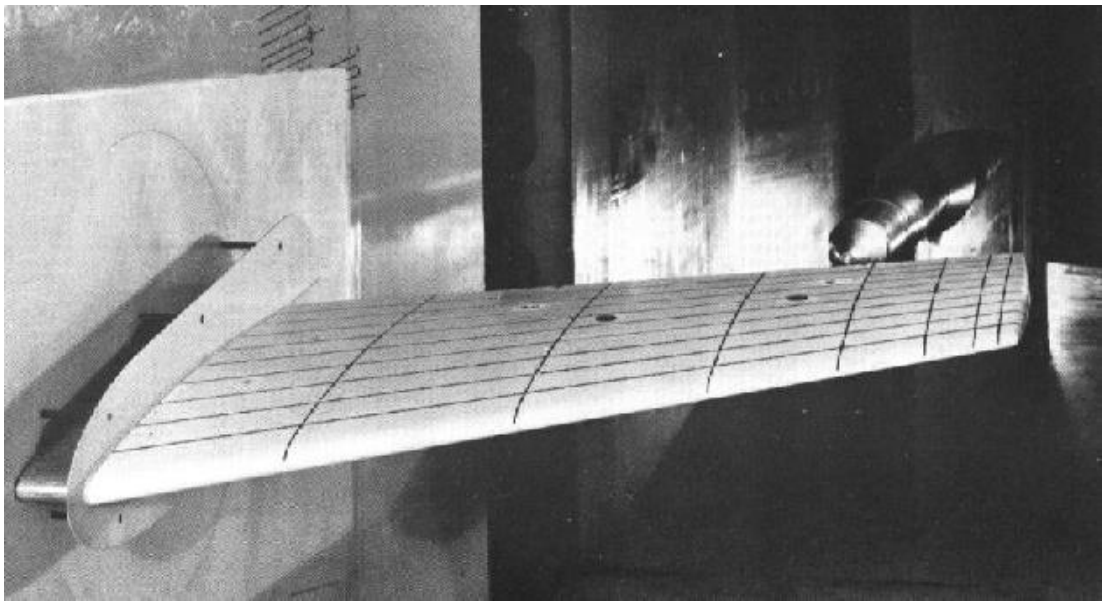

Figure 3.4 : Onera M6 wing **(Schmitt and Charpin, 1979)**

Wind tunnel data from this model called M6-wing have been constituting a good base both for computer program assessment and for understanding various flow phenomena like shock wave-boundary layer interaction or flow separation.

Some experimental data set obtained in the ONERA S2MA wind tunnel at Mach numbers of 0.7, 0.84, 0.88 and 0.92 for angles of attack up to 6 degrees and a Reynolds number of about 12 million is available in the literature. Some geometrical properties of Onera M6 are shown in Figure 3.5.

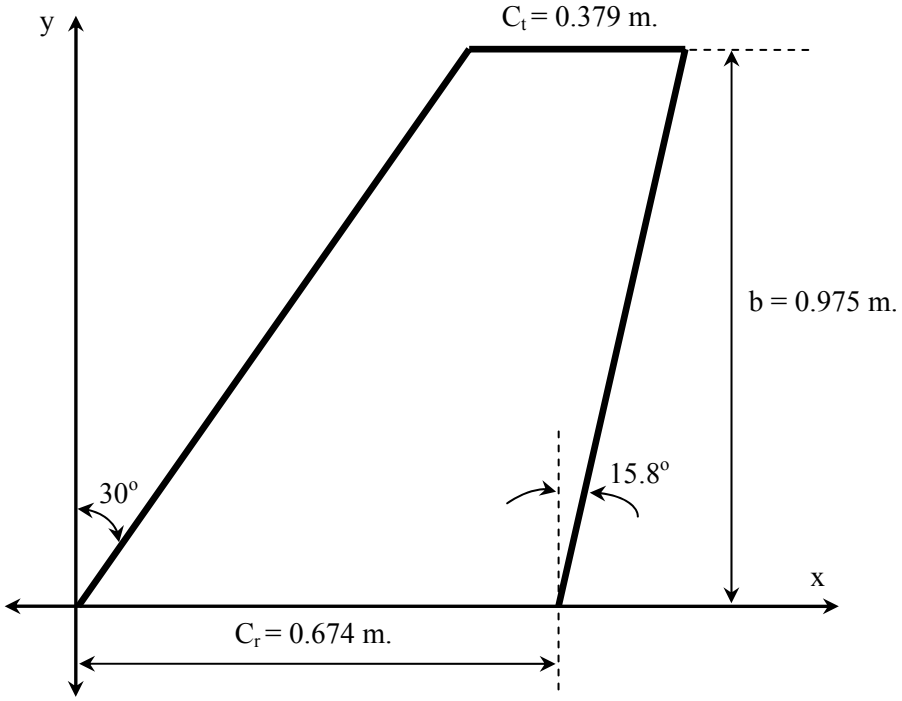

Figure 3.5 : Onera M6 wing

ONERA M6 wing uses symmetric airfoil using the ONERA D section. The geometrical parameters of ONERA-M6 wing is as follows:

Thickness Ratio = 0.098
Sweep Angle of Leading Edge = 30°
Sweep Angle of Trailing Edge =15.78°
Semi-span (b) = 0.975 m
Mean aerodynamic chord (c) = 0.5265 m
Root chord = 0.674 m
Tip chord = 0.379 m
Taper Ratio = 0.5625
Area, S = 0.52 m^2
Aspect Ratio= 3.8
Twist Angle = 0°

ONERA-M6 wing has been a subject for optimization studies and for code verification by several authors. This model was designed to be used for studies

of three-dimensional flows from low to transonic speeds at high Reynolds numbers. It is derived from the ONERA calibration model series M.

3.5 Grid Type

The Euler flow solver ACER3D does not have a mesh generator part. It needs an input mesh file in certain format shown below in Figure 3.6.

nelem *npoin* *nboun*

Coordinates { *x(1)* *y(1)* *z(1)* ... ... *x(npoin)* *y(npoin)* *z(npoin)*

Connectivity for each tetrahedral, at boundary { *p1(1)* *p2(1)* *p3(1)* *p4(1)* *bc_index(1)* ... ... *p1(nboun)* *p2(nboun)* *p3(nboun)* *p4(nboun)* *bc_index(nboun)*

Connectivity for each tetrahedral, in all domain { *p1(1)* *p2(1)* *p3(1)* *p4(1)* ... ... *p1(nelem)* *p2(nelem)* *p3(nelem)* *p4(nelem)*

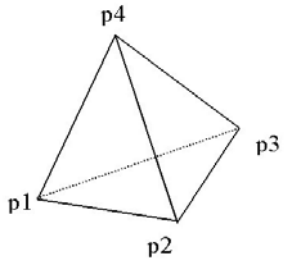

Figure 3.6 : Connectivity of a tetrahedral element

The triangle formed by nodes p1, p2, and p3 is base for boundary element and the apex is p4. bc_index is used to define faces and points that are lying on different boundary surfaces.

3.6 Flow Solver Structure

'**Acer3D**' is a flow solver program, which solves inviscid compressible Euler flow equations on unstructured tetrahedral grids. Serial and parallel versions together with parallel adaptive sensor program are developed in the Ph.D. thesis

study by Yılmaz **(Yilmaz, 2000)**. All programs were coded in FORTRAN language. Some basic features of flow solver are listed below.

- Finite volume space discretization
- Explicit time integration with multi-stage Runge-Kutta time stepping
- Unstructured tetrahedral cells
- 2^{nd} and 4^{th} order artificial dissipations
- Vertex-based scheme with overlapping cells
- Local time stepping
- Implicit residual averaging
- Enthalpy damping

ACER3D **(Yılmaz, 2001)** can read a restart file to carry the solution to further iterations. The restart file is the same as the output file but it must have ".in" extension, in place of ".out" extension. (i.e. "casename.in") Normally ACER3D produces an output file with ".out" extension. In order to restart the program from previous solution, this file must be renamed as ".in"

ACER3D has been run at restart mode at every time. The output part of the program has been modified to write a restart file. In each step, it writes a restart file for the next step. Therefore at the each step ACER3D restarts from the previous step.

This reduces the run time significantly. The CPU time reduces up to 4 times, owing to restarting from the previous solution.

3.7 Force Calculation Method

The flow solver calculates velocities and pressures at each node and writes an output file containing the velocities, pressures, Mach numbers and pressure coefficients on the wing points. From this file, pressure or velocity distributions can be post processed on the wing and symmetry plane or on any section of the flow domain.

However, in Genetic Algorithm, a fitness function must be developed to calculate fitness values of members. In order to define a fitness function, the aim

of the optimization process must be determined. In other words, parameters which are to be maximized or minimized must be determined. Usually, for a wing study case, lift force or lift to drag ratio is tried to be maximized. Besides, the drag force can be minimized with some constraints. Therefore the calculation of the forces acting on the wing is needed.

In order to calculate the forces acting on the wing, pressure values on each element on the wing must be integrated. For this purpose, a subroutine code has been constructed based on a finite element method as in **(Mecitoğlu and Dökmeci 1990)**.

In this method, a local coordinate system is defined for the triangular side of each tetrahedral wall boundary element on the wing. The coordinate systems and unit vectors chosen are shown below in Figure 3.7.

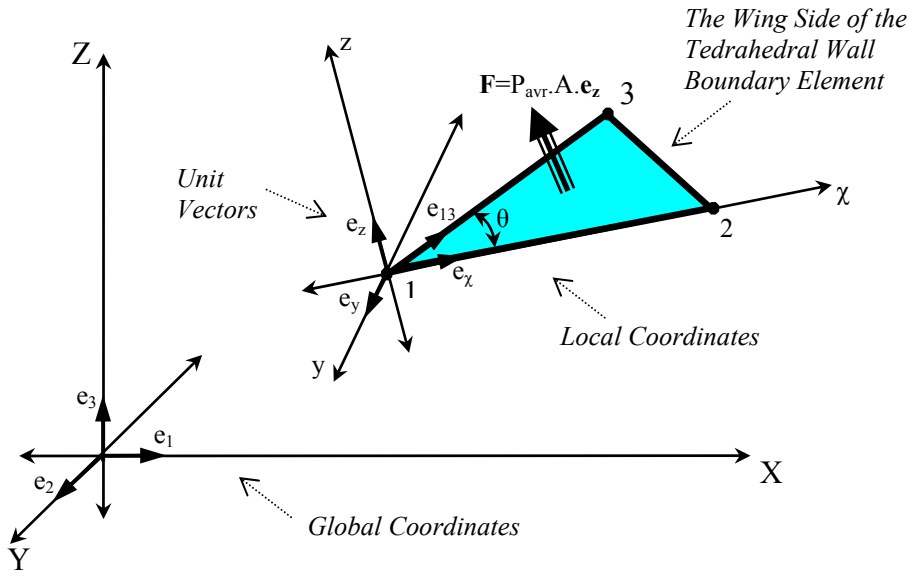

Figure 3.7 : Force calculation method

From the picture, the unit vectors in the local coordinates can be defined as:

$$\vec{e_x} = \frac{x_{21}}{L_{21}}\vec{e_1} + \frac{y_{21}}{L_{21}}\vec{e_2} + \frac{z_{21}}{L_{21}}\vec{e_3} \tag{3.4}$$

$$\overrightarrow{e_{13}} = \frac{x_{31}}{L_{31}}\overrightarrow{e_1} + \frac{y_{31}}{L_{31}}\overrightarrow{e_2} + \frac{z_{31}}{L_{31}}\overrightarrow{e_3} \tag{3.5}$$

The differentials shown in the formulas are defined as:

$$x_{21} = x_2 - x_1 \qquad L_{21} = \sqrt{x_{21}^2 + y_{21}^2 + z_{21}^2} \tag{3.6}$$

Unit vector in the z direction is:

$$\overrightarrow{e_z} = \frac{\overrightarrow{e_x} \times \overrightarrow{e_{13}}}{\sin\theta} \tag{3.7}$$

That is:

$$\overrightarrow{e_z} = \frac{1}{L_{21}L_{31}\sin\theta}\left[(y_{21}z_{31} - y_{31}z_{21})\overrightarrow{e_1} + (z_{21}x_{31} - z_{31}x_{21})\overrightarrow{e_2} + (x_{21}y_{31} - x_{31}y_{21})\overrightarrow{e_3}\right] \tag{3.8}$$

Note that by using this formula, the unit vector in local z direction can be calculated in terms of the global unit vectors. Then the force vector can be calculated as:

$$\overrightarrow{F} = P_{avr}.A.\overrightarrow{e_z} \tag{3.9}$$

Because the differences between the pressure values at the corner nodes are not much, therefore the pressure on the triangular area can be taken as the average pressure:

$$P_{avr} = \frac{1}{3}(P_1 + P_2 + P_3) \tag{3.10}$$

The area of the triangle can be calculated by using the lengths of its sides:

$$A = \sqrt{u(u - L_{21})(u - L_{32})(u - L_{31})} \tag{3.11}$$

$$u = \frac{1}{2}(L_{21} + L_{32} + L_{31}) \tag{3.12}$$

ACER3D uses non – dimensional parameters like:

$$P_{nd} = \frac{\rho_{nd} U_{nd}^2}{\gamma M^2} = \frac{\rho U^2}{\rho_\infty U_\infty^2} \cdot \frac{1}{\gamma M^2} \qquad \rho_{nd} = \frac{\rho}{\rho_\infty} \qquad U_{nd} = \frac{U}{U_\infty} \tag{3.13}$$

Note that the subscript nd indicates non-dimensional values. Hence the lift force becomes:

$$L = L_c . \rho_\infty U_\infty^2 \tag{3.14}$$

Where, L_c is the calculated lift force by integration of non-dimensional pressure values. Hence the lift coefficient can be calculated as:

$$\frac{c_L}{2} \rho_\infty U_\infty^2 S = L_c \rho_\infty U_\infty^2 \qquad \Rightarrow \qquad c_L = \frac{2L_c}{S} \tag{3.15}$$

3.8 Parallel Processing Essence

The solution of a flow condition by using the Euler flow solver ACER3D takes approximately 10 hours with a 1.3 GHz. Pentium – IV processor. Normally an optimization process with a Genetic Algorithm needs approximately 30 - 100 iterations (generations) each of which has 12 - 30 population members. This means that the whole process would take 5-40 months which is a tremendous time for an optimization process and not feasible.

This is not an acceptable time to get the results and analyze them. It must be reduced significantly, in order to have an efficient optimization process. Reducing this time can be possible by using the previous results as a re-starting point, by using the dynamic mesh method to modify the mesh and parallel processing.

Main structure of the parallel processing is shown in Figure 3.8. In serial calculations flow solutions take approximately 95 % of the total time. By making this portion of the calculation parallel, the total calculation time can be reduced up to 7 times.

The program starts as if serial. The processor zero reads input data, calculates the new airfoil coordinates and the new mesh structures by using dynamic mesh method. The other 13 processors go to just before the flow solution and wait the processor zero.

After all mesh structures are calculated and written in the separate files, all processors start to solve the flow parameters of each mesh structure. 14 processors solve 14 new mesh structures of 14 new members of the current generation. Each processor writes the result file of each member. Later the processor zero calculates forces; fitness values for all members and performs genetic operations (crossover, mutation etc.) while the other 13 processors wait for the next step of the flow solution. The program repeats this procedure for each generation. Any communication and synchronization between the processors are done using the MPI library which has parallel functions or subroutines. **(Tai, 2004)** The code is run on a SUN parallel computer having 64GB RAM and 32 CPUs. **(Vatandaş et al., 2004e)**

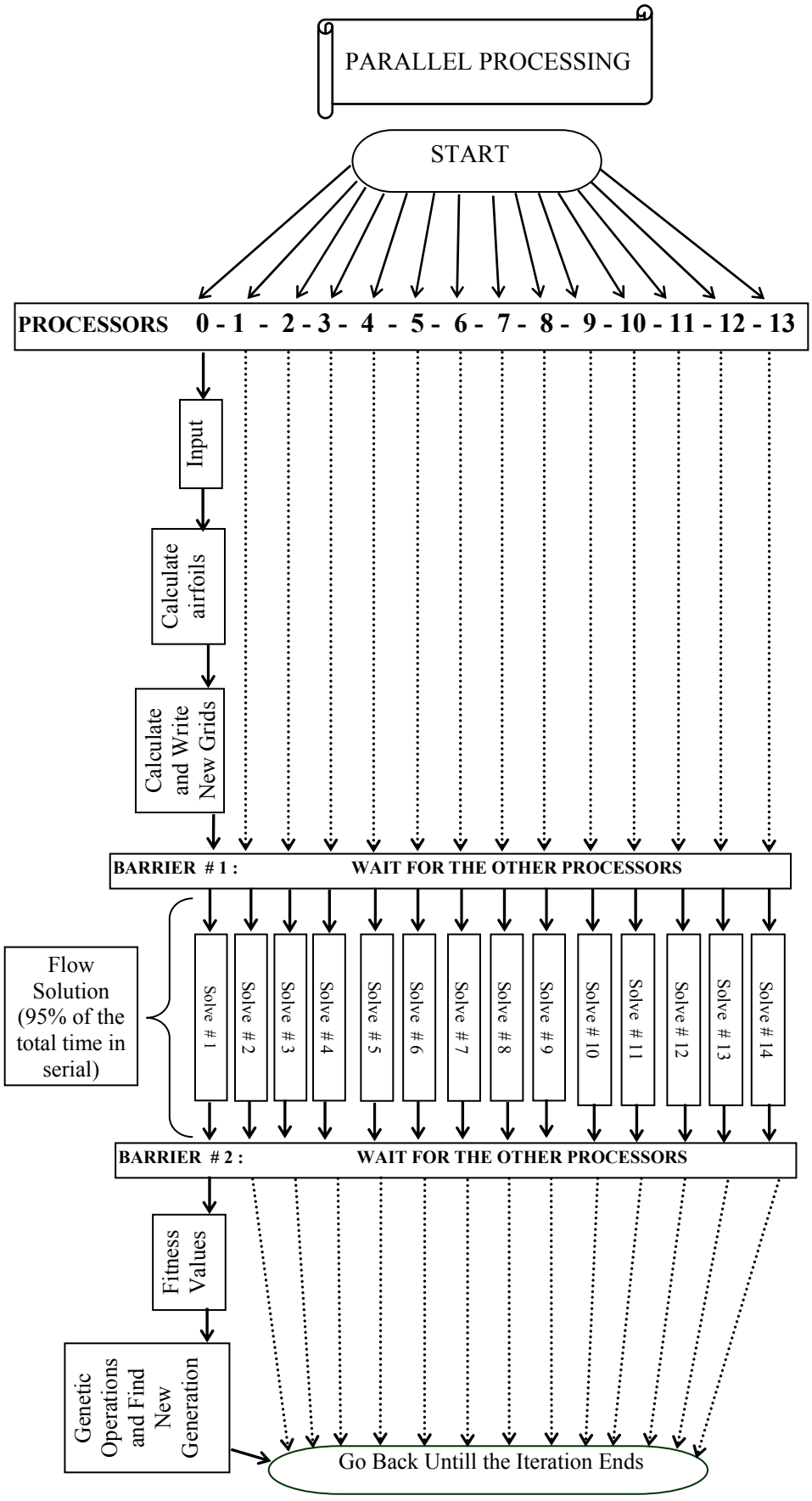

Figure 3.8 : Main outline of the parallel processing

3.9 Design Criteria

In the application of the developed process in this work, Onera M6 wing has been chosen. This wing has been used in the verification of CFD codes (ONERA). The aim of the optimization process is to minimize the inviscid drag force while holding the lift force approximately at the same level of the original (or design) lift value. At the second stage the thickness ratio was also held fixed, at the third stage the taper ratio was added to the design variables.

The flow conditions are:

Mach Number: 0.84

Angle of Attack: 3.04

Initial (starting) Model: Onera M6 Wing

Thickness Ratio: 9.79243E-02

Taper Ratio: 0.562315

Original (Design) Lift Force (calculated from non-dimensional pressure values): 3.278321E-03

Original Drag Force (calculated from non-dimensional pressure values): 7.386871E-02

Original (Design) Lift Coefficient: 0,2841

Original Drag Coefficient: 0,0126

4. RESULTS AND DISCUSSIONS

4.1 Design without Thickness Ratio Constraint

4.1.1 Progress in the Generations

In the optimization process, there are 14 members in each generation. These are 14 Onera M6 wing planforms that have different wing sections. All of them are solved by using ACER3D and their lift and drag forces are calculated.

By using these forces, the fitness values are calculated for each member. The fitness function is taken as:

$$f(i) = C_D + a(C_L - C_{Ld})^2 \quad (4.1)$$

$$\text{fitness value} = 1/f(i) \quad (4.2)$$

C_D : Drag coefficient calculated

C_L : Lift coefficient calculated

C_{Ld} : Design lift coefficient (The calculated lift coefficients are desired to be close to this value)

a : Constant parameter to define the weight of the lift coefficient constraint

As it can be seen from the above formula (equation (4.1) and (4.2)), if the drag coefficient is getting higher or the lift coefficient is diverging from the design lift coefficient determined before, the fitness value becomes lower.

The average fitness value for each generation and the maximum fitness value (i.e. the best member found in that generation) are shown in Figure 4.1.

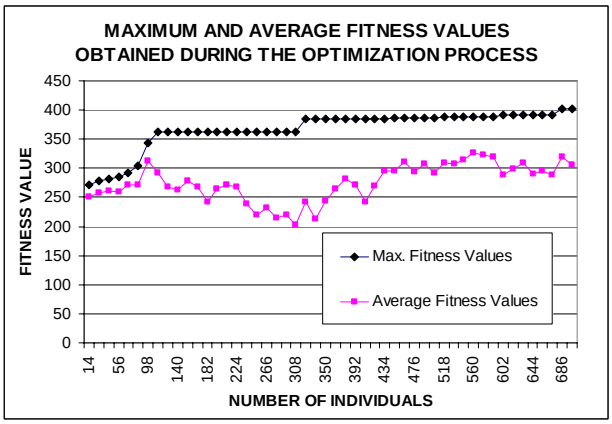

Figure 4.1 : Change in the average fitness and the development of the maximum fitness value

The average fitness value shown in Figure 4.1 can be altered in different ways. The important parameter is the maximum fitness value (or the best member) obtained in each generation.

The best member is kept in each generation and carried into the next generation. So the best member found in each generation can not be worse than the best member of the previous generation.

ACER3D calculates non-dimensional pressure values on all mesh nodes. These pressure values are then integrated and drag force is calculated. The progress of calculated drag forces for the best member of each generation is illustrated in Figure 4.2**.**

The fitness function in equation (4.1) is arranged so that the lift force can be held fixed. However depending on the weighting constant a, there may be slight changes in the lift forces. As it can be seen in Figure 4.3, these changes are kept in a small interval.

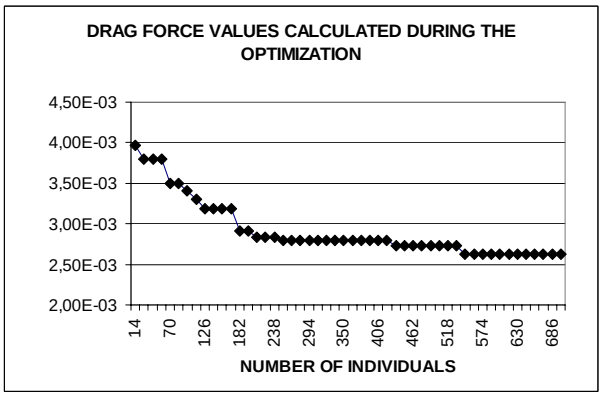

Figure 4.2 : Change in the drag force calculated from non-dimensional pressure values

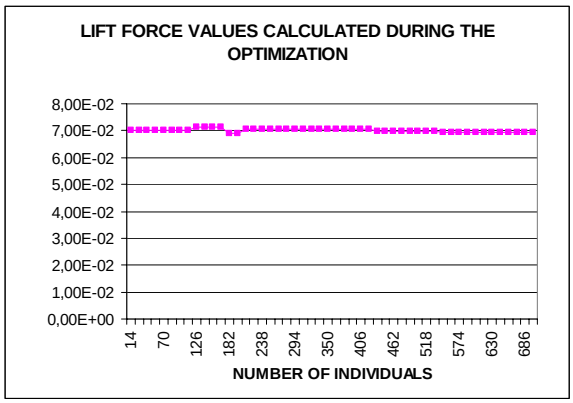

Figure 4.3 : Change in the dimensionless lift calculated from non-dimensional pressure values during the optimization

For the initial population, the wing section of Onera M6 is reproduced by altering its thickness ratio. The initial population is shown in Figure 4.4.

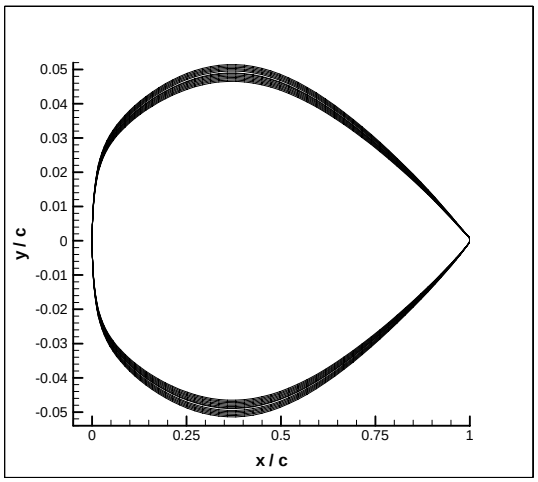

Figure 4.4 : Wing sections of the initial population (14 members)

In the following stages, the wing sections are reproduced according to their fitness values based on the genetic processes (crossover, mutation etc.). For instance, the wing sections found in 22^{th}, and 50^{th} generations are shown in Figure 4.5 and Figure 4.6 respectively.

In these figures, airfoils are exaggerated in y-axis, in order to make the small differences noticeable between the airfoils.

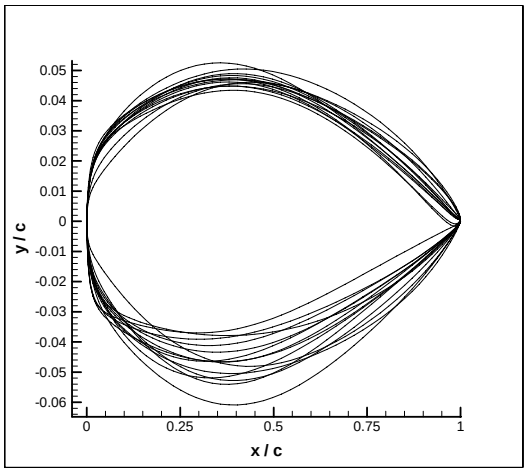

Figure 4.5 : Wing sections found in the 22th population (14 members)

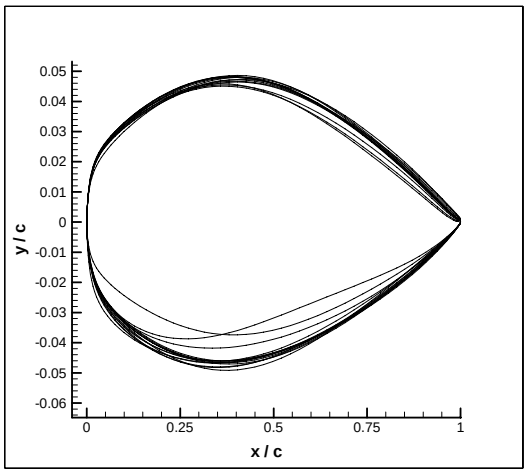

Figure 4.6 : Wing sections of the 50th population (14 members)

4.1.2 Change in Mesh Structures

The unstructured tetrahedral mesh is modified according to the change in wing section by using dynamic mesh technique and the new mesh structures are calculated for all members of a generation. For instance, the meshes calculated for the initial and the best member wing sections are shown in Figure 4.7 and Figure 4.8.

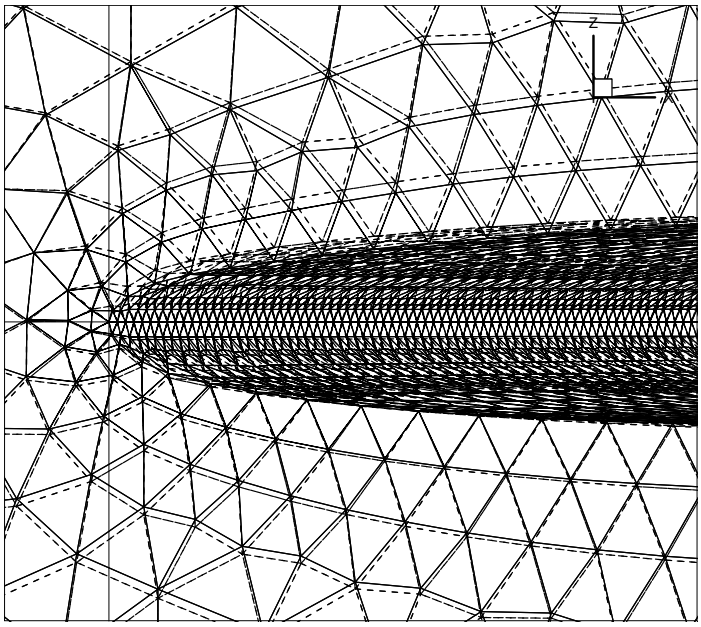

Figure 4.7 : The mesh structures of the initial (dashed line) and the best wing found at the 50th population (solid line)

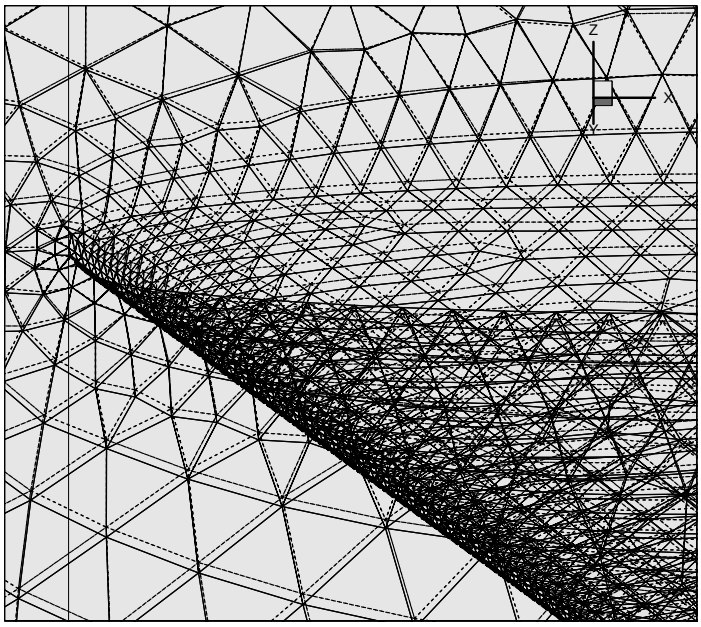

Figure 4.8 : The mesh structures of the initial (dashed line) and the best wing found at the 50th population (solid line)

4.1.3 Change in the Pressure Distribution

In Figure 4.9, the differences between pressure coefficient distributions of the initial wing and the best member produced in the 50^{th} generation can be seen.

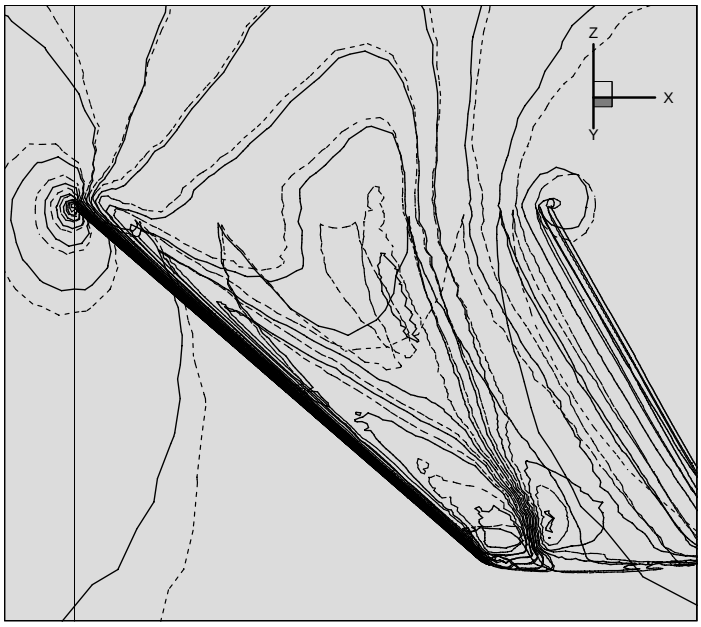

Figure 4.9 : The Cp distributions of the initial (dashed line) and the best wing found at the 50th population (solid line)

The Cp and Mach number distributions over the root sections of the initial wing and the wing obtained at the 50th step are shown in Figure 4.10 and Figure 4.11 respectively.

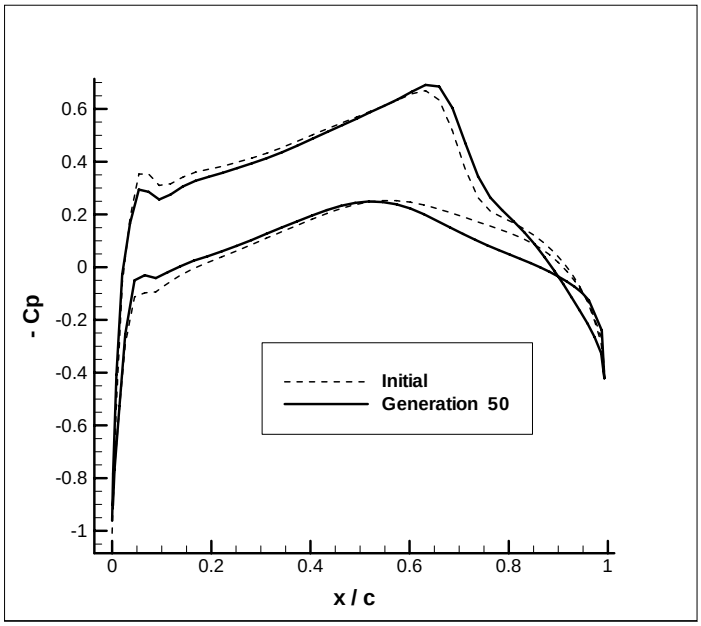

Figure 4.10: The Cp distributions of the initial and the best wing found at the 50th population over the root section

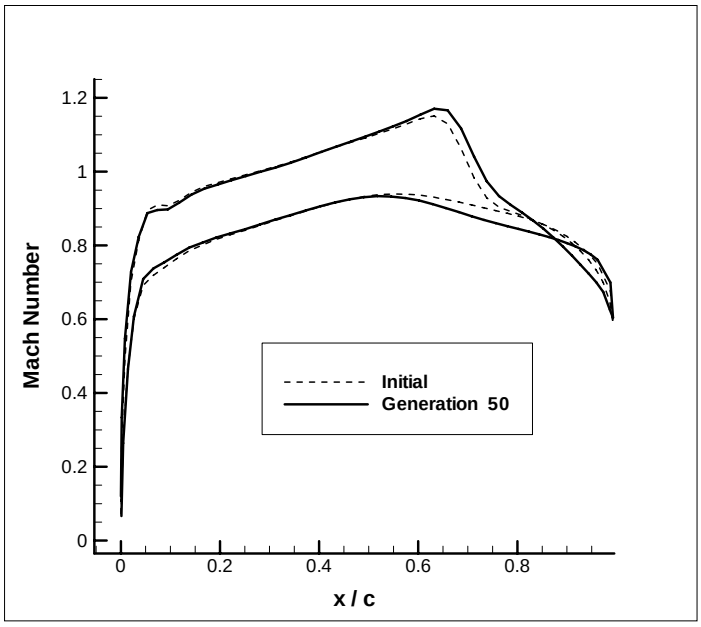

Figure 4.11: The Mach number distributions of the initial and the best wing found at the 50th population over the root section

The Cp distribution changes over the wing sections at the stations 0.44b and 0.8b are shown in Figure 4.12 and Figure 4.13 respectively.

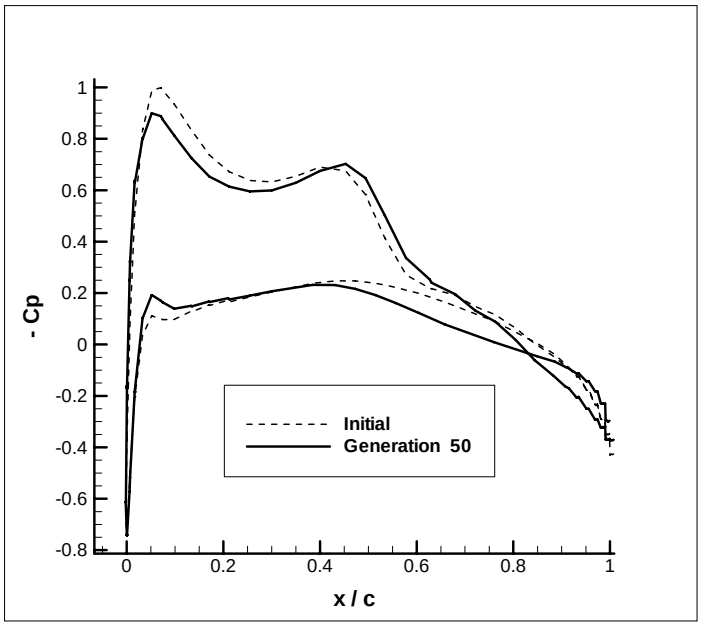

Figure 4.12: The Cp distributions of the initial and the best wing found at the 50th population over the section at 0.44b

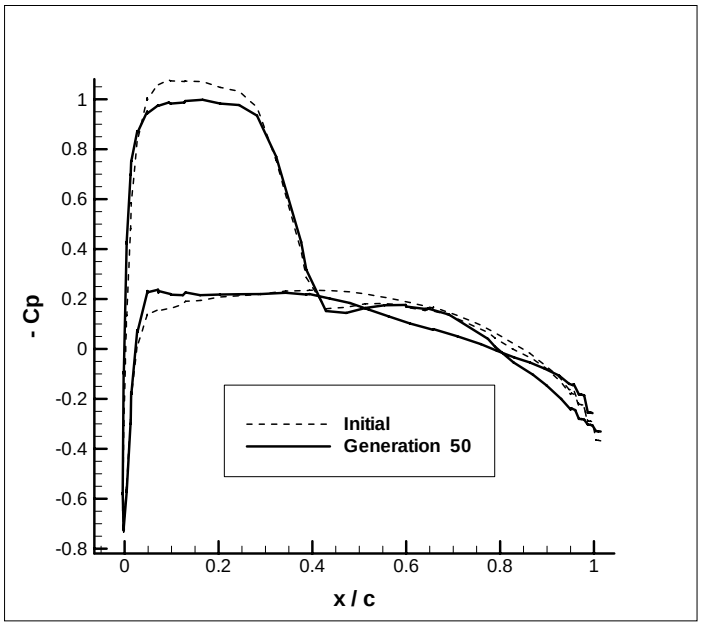

Figure 4.13: The Cp distributions of the initial and the best wing found at the 50th population over the section at 0.8b

4.1.4 The Best Wing Section Geometries Found by Genetic Processes

In Figure 4.14 the best members obtained in different stages are shown. It can be seen from this figure that the wing section has become thinner. This figure is also exaggerated in y direction to make the small differences between wing sections visible.

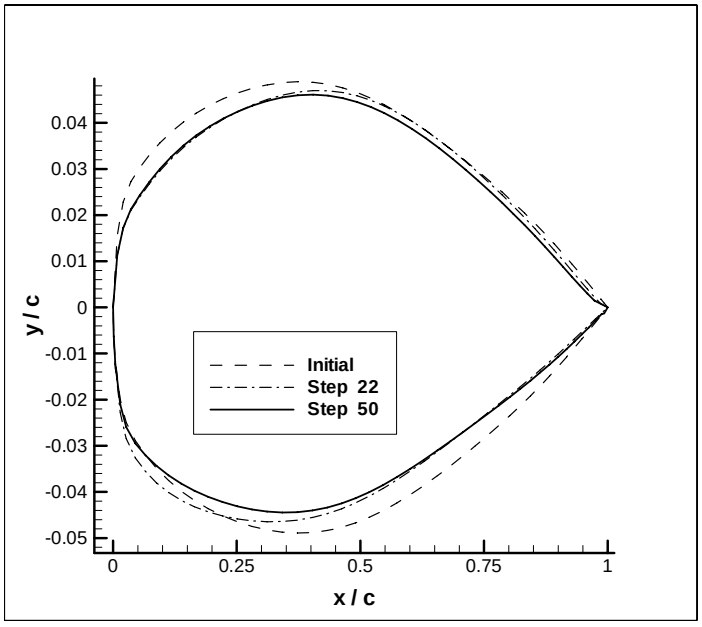

Figure 4.14: Wing sections of the initial and the best members found at the steps 22 and 50

During this process the lift coefficient has been tried to be held fixed, while the drag coefficient has been reduced about 25 percent. The best wing section obtained at the 50^{th} generation is shown one to one scale in Figure 4.15.

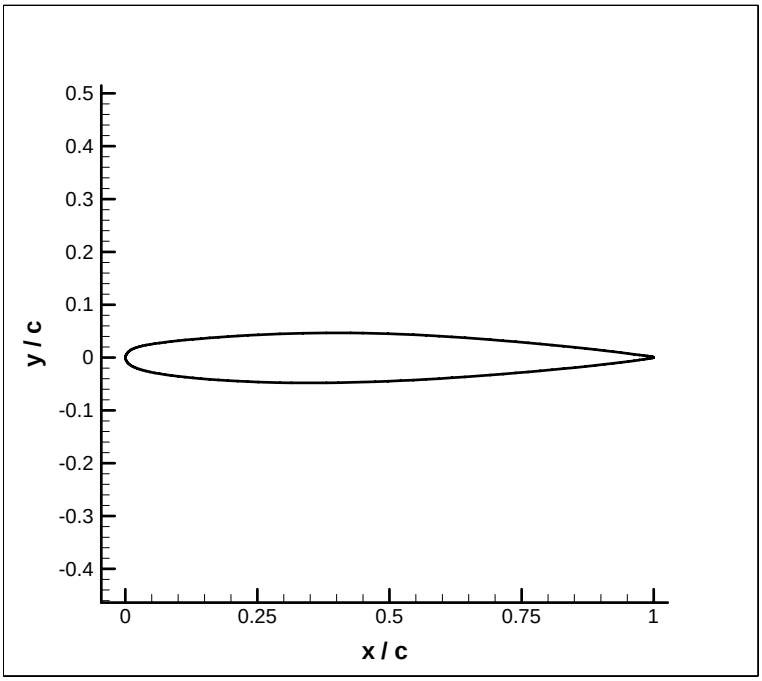

Figure 4.15: Wing section of the best member found (at normal scale).

It can be thought that decreasing the drag force without holding the thickness ratio and letting the wing section become thinner is an easy way of this kind of work. However, this application has been performed to see if the optimization process is working in the expected direction.

4.2 Results with Thickness Ratio Constraint

4.2.1 Progress in Generations

In this application, there are also 14 members i.e. 14 Onera M6 wing planforms that have different wing sections in each generation. All of them are solved by using the Euler flow solver ACER3D and their lift and drag forces are calculated. In this part, thickness ratios are also calculated for all members.

The original thickness ratio of Onera M6 wing is taken as design thickness ratio value. The fitness function is determined such a way that the process would keep the best member around design lift and thickness ratio values as shown in the following equation.

$$f(i) = C_D + a(C_L - C_{Ld})^2 + b\,(Th - Th_d)^2 \quad (4.3)$$

$$\text{fitness value} = 1/f(i) \quad (4.4)$$

C_D : Drag coefficient calculated

C_L : Lift coefficient calculated

C_{Ld} : Design lift coefficient

a : Constant parameter to define the weight of the lift coefficient constraint

Th : Thickness ratio of the produced wings

Th_d : Design thickness ratio

b : Constant parameter to define the weight of the thickness ratio constraint

As it can be seen from the formula, if the drag coefficient is getting higher or the lift coefficient and thickness ratio are diverging from the design lift coefficient and thickness ratio determined before, the fitness value becomes lower.

The average fitness value for each generation and the maximum fitness value (i.e. the best member found in that generation) are shown in Figure 4.16.

The improvement in drag force during the optimization process is shown in Figure 4.17. Because of the fitness function, the code searches for new members that have thickness ratios and lift forces close to the original (or design) values. Therefore both the thickness ratio and lift force remain almost unchanged as shown in Figure 4.18**.**

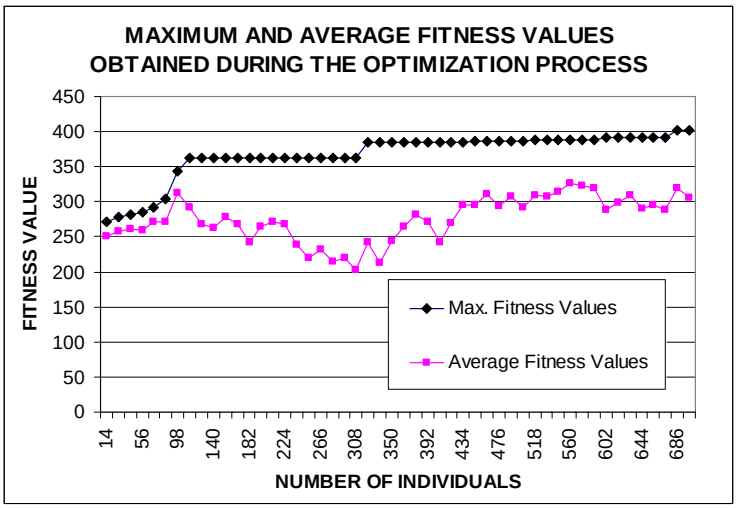

Figure 4.16: Change in the average fitness and the development of the maximum fitness value

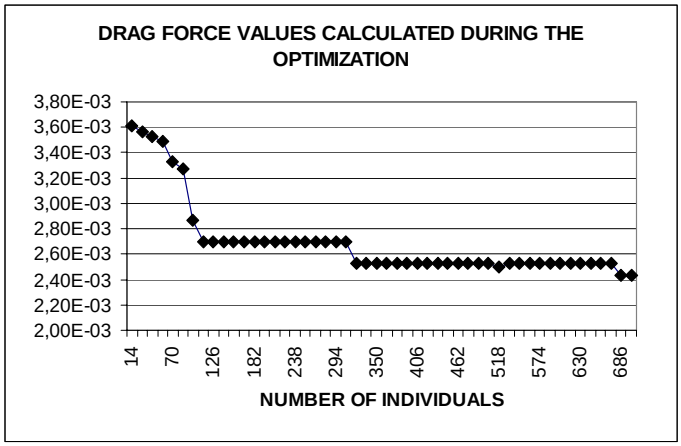

Figure 4.17: Change in the drag force calculated from non-dimensional pressure values

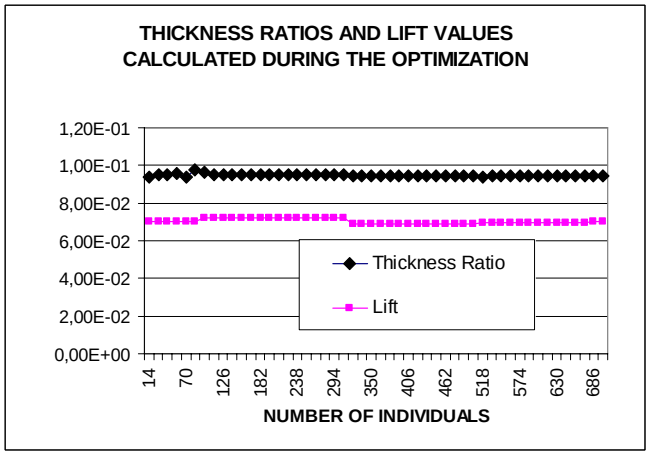

Figure 4.18: Change in the lift calculated from non-dimensional pressure values during the optimization

The wing sections found in each generation can alter in different ways as shown in Figure 4.19 and Figure 4.20 as the genetic process is searching the better fitted members.

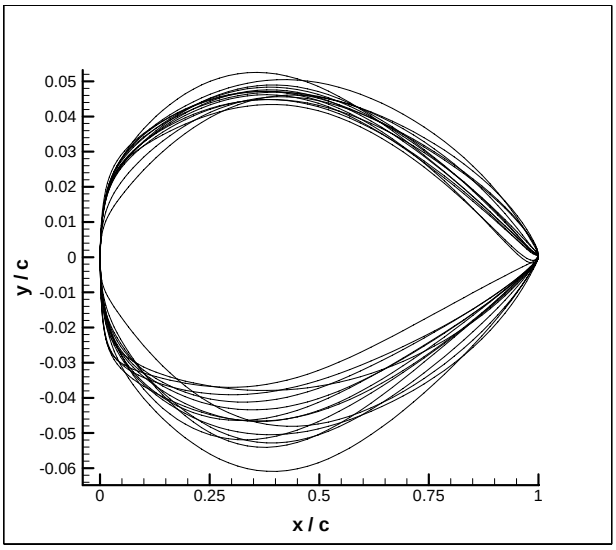

Figure 4.19: Wing sections of the 22th population (14 members)

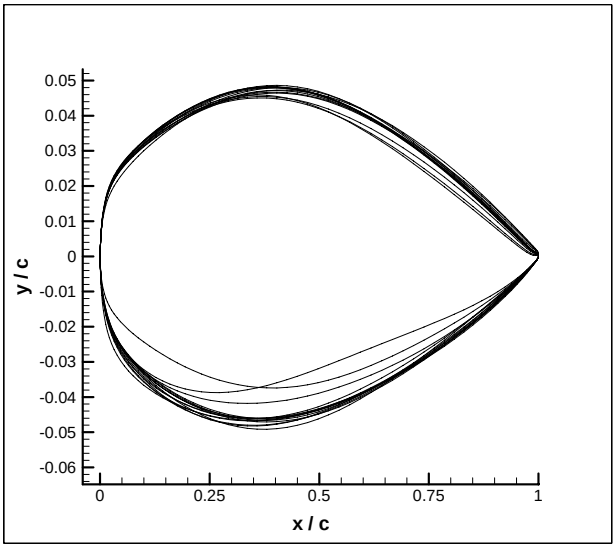

Figure 4.20: Wing sections of the 50th population (14 members)

4.2.2 Mesh Structures Modification

The changes in mesh structures are very small due to the small changes in wing sections (Figure 4.21).

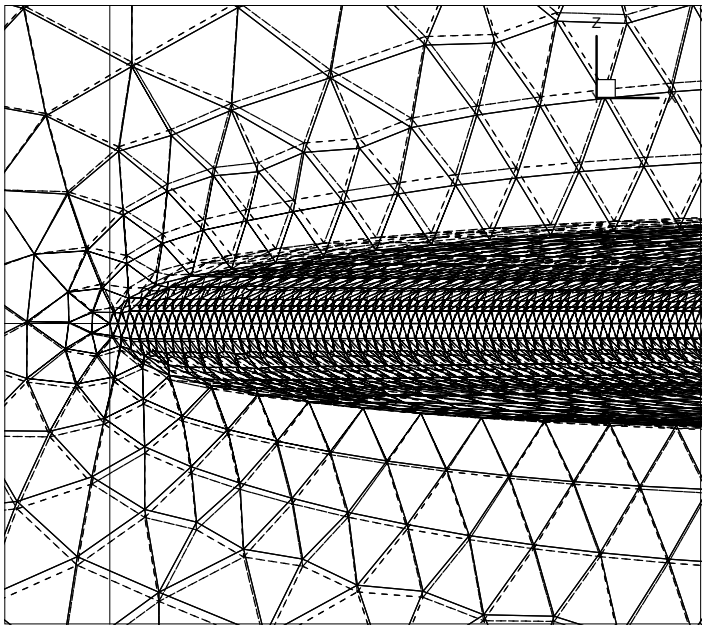

Figure 4.21: The mesh structures of the initial (dashed line) and the best wing found at the 50th population (solid line)

4.2.3 Progress in the Pressure Distributions

The Cp distribution contours are shown in Figure 4.22 in a 3-D view. Cp and Mach number distribution over the root sections are shown in Figure 4.23 and Figure 4.24 respectively.

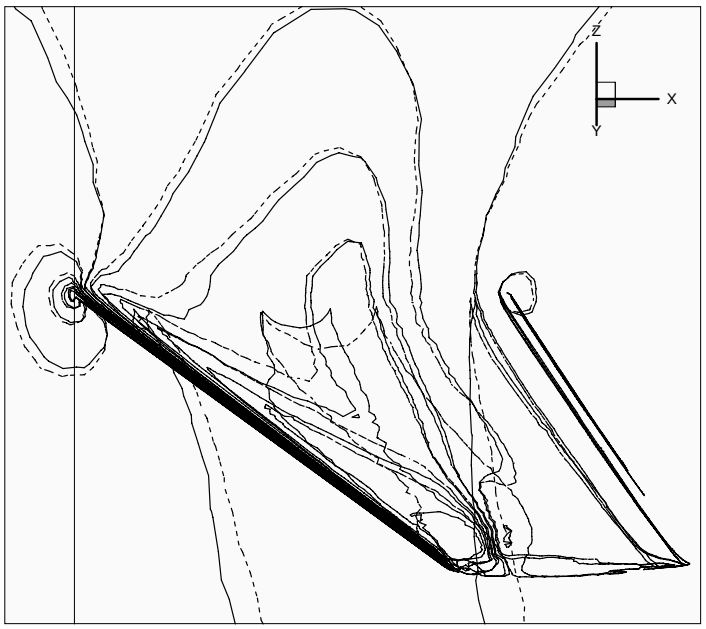

Figure 4.22: The Cp distributions of the initial (dashed line) and the best wing found at the 50th population (solid line)

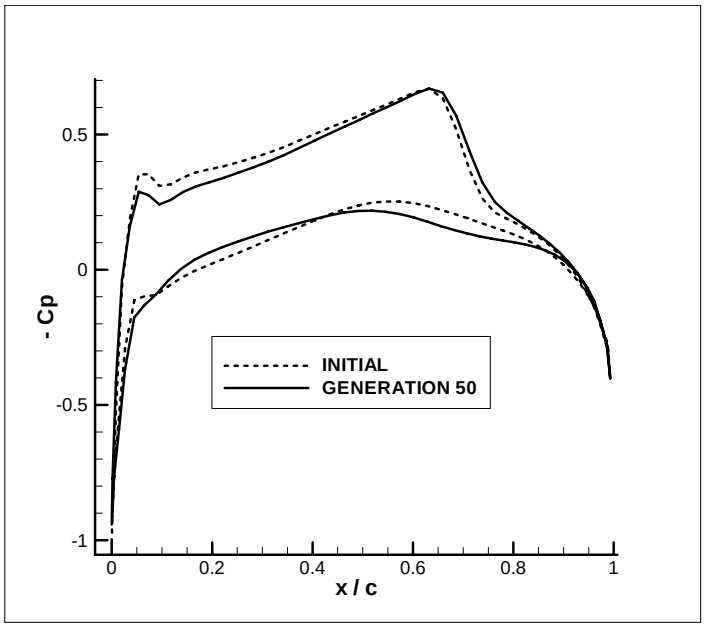

Figure 4.23: The Cp distributions of the initial and the best wing found at the 50th population over the root section

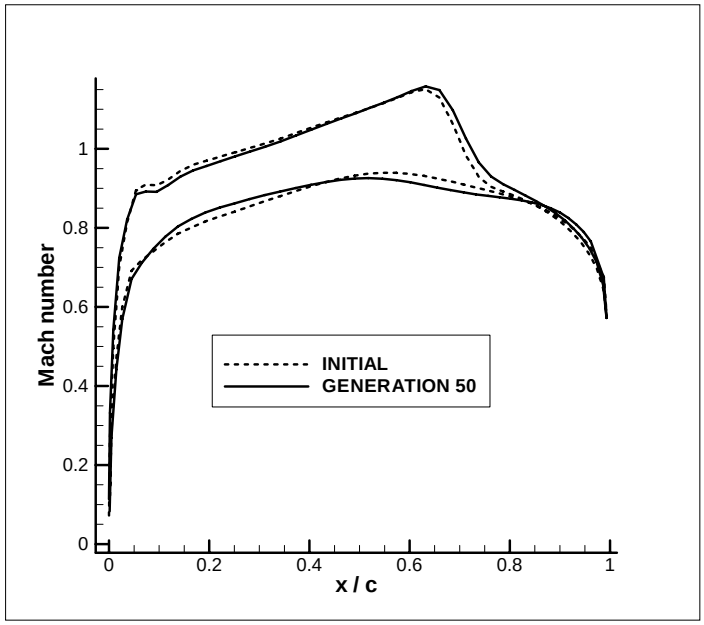

Figure 4.24: The Mach number distributions of the initial and the best wing found at the 50th population over the root section

The Cp distributions over the sections at the stations 0.2b, 0.44b and 0.8b are shown in Figure 4.25, Figure 4.26 and Figure 4.27 respectively.

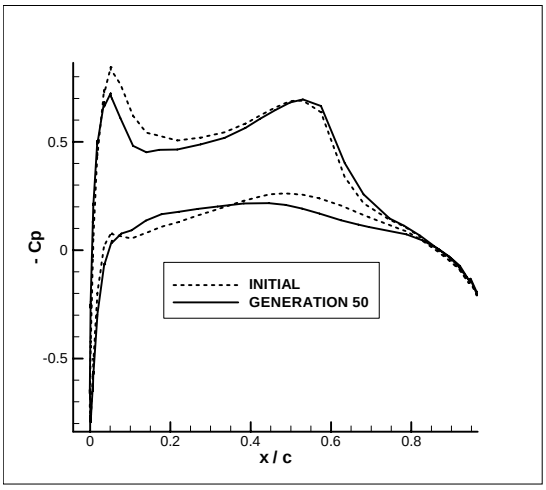

Figure 4.25: The Cp distributions of the initial and the best wing found at the 50th population over the section at 0.2b

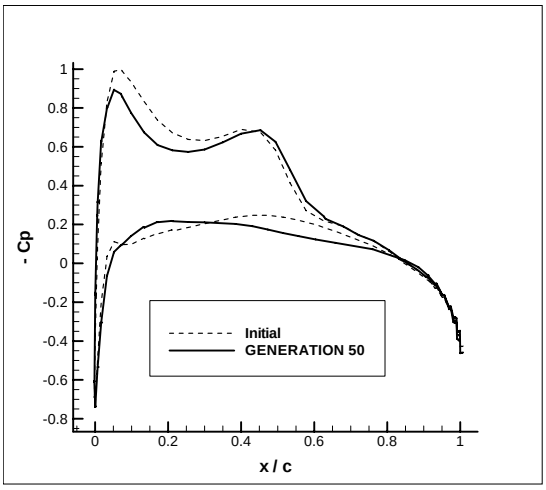

Figure 4.26: The Cp distributions of the initial and the best wing found at the 50th population over the section at 0.44b

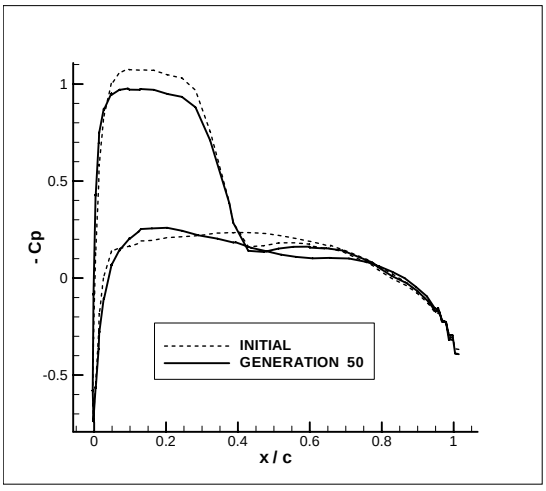

Figure 4.27: The Cp distributions of the initial and the best wing found at the 50th population over the section at 0.8b

4.2.4 The Best Wing Sections Found by Genetic Processes

In Figure 4.28, the best members calculated in different generations are shown. In Figure 4.29, the best members obtained in different stages -with and without thickness ratio constraint- are shown. In Figure 4.29, it can be seen that the wing section has become much thinner in the optimization process without thickness ratio constraint. In Figure 4.30, the last obtained wing section in the optimization process is shown at its normal scale.

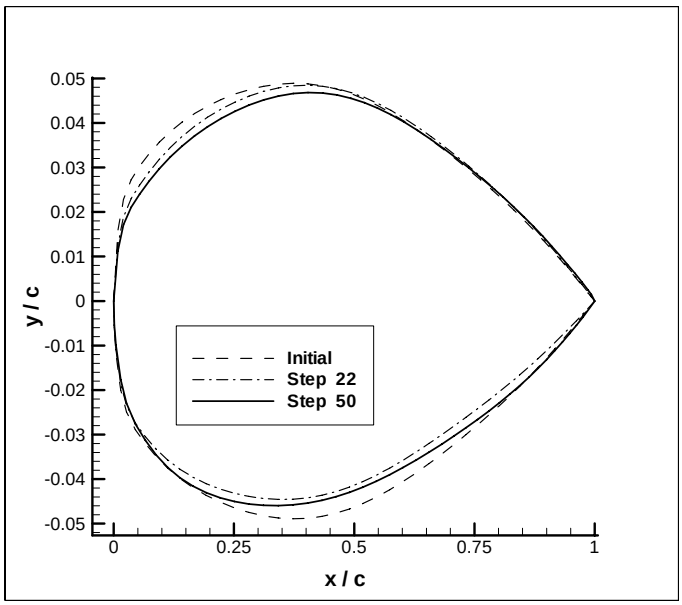

Figure 4.28: The best members found at the different stages (with thickness ratio constraint)

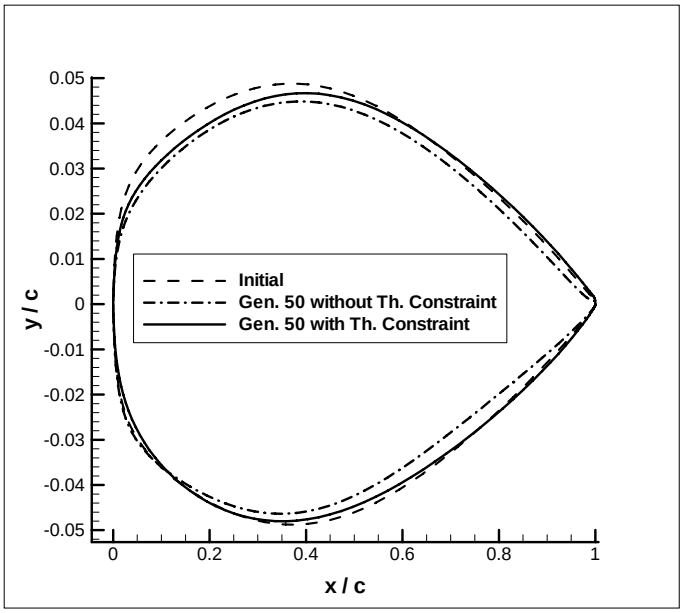

Figure 4.29: Wing sections of the initial and the best members found at the step 50 without and with thickness ratio constraint

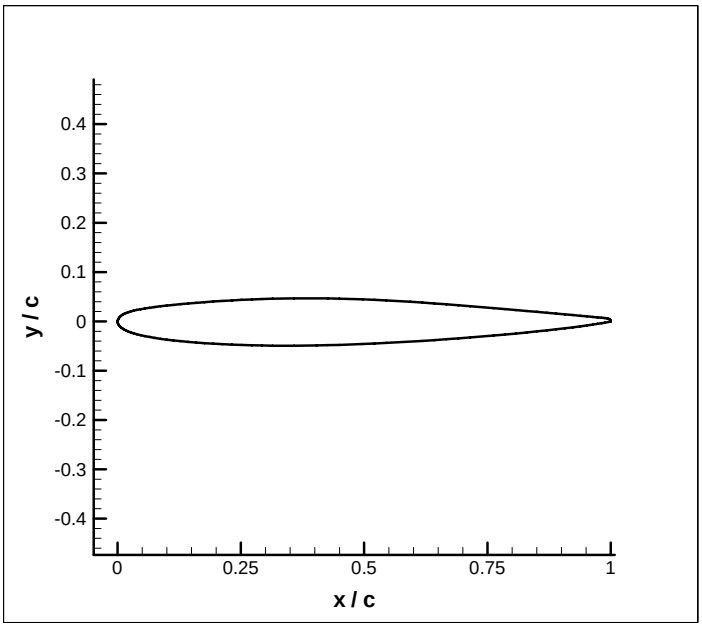

Figure 4.30: Wing section of the best member found (at normal scale)

As it can be seen in Figure 4.29 the thickness of the wing is a little lowered even with a thickness ratio constraint. This is avoidable by adjusting the weighting constant (i.e. b) of the thickness ratio in the fitness function. However, there is a cost of this. Much more generations would possibly be needed to achieve a good solution.

4.3 Solution with Thickness Ratio Constraint and Design Variable Taper Ratio

4.3.1 Improvement in the Generations

In this part of the optimization, the taper ratios of the wings are added as a design variable to the process. This addition was made to control points which define each member. Therefore taper ratio of each wing becomes a gene in its chromosomes. Thus, fitness function for this stage is the same as previous one.

$$f(i) = C_D + a(C_L - C_{Ld})^2 + b(Th - Th_d)^2 \quad (4.5)$$

$$\text{fitness value} = 1/f(i) \quad (4.6)$$

C_D : Drag coefficient calculated

C_L : Lift coefficient calculated

C_{Ld} : Design lift coefficient

a : Constant parameter to define the weight of the lift coefficient constraint

Th : Thickness ratio of the produced wings

Th_d : Design thickness ratio

b : Constant parameter to define the weight of the thickness ratio constraint

As it can be seen from the formula as in the previous application, if the drag coefficient is getting higher or the lift coefficient and thickness ratio are diverging from the design lift coefficient and thickness ratio determined before, the fitness value becomes lower.

The average fitness value for each generation and the maximum fitness value (i.e. the best member found in that generation) are shown in Figure 4.31.

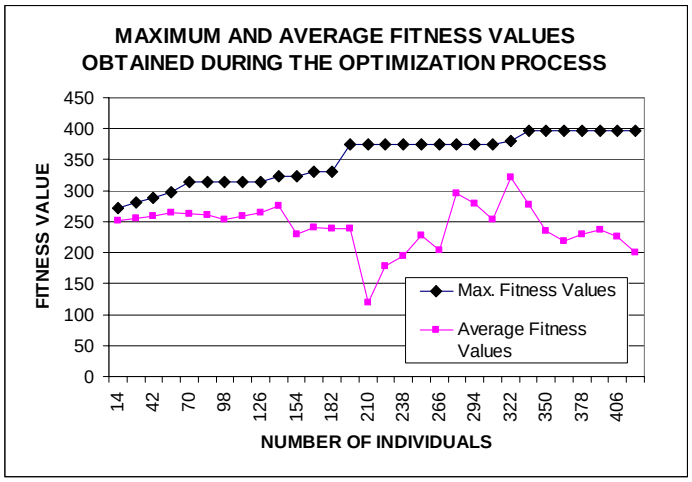

Figure 4.31: Change in the average fitness and the development of the maximum fitness value

As the same as before, the maximum fitness value cannot be lowered because of elitism. The drag force improvement shown in Figure 4.32 is more rapid at the initial steps with the variable taper ratio. Drag forces reach almost the same values at the end with and without a taper ratio design variable. However with a taper ratio design variable it reaches a converged level about 30% faster. As it can be seen in Figure 4.33, lift values and thickness ratios again remain in a small interval.

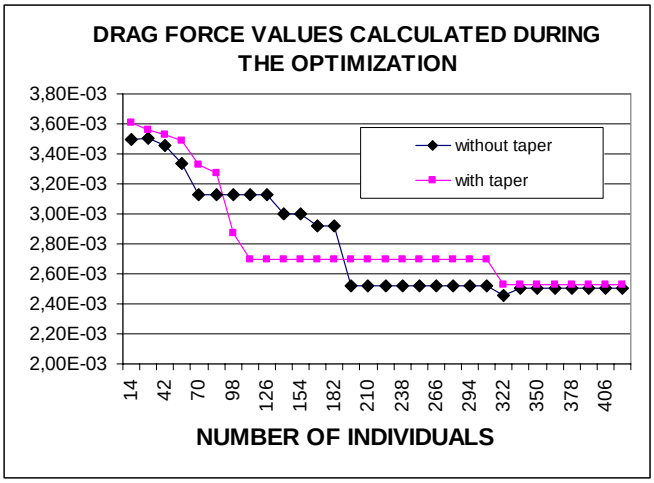

Figure 4.32: Progresses in the drag forces calculated from non-dimensional pressure values with and without a taper ratio design variable

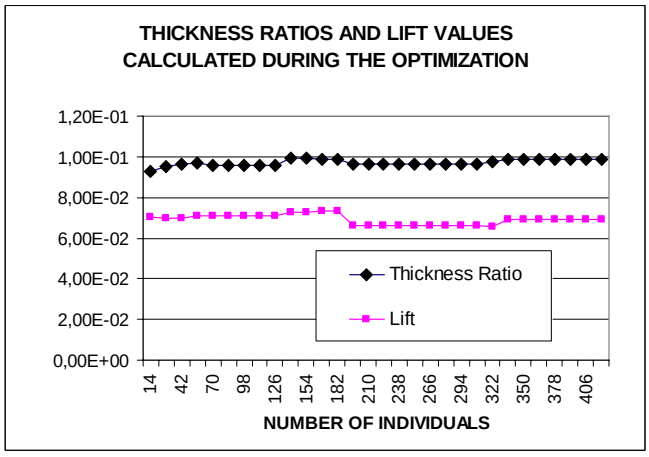

Figure 4.33: Change in the thickness ratio and the lift force

History of taper ratios found for the best members of each generation is shown in Figure 4.34.

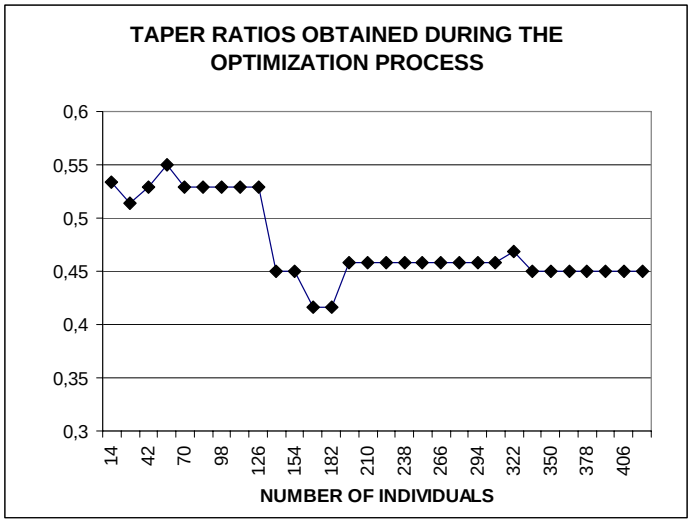

Figure 4.34: History of the taper ratios calculated during the optimization process

The taper ratio is reduced as expected. However, it cannot be dropped to much less values. An increase is observed at the later steps. Because the process is not only trying to minimize the drag force, but it is also trying to keep the lift force close to the original level.

In the initial population, the wing section of Onera M6 is reproduced by changing its thickness ratio. The initial population is shown in Figure 4.35.

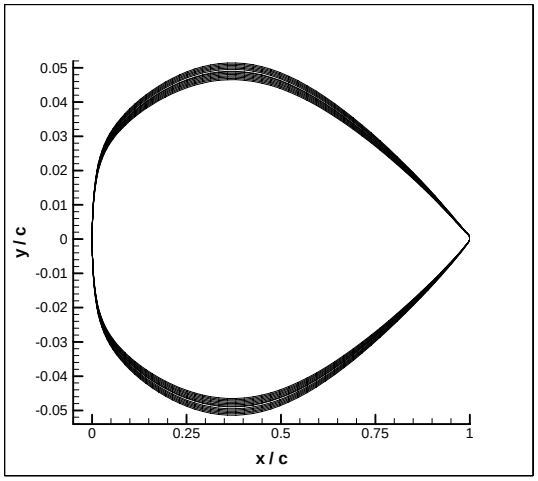

Figure 4.35: Wing sections of the initial population (14 members)

In the following stages, similar to the previous applications, the wing sections are reproduced according to their fitness values based on the genetic process (crossover, mutation etc.). The wing sections found in 10^{th} and 30^{th} generations are shown in Figure 4.36 and Figure 4.37 respectively.

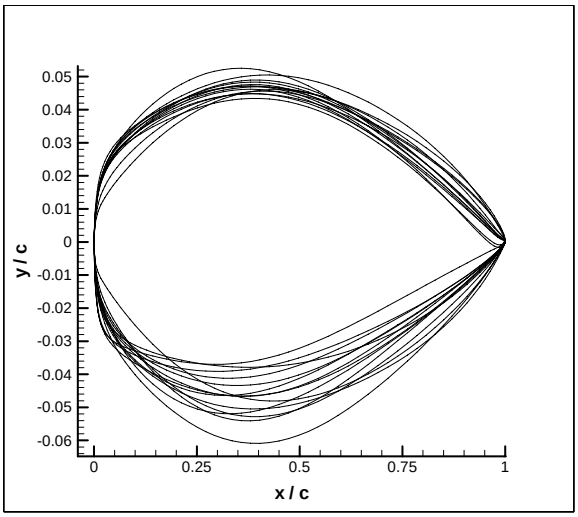

Figure 4.36: Wing sections of the 10th population (14 members)

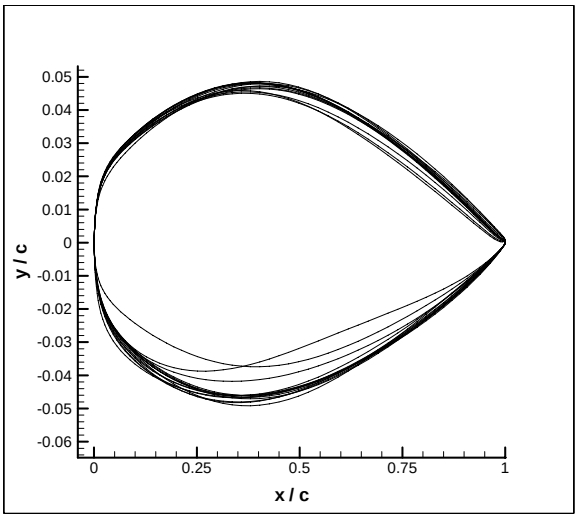

Figure 4.37: Wing sections of the 30th population (14 members)

4.3.2 Change in the Geometry and the Mesh Structures

The unstructured tetrahedral mesh is modified according to the change in wing sections by using dynamic mesh technique and for all members of a generation; new mesh structures have been adapted. For instance, the meshes calculated for two different wing sections are shown in Figure 4.38 and Figure 4.39.

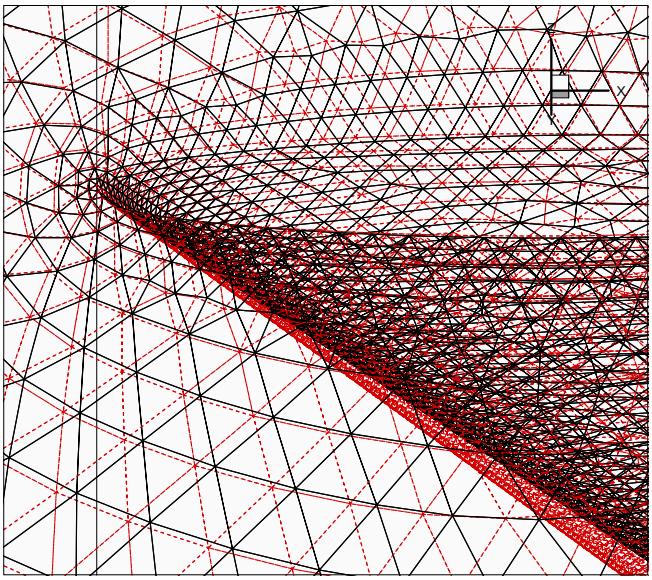

Figure 4.38: The mesh structures of the initial (dashed line) and the best wing found at the 30th population (solid line)

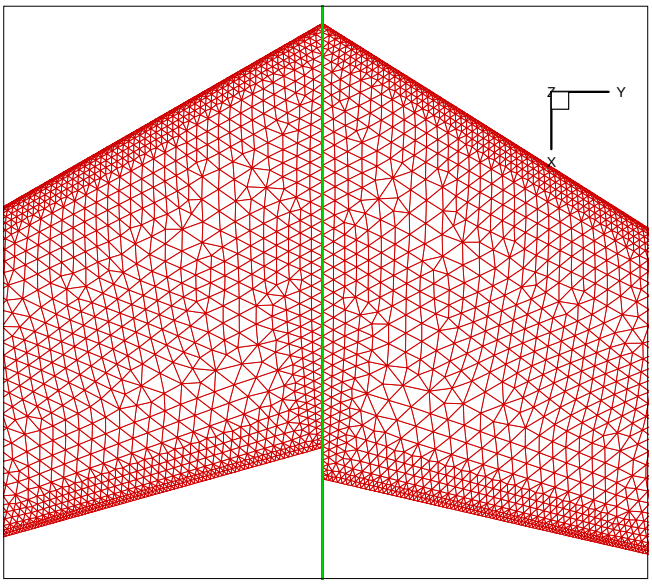

Figure 4.39: The mesh structures of the initial (left) and the best wing found at the 30th population (right)

As it can be seen in Figure 4.34the taper ratios are reducing from 0.56 to about 0.45. The change in wing platform, because of this reduction in the taper ratio, is shown in Figure 4.40.

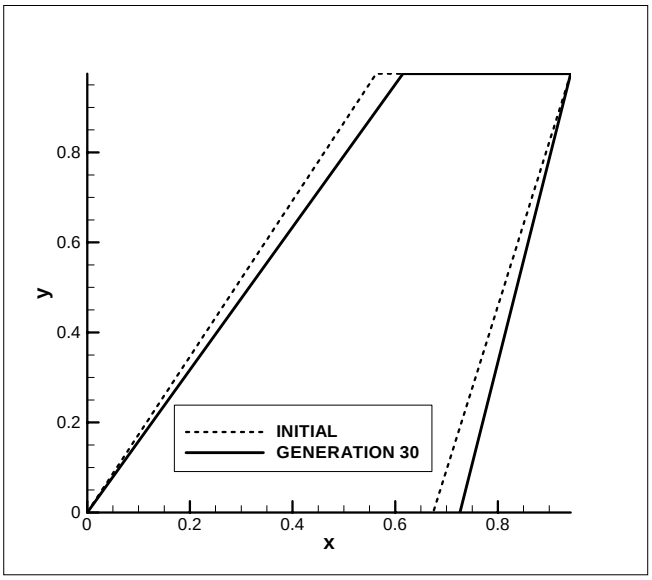

Figure 4.40: The difference between the initial wing planform and the best member found at the 30th generation

4.3.3 Development in Pressure Distribution

In Figure 4.41 and Figure 4.42, the differences between pressure coefficient distributions of the initial wing and the best member produced in the 30th generation can be seen.

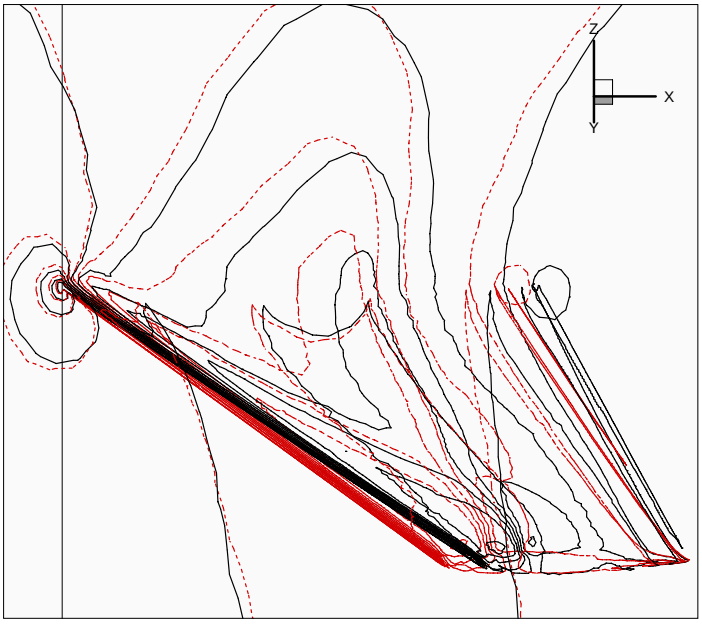

Figure 4.41: The Cp distributions of the initial (dashed line) and the best wing found at the 30th population (solid line)

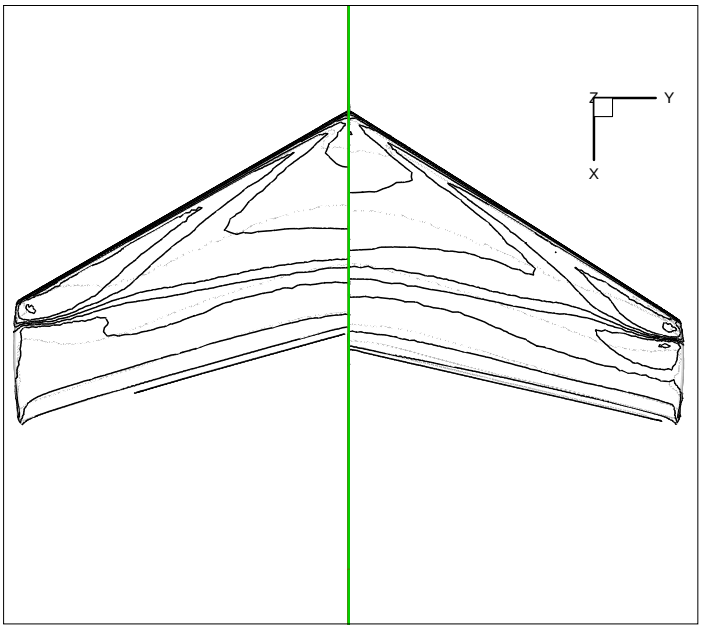

Figure 4.42: The Cp distributions of the initial (left) and the best wing found at the 30th population (right)

The Cp and Mach number distributions over the root sections of the initial wing and the wing obtained 30th step are shown in Figure 4.43 and Figure 4.44.

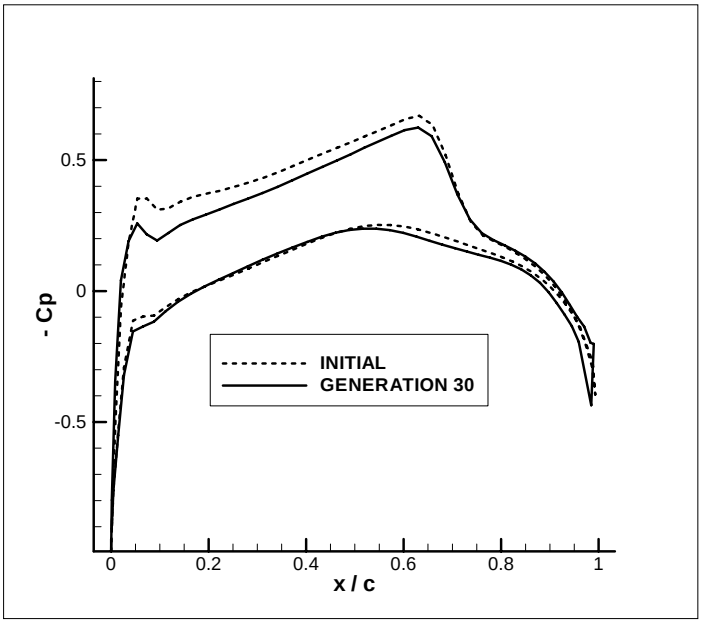

Figure 4.43: The Cp distributions of the initial and the best wing found at the 30th population over the root section

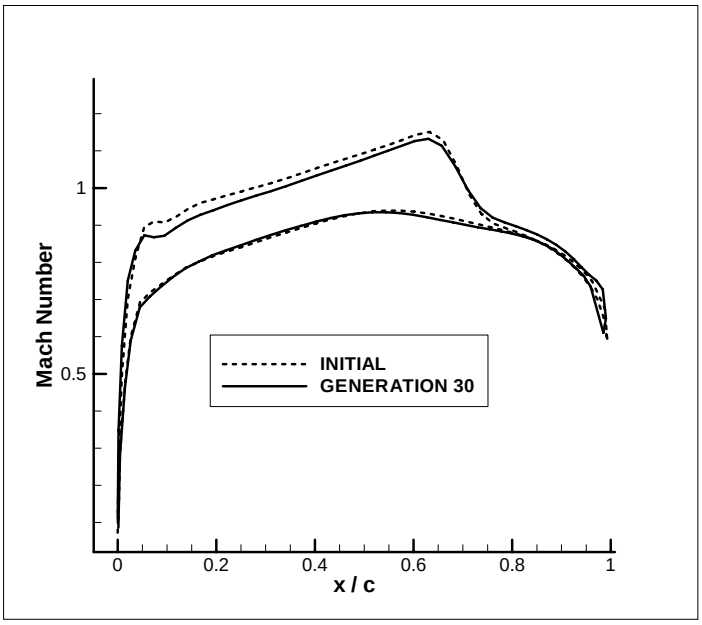

Figure 4.44: The Mach number distributions of the initial and the best wing found at the 30th population over the root section

The Cp distributions over the sections at the wing stations 0.44b and 0.8b are shown in Figure 4.45 and Figure 4.46 respectively.

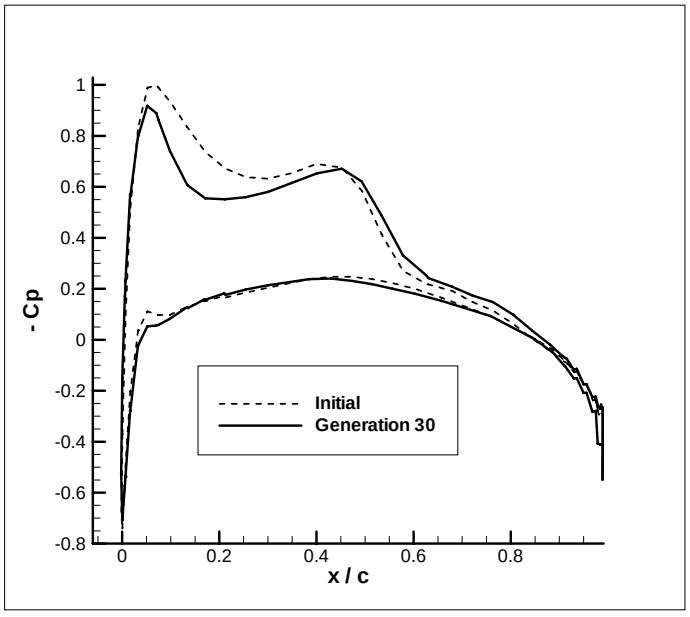

Figure 4.45: The Cp distributions of the initial and the best wing found at the 30th population over the section at 0.44b

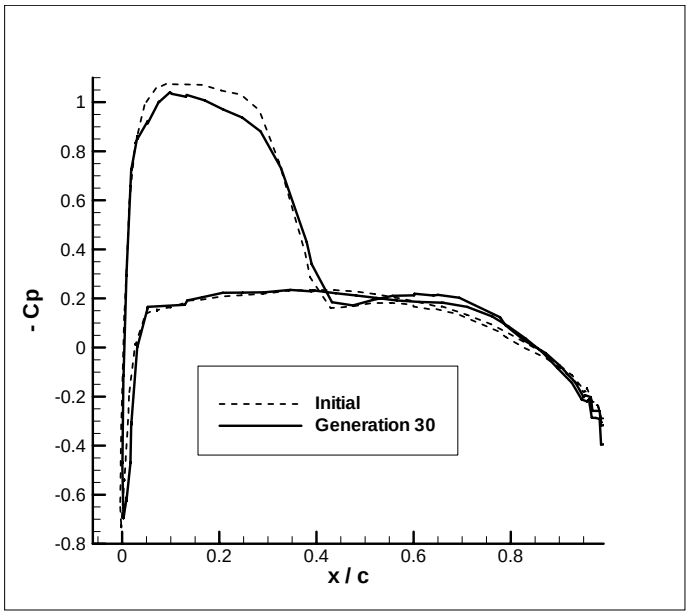

Figure 4.46: The Cp distributions of the initial and the best wing found at the 30th population over the section at 0.8b

4.3.4 The Best Wing Sections Found by Genetic Processes

In Figure 4.47, the best member obtained in 30 generations is compared with the initial wing.

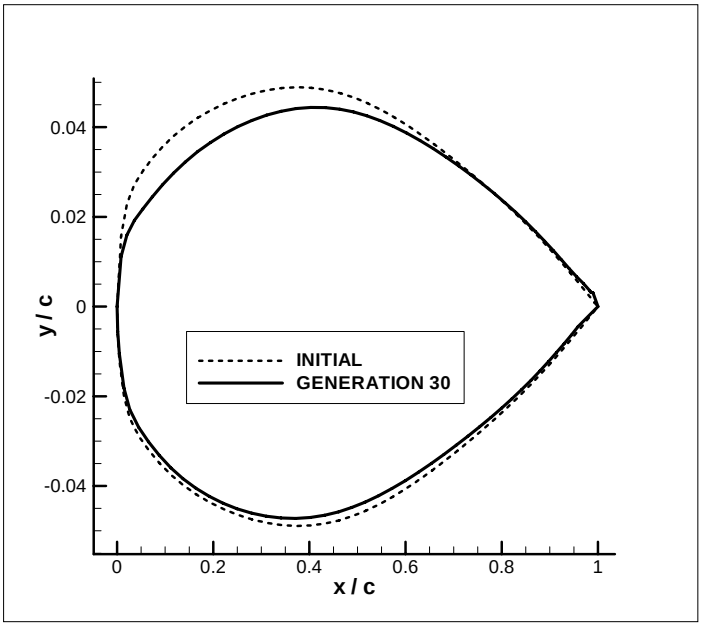

Figure 4.47: Wing sections of the initial and the best members found at the step 30

The best wing section obtained at the 30th generation is shown at its normal scale in Figure 4.48.

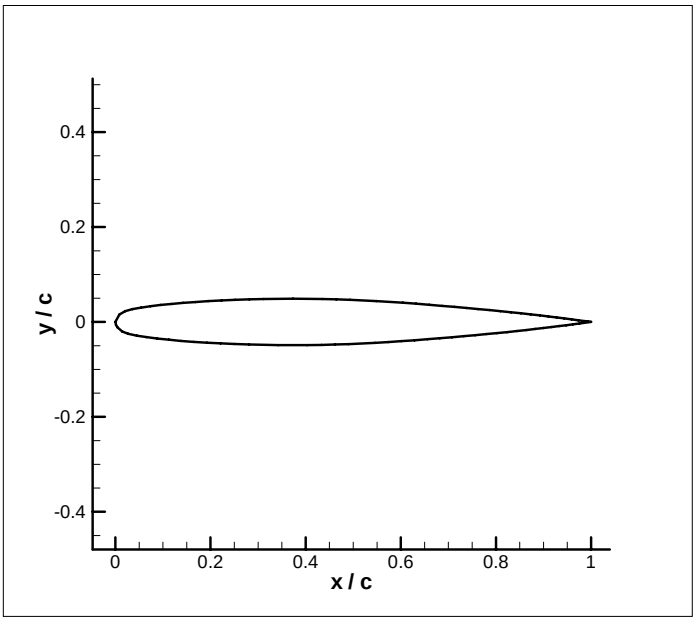

Figure 4.48: Wing section of the best member found (at normal scale)

It is observed that especially the leading edge parts of the wing sections become thinner.

4.4 Application to a Finer Mesh (with Thickness Ratio Constraint and Design Variable Taper Ratio)

4.4.1 Progress in Generations

In this section, the wing optimization process with thickness ratio constraint and the taper ratio design variable is applied to a finer mesh structure of Onera M6 wing. The same as before, there are 14 members in each generation. These are 14 Onera M6 wing planforms that have different wing sections. The fitness function is taken as the same as before:

$$f(i) = C_D + a(C_L - C_{Ld})^2 + b(Th - Th_d)^2 \quad (4.7)$$

$$\text{fitness value} = 1/f(i) \quad (4.8)$$

C_D : Drag coefficient calculated

C_L : Lift coefficient calculated

C_{Ld} : Design lift coefficient

a : Constant parameter to define the weight of the lift coefficient constraint

Th : Thickness ratio of the produced wings

Th_d : Design thickness ratio

b : Constant parameter to define the weight of the thickness ratio constraint

The average fitness value for each generation and the maximum fitness value (i.e. the best member found in that generation) are shown in Figure 4.49.

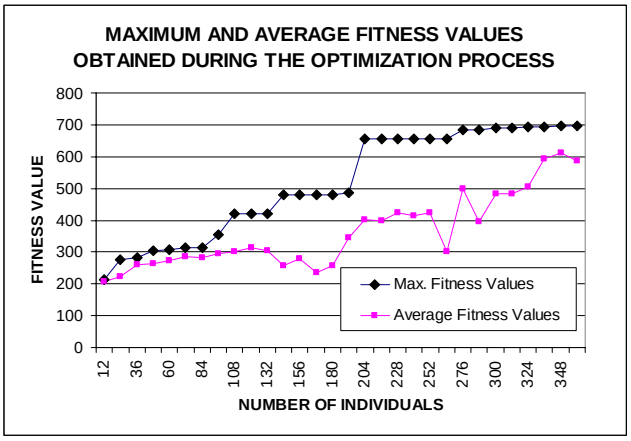

Figure 4.49: Change in the average fitness and the development of the maximum fitness value

The important parameter, in Figure 4.49**,** is the maximum fitness value (or the best member) obtained in each generation. The average fitness value shown can be altered in different ways.

The best member is kept in each generation and taken to the next generation. So the best member found in each generation would be, at least, as the same as the best member of the previous generation. The drag force reduction is shown in Figure 4.50.

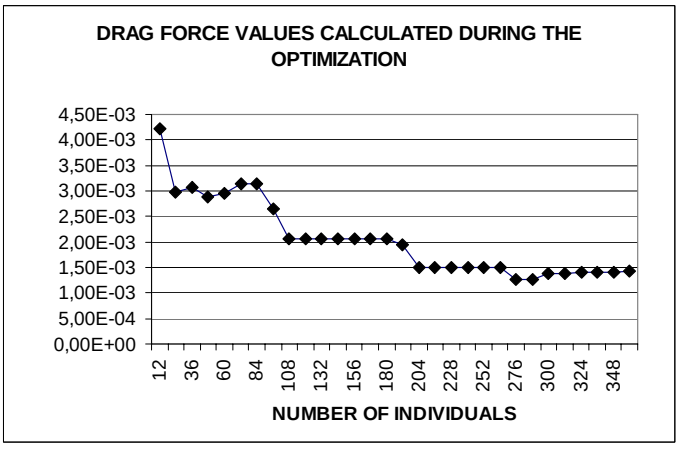

Figure 4.50: Change in the drag force calculated from non-dimensional pressure values during the optimization process

As it can be seen in Figure 4.51, the change in the thickness ratio and the lift forces is very low. In Figure 4.52, taper ratio development is shown. The taper ratio is lowered and converged to 0.35.

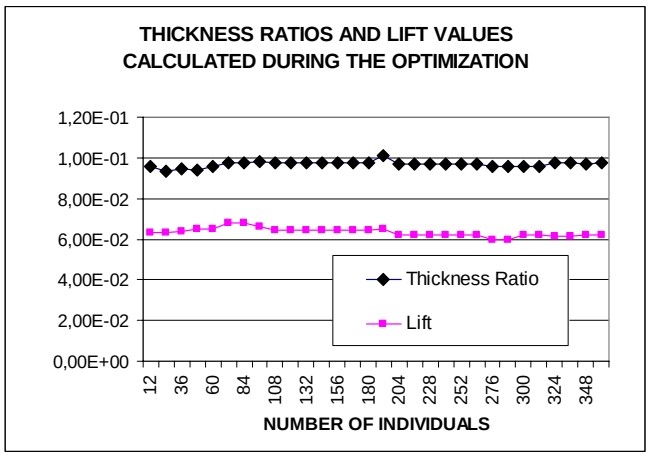

Figure 4.51: Change in the thickness ratio and the dimensionless lift force calculated from non-dimensional pressure values

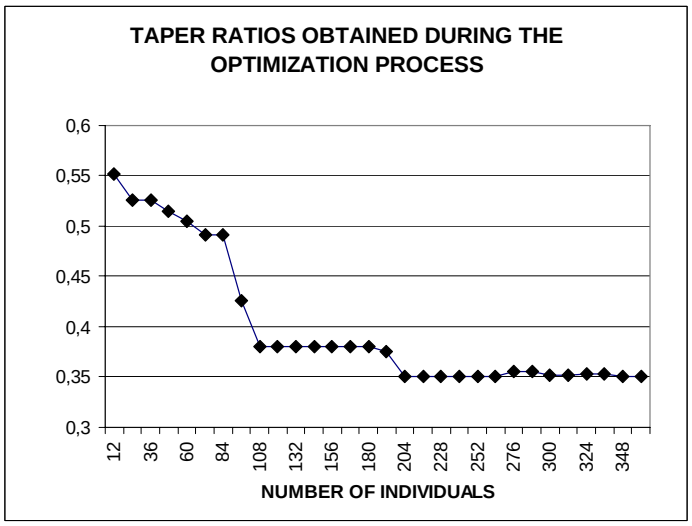

Figure 4.52: Progress in taper ratio values

The wing sections found in 10th and 30th generations are shown in Figure 4.53 and Figure 4.54 respectively.

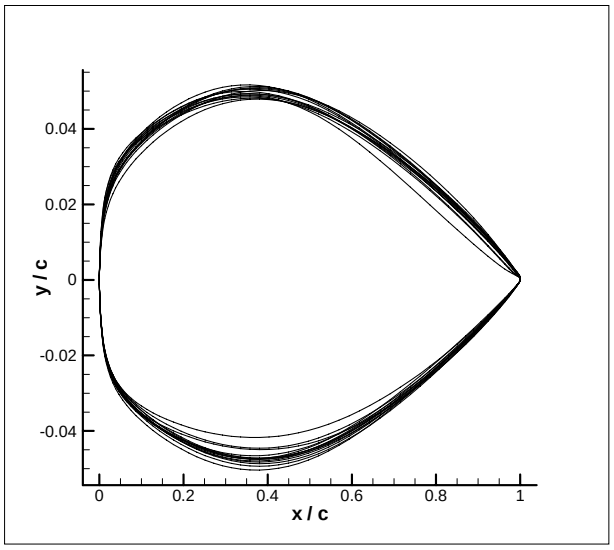

Figure 4.53: Wing sections of the 10th population (14 members)

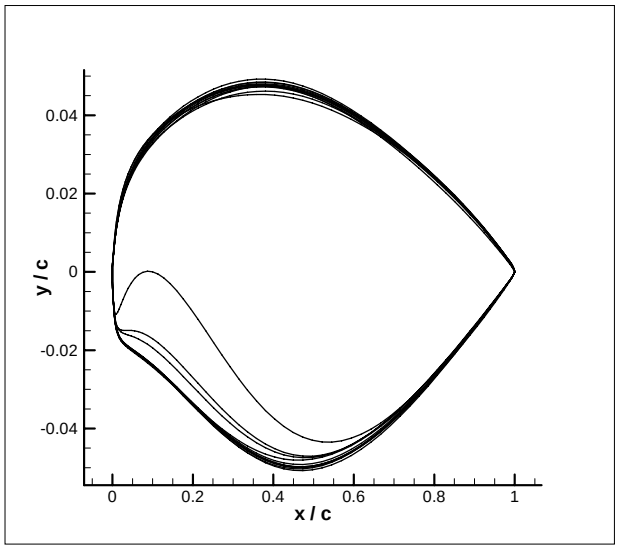

Figure 4.54: Wing sections of the 30th population (14 members)

4.4.2 Change in the Geometry and the Mesh Structures

The unstructured tetrahedral mesh is modified according to the change in wing sections by using dynamic mesh technique and new mesh structures have been adapted for all members of a generation. For instance, the meshes calculated for the initial and the last wing sections are shown in Figure 4.55.

In Figure 4.56**,** the mesh structure of initial Onera M6 wing (on the left hand side) and the mesh of the best member found at 30^{th} step are shown.

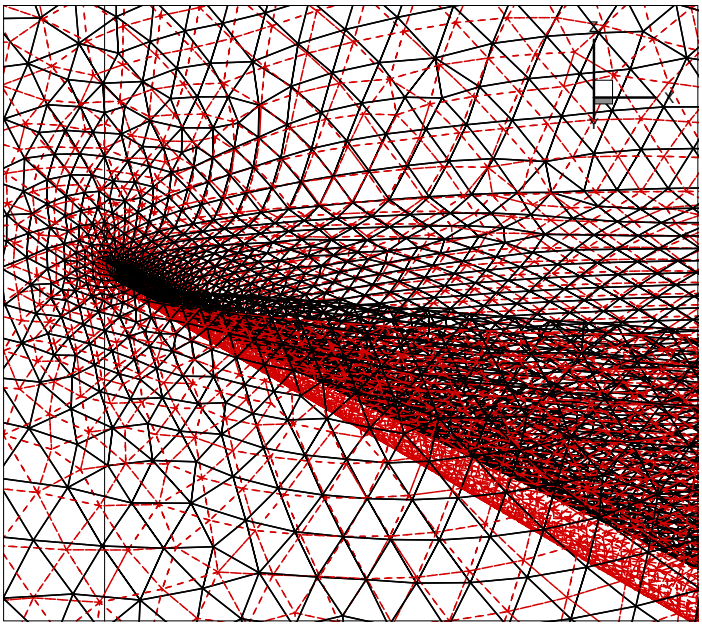

Figure 4.55: The mesh structures of the initial (dashed line) and the best wing found at the 30th population (solid line)

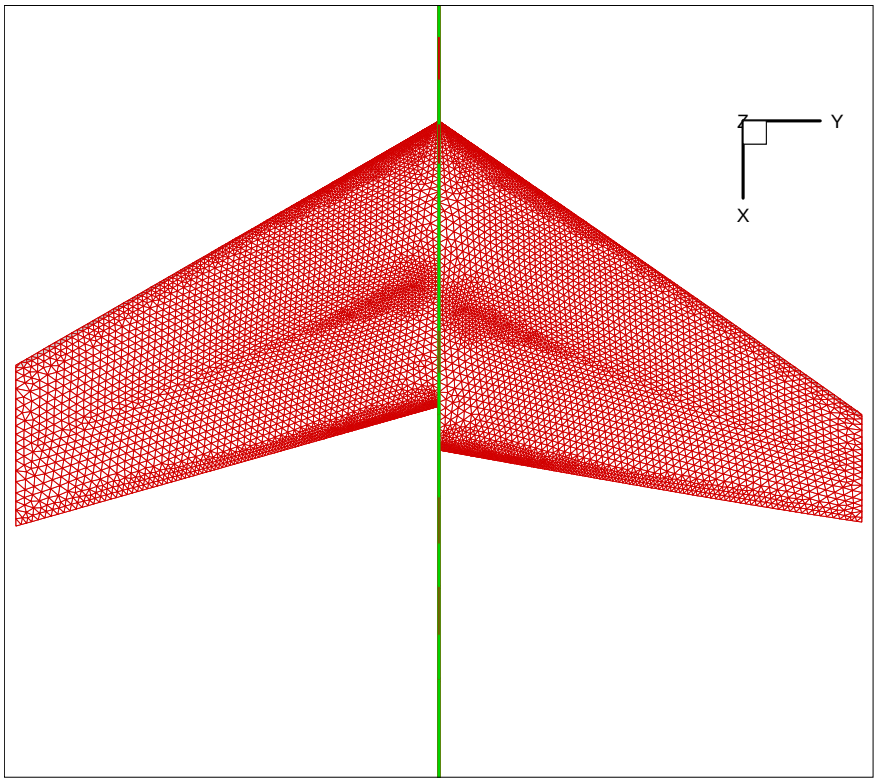

Figure 4.56: The mesh structures of the initial (left) and the best wing found at the 30th population (right)

In this application, it is observed that the taper ratio has been reduced to a lower value (i.e. 0.35). Besides, the drag force is able to be reduced to a lesser value.

The planforms of original Onera M6 wing and optimized wing are shown in Figure 4.57.

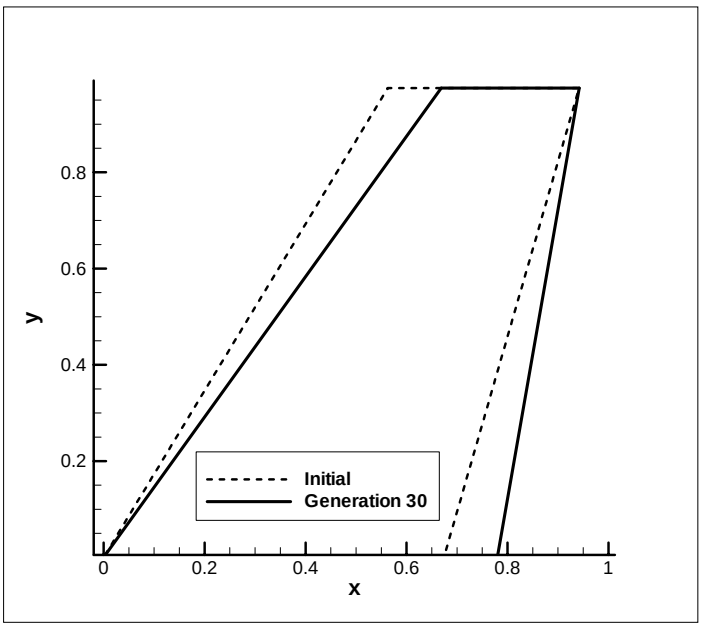

Figure 4.57: The difference between the initial wing planform and the best member found at the 30th generation.

4.4.3 Change in the Pressure Distribution

In Figure 4.58 and Figure 4.59, the differences between pressure coefficient distributions of the initial wing and the best member produced in the 30th generation can be seen.

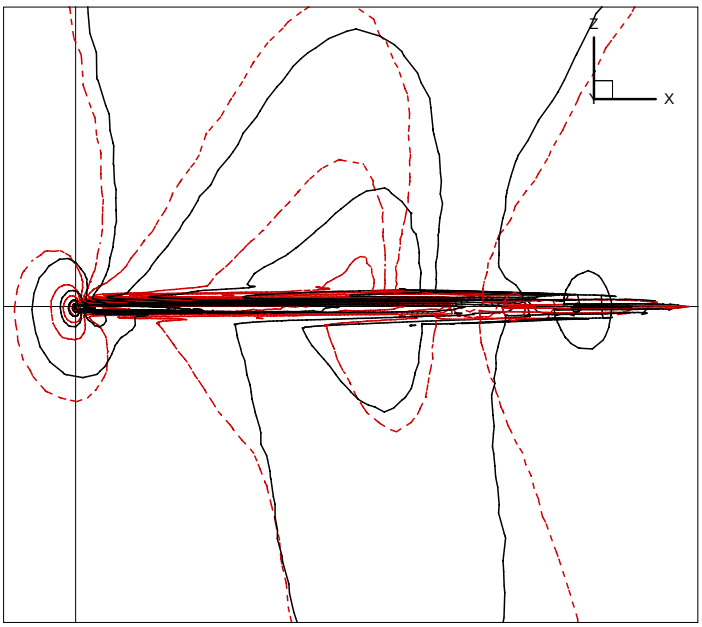

Figure 4.58: The Cp distributions of the initial (dashed line) and the best wing found at the 30th population (solid line)

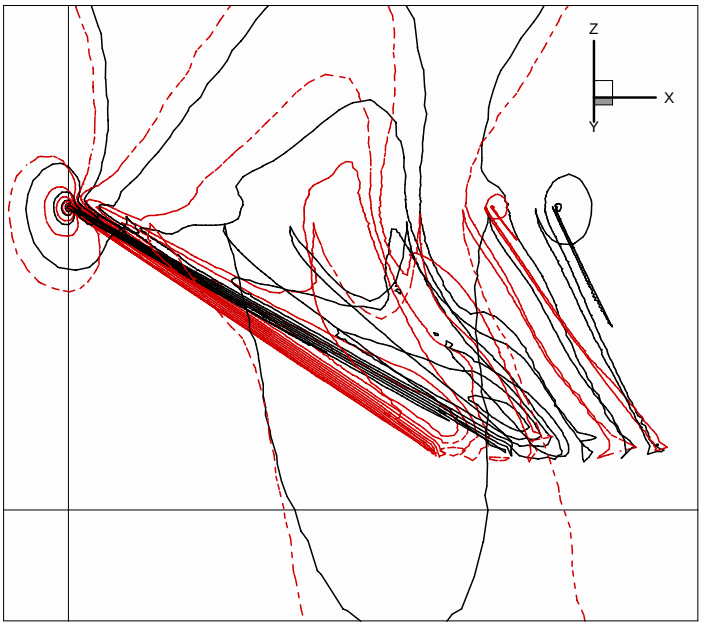

Figure 4.59: The Cp distributions of the initial (dashed line) and the best wing found at the 30th population (solid line)

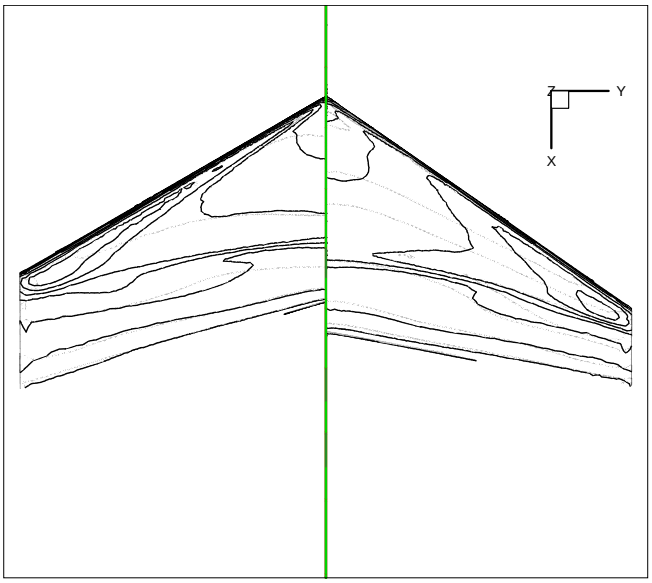

Figure 4.60: The Cp distributions of the initial (left) and the best wing found at the 30th population (right)

In Figure 4.60, the pressure contours are shown from the top view. The Cp and Mach number distributions over the 0.44b sections of the initial wing and the wing obtained 30th step are shown in Figure 4.61 and Figure 4.62.

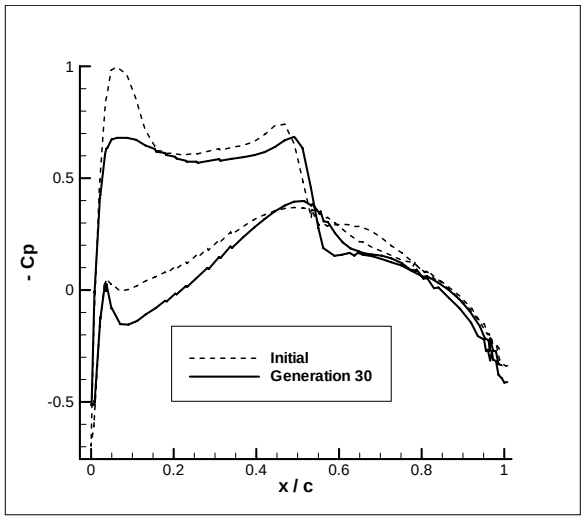

Figure 4.61: The Cp distributions of the initial and the best wing found at the 30th population over the section at 0.44b

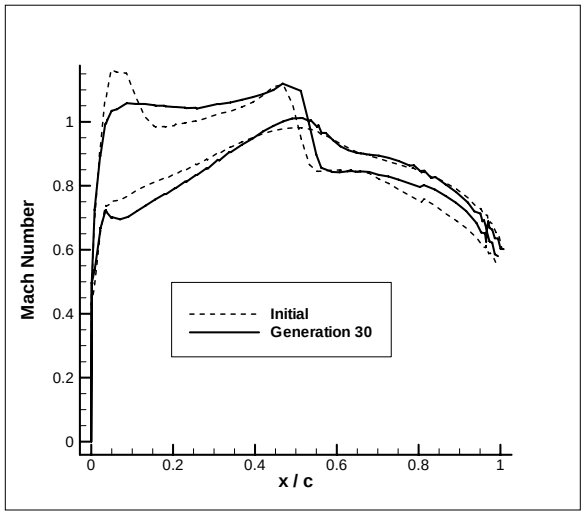

Figure 4.62: The Mach number distributions of the initial and the best wing found at the 30th population over the section at 0.44b

The Cp and Mach number distributions over the 0.8b sections of the initial wing and the wing obtained 30th step are shown in Figure 4.63 and Figure 4.64**.**

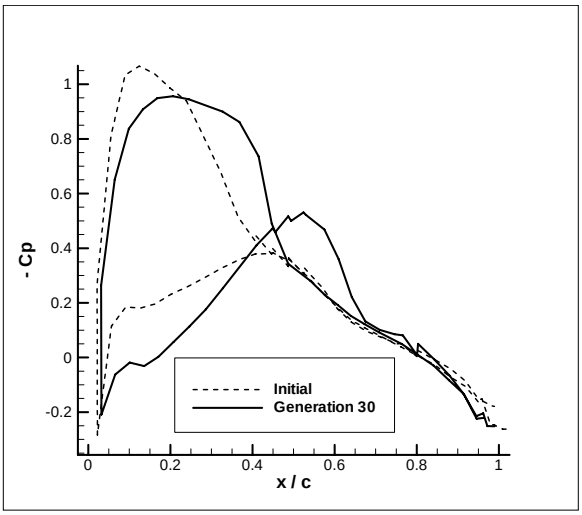

Figure 4.63: The Cp distributions of the initial and the best wing found at the 30th population over the section at 0.8b

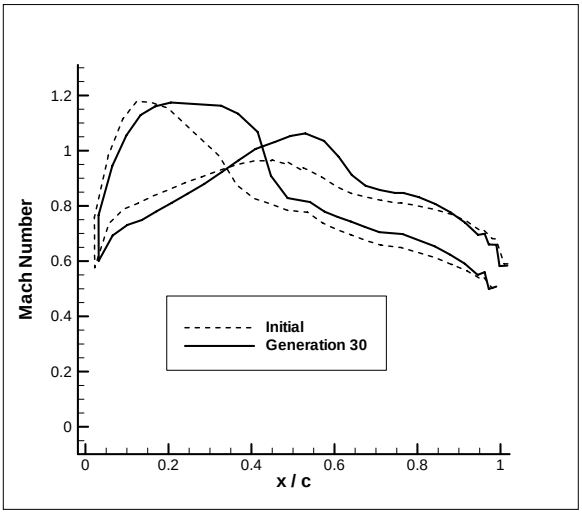

Figure 4.64: The Mach number distributions of the initial and the best wing found at the 30th population over the section at 0.8b

4.4.4 The Best Wing Sections Found by Genetic Processes

In Figure 4.65, the best members obtained in different stages are shown.

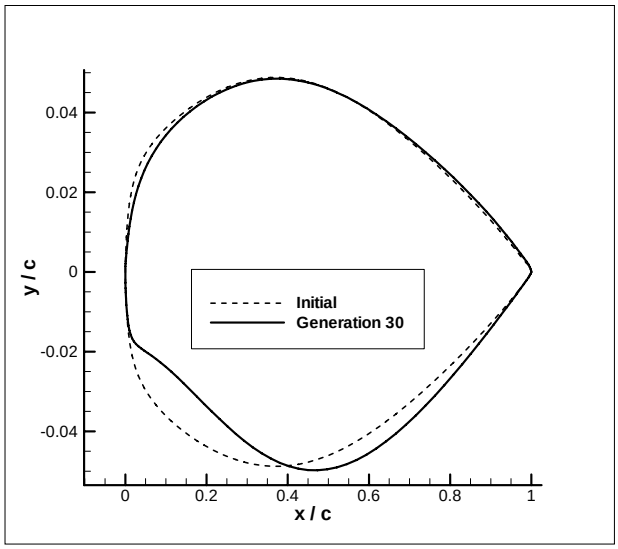

Figure 4.65: Wing sections of the initial and the best members found at the step 30

During this process, the lift coefficient has been tried to be held fixed, while the drag coefficient has been reduced 25 percent. The best wing section obtained at the 30th generation is shown at its normal scale in Figure 4.66.

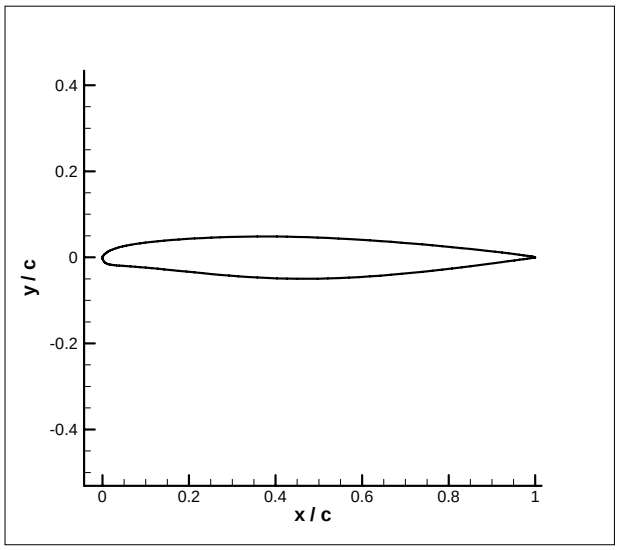

Figure 4.66: Wing section of the best member found (at normal scale)

5. EVALUATION AND CONCLUSION

Today, evolutionary type of algorithms is entering in many engineering fields. The time-consuming flow solvers and gradient type optimization techniques have not been preferred recently. Instead, flow solvers are carried into parallel computing type machines and optimizations are carried out by evolutionary techniques.

Throughout this study, Onera M6 wing has been successfully optimized on two parameters, the wing section and the taper ratio by combining recent preferable approach i.e. parallel computing and evolutionary techniques. For the 3-D models developed during the optimization stages, the mesh structures required are obtained by dynamic mesh technique **(Batina, 1991)**. The code developed for this aim is robust and faster than the codes, which are only producing mesh by classical techniques. The flow solver ACER3D **(Yılmaz, 2000)** has been successfully adapted to this optimization to obtain the fitness values for each member. Because the operating time of the program is very long, on account of low capacity computer resources, parallel processing has been used. Obviously the strategy applied here can be used for any slowly deforming complex geometries, as long as an effective combination of the genetic algorithm and dynamic mesh be succeeded.

The best member is kept in each generation and taken to the next generation. So the best member found in each step cannot be worse than the best member of the previous one. This is called “elitism”.

The CPU time of the initial step in dynamic mesh method is approximately the same as mesh generation time. However, later steps of dynamic mesh technique need much less time than the first step. Therefore, especially, if a lot of configurations are to be considered, the dynamic mesh method offers more advantage.

Onera M6 wing is already a developed transonic wing. Therefore starting from this wing at transonic Mach numbers may lead some difficulties for improvements in the aerodynamic parameters throughout genetic optimization.

In the dynamic mesh technique the predictor – corrector procedure has been found to be more efficient than simply performing Jacobi iterations because much less iterations are required to achieve acceptable convergence. **(Batina, 1991)**

However, at the first step, because no prediction from the previous step is available, initial displacements are taken as proportional to geometry change in the body. At the second step, initial displacements are obtained from the first step. For the third step and further, initial displacements are taken from the previous two steps. In case an accurate solution is desired iterations can be increased up to 1000. The differences between the first step and others are really high. While the first step is reaching to a specified criterion in about 1000 iterations, the others reach in 30, 20 or 5 iterations.

Although calculating the neighboring points for each node is also time consuming process. This is needed only once for an initial grid. Therefore it is calculated once and written in a data file and later the program reads those data from the file. Unless the initial mesh structure is changed, there is no need to run this portion of the code. Reading from the file is enough and very much faster than calculating.

The slight differences between geometries give the opportunity to use dynamic mesh technique to easily re-generate mesh. Frankly, the drawback of this technique is requirement of the slight changing of geometry in each step.

To get satisfactorily accurate results, number of the short runs required is changing between 400 – 3000 for the considered geometry. Normal run time of the flow solver ACER3D is 10 hours. This does not include mesh generation. Mesh generation takes approximately 8-10 minutes depending on the computer's capability **(Van der Burg, 2005)**. This means that the total run time of the optimization process with genetic algorithm would reach up to 4 - 40 months with a 1.3 GHz. P-IV PC.

This is not acceptable and feasible time for a numerical calculation. In order to make this process applicable, the both software and hardware conditions must be improved. By restarting the flow solver from previous solution and using the dynamic mesh technique for re-meshing the new population members, this time can be reduced up to 3 times. By using the parallel processing the total run time can be decreased up to 7 times.

Aerodynamic force, lift and drag, calculations have been done by using a finite element method. The pressure value for each triangular wall boundary face is taken as the average of the pressures on the corner nodes. Then the total forces are calculated by a numerical integration as in **(Mecitoğlu and Dökmeci 1990)**.

From the results, it is observed that the optimization process is working as expected. The drag coefficient was reduced by about 25 percent. While this has been done, its lift coefficient is tried to be close to the design value determined at the beginning. This is done by arranging the fitness function. At the 50^{th} generation, for example, the difference between the lift coefficient of the best member and the design lift coefficient value is about 1 percent and the difference between thickness ratios is 3 percent.

The designer should decide how much important the changes (of course depend on the problem and purposes) in these constraints are. If they are to be kept in certain intervals at the design values more strictly, then the weighting constants in the fitness function should be increased. However the cost of this would be higher number of iterations to achieve a good solution.

The taper ratio is getting smaller while the code is trying to minimize the drag force. But it cannot be reduced to very small values and is kept almost the same at later steps, because the program is expected not only to reduce the drag force, but also to hold the lift force close to the design value.

It is possible to develop this study to further steps. For aerodynamic wing design problems, one of the most important parameter to be considered is pitching moment. Pitching moment coefficient must be kept, while changing the wing configuration. Otherwise the wing configuration may not be suitable for general aircraft design considerations. Therefore the pitching moment coefficient can be added as a design constraint to fitness function.

In this work, the shape of the wing section is thought as fixed along the wing. It is also possible to define different control points for different stations of the wing. But this would increase the number of parameters to be optimized. Therefore it can expand the size and the time of calculation and the code may need more computer resources. Besides a variable section wing can bring a disadvantage about manufacturing difficulties.

A Navier – Stokes solver can be employed to calculate flow parameters of each wing on account of accuracy considerations. Therefore it would be possible to calculate pressure values more precisely and to find drag forces even at sub-sonic flow regimes. However, a Navier-Stokes solver would increase calculation time and much more computer resources will be needed.

This type of numeric solutions actually needs huge computer resources. If today's computer capabilities are considered, parallel processing would be ineluctable. To overcome this difficulty, hybrid methods can be worked on. For instance, a genetic algorithm technique together with neural network method can achieve a reasonable solution in a much less time.

REFERENCES

Al Geist, Beguelin, A., Dongarra, J., Jiang, W., Manchek, R. and Sunderam, V., 1994. PVM: Parallel Virtual Machine, a Users' Guide and Tutorial for Networked Parallel Computing, *the MIT Press,* Cambridge-MA-USA

Baker J. E., 1987. Reducing Bias and Inefficiency in the Selection Algorithm, *Proceedings of the Second International Conference on Genetic Algorithms*, Morgan Kaufmann Publishers, pp.14-21.

Barney B., 2005. Lawrence Livermore National Laboratory, University of California, http://www.llnl.gov/computing/tutorials/mpi (July 2005)

Batina, J.T., 1990. Unsteady Euler Airfoil Solutions Using Unstructured Dynamic Meshes*, AIAA Journal*, Vol. 28, No. 8, pp. 1381-1388. August.

Batina, J.T., 1991. Unsteady Euler Algorithm with Unstructured Dynamic Mesh for Complex-Aircraft Aerodynamic Analysis, *AIAA Journal*, Vol. 29, No. 3, pp. 327-333. March.

Benson, T., 2004. NASA Glenn Learning Technologies Home Page http://www.grc.nasa.gov/WWW/K-12 (December, 2004)

Chung, H. S., 2004. Multidisciplinary Design Optimization of Supersonic Business Jets Using Approximation Model-Based Genetic Algorithms *Ph. D. Thesis* the Department Of Aeronautics and Astronautics and the Committee on Graduate Studies of Stanford University, March

De Falco, I. 1997. an Introduction to Evolutionary Algorithms and their Application to the Airfoil Design Problem- Part II: the Results, *Lecture Series 1997-05*, Von Karman Institute for Fluid Dynamics.

De Falco, I. Cioppa, A. D., Balio, R. D. and Tarantino, E., 1996. Breeder Genetic Algorithms for Airfoil Design Optimization, *IEEE Int. Conf. on Evolutionary Computing*, Nagoya, Japan.

De Falco, I. Cioppa, A. D., Lazzetta, A. and Tarantino, E., 1998. M_{ijn} Mutation Operator for Airfoil Design Optimization, *Soft Computing in Engineering Design and Manufacturing*, Springer Verlag, p.211-220.

Dulikravich, G.S. 1991. Aerodynamic shape design and optimization, *Tech. Rep. 91-0476, AIAA paper*.

Ermiş M., Ülengin F., Hacıoğlu A., 2002. Vibrational Genetic Algorithm (VGA) for Solving Continuous Covering Location Problems, *Lecture Notes in Computer Science*, Volume 2457, pp 293-302.

Eshelman L.J. and Schaffer J. D., 1993. Real Coded Genetic Algorithms and Interval Schemata, *Foundations of Genetic Algorithms 2,* Morgan Kaufmann Publishers, pp187-202.

Fanjoy, D. W., 2001. Aerodynamic Shape and Structural Topology Design of Helicopter Rotor Cross-Sections Using a Genetic Algorithm *Ph.D., Purdue University* Major Professor: William A. Crossley, August.

Filippone, A, 2004. Advanced Topics in Aerodynamics, Aerodynamic Drag, Release 3.8.3 October 1, *The University of Manchester, Dept. Mechanical, Aerospace, Civil Engineering P.O. Box 88, Manchester M60 1QD United Kingdom,* http://aerodyn.org/Drag/speed-drag.html#tdrag

Fostar, I., 1995. Designing and Building Parallel Programs, *Addison-Wesley Pub* New York, NY, 1995.

Foster, N.F. and Dulikravich, G.S., 1997. Three Dimensional Aerodynamic Shape Optimization Using Genetic and Gradient Search Algorithms, *Journal of Spacecraft and Rockets*, Vol. 34, No. 1

Golberg, D.E., 1989. Genetic Algorithms in Search, Optimization & Machine Learning, *Addison-Wesley Publishing Company, Inc. Reading*

Gundlach, J. F. 1999. Multidisciplinary Design Optimization and Industry Review of a 2010 Strut-Braced Wing Transonic Transport *Master of Science Thesis* submitted to the Faculty of the Virginia Polytechnic Institute and State , Aerospace Engineering, June 7, Blacksburg, Virginia

Gundlach, J. F. 2004. Multi-Disciplinary Design Optimization of Subsonic Fixed-Wing Unmanned Aerial Vehicles Projected Through 2025, *Ph.D. Thesis* submitted to the Faculty of the Virginia Polytechnic Institute and State University, Aerospace Engineering, February 9, 2004 Blacksburg, Virginia

Hacıoğlu, A. and İ. Özkol, 2001. Modified BLX-α: Double Directional Alpha Method, *Sixteenth International Symposium On Computer And Information Sciences* (ISCIS XVI) 5-7 Nov.

Hacıoğlu, A. and Özkol, İ., 2002. Vibrational Genetic Algorithm as a New Concept in Aerodynamic Design, *Aircraft Engineering and Aerospace Technology*, Vol. 74, No. 3, pp. 228-236.

Hacıoğlu A. and Özkol İ., 2003a. Transonic Airfoil Design and Optimization by Using Vibrational Genetic Algorithm, *Aircraft Engineering and Aerospace Technology*, Vol.75, No:4.

Hacıoğlu, A., 2003b. Aerodinamik Dizayn ve Optimizasyonda Genetik Algoritma Kullanımı, *Doktora Tezi,* İ.T.Ü. Fen Bilimleri Enstitüsü, Uçak Mühendisliği Programı, İstanbul.

Hacıoğlu, A. ve Özkol, İ., 2005. Inverse Airfoil Design by Using an Accelerated Genetic Algorithm via Distribution Strategies, *Inverse Problems in Science and Engineering*, Vol. 13, No. 6, 563-579.

Hacıoğlu, A., 2005a, A Novel Usage of Neural Network in Optimization and Implementation to the Internal Flow Systems, *Aircraft Engineering and Aerospace Technology*, Vol. 77, No. 5.

Haftka, R.T. and Gürdal, Z., 1992. Elements of Structural Optimization 3rd ed., *Kluwer Academic, Boston*, MA.

Hendrickson, R., Roman, D. and Rajkovic, D., 1997. The importance of Drag, Applied Computational Aerodynamic

Hirsch, C., 1988. Numerical Computation of Internal and External Flow, Vol. 1 *John Wiley & Sons*.

Hu, Z., 2003. Application of Heuristic Optimization in Aircraft Design *Ph. Thesis* Submitted to the Henry Edwin Sever Graduate School of Washington University, December, Saint Louis, Missouri

Jameson, A. 1988. Aerodynamic design via Control Theory, *Tech. Rep. 88-64*, ICASE, 1988.

Jones, B. R., Crossley, W. A. and Lyrintzis, A. S., 2000. Aerodynamic and Aeroacoustic Optimization of Airfoils via a Parallel Genetic Algorithm, *Journal of Aircraft*, Vol. 37, No. 6.

Kim, H.-J. and Rho, O.-H. 1998. Aerodynamic Design of Transonic Wings Using the Target Pressure Optimization Approach, *Journal of Aircraft*, Vol. 35, No. 5.

Klein, M. and Sobieczky, E., 2001. Sensivity of Aerodynamic Optimization to Parameterized Target Functions, *Proc. Int. Symp. On Inverse Problems in Engineering Mechanics* (ISIP 2001), Nagona, Japan.

Liang, Y., 2003. Accelerated Strategies of Evolution Computation for Optimization and their Application *Ph.D. Thesis*, the Chinese University of Hong Kong, November.

Liu, W., Emerson, D. and Ashworth, M., 2005. A parallel and Adaptive Refinement Algorithm of FE Multigrids for Solving Flow Problems, *Finite Element for Flow Problems FEF05 IACM Special Interest Conference supported by ECCOMAS*, April 4-6, Swansea, Wales, UK

Mali, V., Sudhakar, K. and Chatterjee, A. , Optimization of L/D for ONERA-M6 Wing Using ADIFOR and EULER *Department of Aerospace Engineering*, IIT Bombay, Mumbai 400 076

MCS, Mathematics and Computer Science Division, Argonne National Laboratory, 9700 South Cass Avenue Argonne, Illinois 60439-4844, USA http://www-unix.mcs.anl.gov/mpi/ (July 2005)

Mecitoğlu, Z., Dökmeci, M.C. , 1990. Vibration Analysis Stiffened Cylindrical Thin Shell *Proc. 17th Congress of the International Council of Aeronautical Sciences* pp. 986-993, Stockholm.

Nicolai, L. M., 2002. Estimating R/C Model Aerodynamics And Performance *Lockheed Martin Aeronautical Company,* June.

Obayashi, S. and Takanashi, S., 1995. Genetic Optimization of Target Pressure Distributions for Inverse Design Methods, *Proc. 12th AIAA Computational Fluid Dynamics Conf.*, San Diego.

Obayashi, S. Yamaguchi Y. and Nakamura, T. 1997. Multiobjective Genetic Algorithm for Multidisciplinary Design of Transonic Wing Planform, *Journal of Aircraft*, Vol. 34, Sept./Oct.

Obayashi, S., 1998a. Multidisciplinary Design Optimization of Aircraft Wing Planform Based on Evolutionary Algorithms, *Dept. of Aeronautical*

Engineering, Tohoku University, Japan, 0-7803-4778-1/98 © 1998 IEEE

Obayashi, S., Nakahashi, K., Oyama, A. and Yoshino, N., 1998b. Design Optimization of Supersonic Wings Using Evolutionary Algorithms, *ECCOMAS 98, Published in 1998 by John Wiley & Sons, Ltd.*

ONERA The French Aeronautics and Space Research Center, www.onera.fr (July 2005)

Oyama, A. Obayashi, S. Nakahashi, K. and Hirose, N., 1998. Coding by Taguchi Method for Evolutionary Algorithms Applied to Aerodynamic Optimization, *Proceedings of the Fourth ECCOMAS Computational Fluid Dynamics Conference*, Athens, John Wiley & Sons Ltd, Chichester, September.

Ozkol I. and Komurgoz G., 2005. Determination of the Optimum Geometry of the Heat Exchanger Body Via a Genetic Algorithm *Numerical Heat Transfer*, Part A, Vol: 48, pp. 283-296.

Quagliarella D. and Della Cioppa, A. 1994. Genetic Algorithms Applied to the Aerodynamic Design of Transonic Airfoil, *Proc. 12th AIAA Aplied Aerodynamics Conference*, Colorado Springs, AIAA-94-1896-CP, s. 686-693.

Quagliarella D. and Vicini, A. 1999. Designing High-Lift Airfoils Using Genetic Algorithms, *Proceedings of EUROGEN'99*, Jyväskylä, Finland.

Schmitt, V. and Charpin, F., 1979**.** Pressure Distributions on the ONERA-M6-Wing at Transonic Mach Numbers, *Experimental Data Base for Computer Program Assessment.* Report of the Fluid Dynamics Panel Working Group 04, AGARD AR 138, May.

Schuhmacher, G., Murra, I., Wang, L., Laxander, A., O'Leary, O.L. and Herold, M., 2001. Multidisciplinary Design Optimization of a Regional Aircraft Wing Box *American Institute of Aeronautics and Astronautics*, (Fairchild Dornier GmbH, 82230 Wessling, Germany)

Slater, J. W., NASA John H. Glenn Research Center http://www.grc.nasa.gov/WWW/wind/valid/m6wing/m6wing02/m6wing02.html (July 2005)

Slooff, J.W. and Schmidt, W., 2000. Computational Aerodynamics Based on the Euler Equations, *AGARD-AG-325*.

Tai, C.H., Zhao, Y., Liew, K.M., 2004. Parallel computation of unsteady three-dimensional incompressible viscous flow using an unstructured multigrid method *Computer & Structures*, 82 (2004) pp.2425-2436

Tezduyar, T.E., Sathe, S., Senga, M. and Stein, K., 2005. Space Time Techniques For Fluid-Structure Interactions*, Finite Element for Flow Problems FEF05 IACM Special Interest Conference* supported by ECCOMAS, April 4-6, 2005, Swansea, Wales, UK

Tong, S. S., 1985, Design of aerodynamic bodies using artificial intelligence/expert system technique, *Tech. Rep. 85-0112,* AIAA paper.

Tse D.C.M. and Chan L.Y.Y., 1999. Application of Micro Genetic Algorithms and Neural Networks for Airfoil Design Optimization, *RTO MP-035 RTO-MP-035, Aerodynamic Design and Optimisation of Flight Vehicles in a Concurrent Multi-Disciplinary Environment*.

Van der Burg, J.W. FASTFLO I - Fully automatic CFD system for inviscid flow simulations, *http://www.fastflo.nl/publication.html* (July 2005)

Vanderplaats, G. N., 1984, Numerical Optimization Techniques for Engineering Design: with applications, *Mc Graw Hill*.

Vatandaş, E., Özkol, İ. and Kaya, M.O., 2003. Implementation of the Dynamic Mesh Methods on Genetically Obtained Mesh Structures for 3-D Geometries *Proceedings of International Congress on Evolutionary Methods for Design, Optimization and Control with Applications to Industrial Problems*, EUROGEN'03, Barcelona, Spain

Vatandaş, E. and Özkol İ., 2004a. Genetik Algoritma İle Elde Edilen 3 Boyutlu Kanat Modelleri İçin Yeni Ağ Yapılarının 'Dinamik Ağ' Yöntemiyle Bulunması, *Kayseri V Havacılık Sempozyumu*, KAYSERİ, 14 Mayıs.

Vatandaş, E., Özkol, İ. and Kaya, M.O., 2004b. Using The Dynamic Mesh Method For Genetically Obtained Wing Structures *Aircraft Engineering & Aerospace Technology*, Vol.76, No.3, pp. 314-319.

Vatandaş, E., Özkol, İ., 2004c. On Effective Combination Of Heuristic Algorithms And Dynamic Meshes In CFD Applications *Proceedings Of 5th International Bi-Annual ASME/JSME Symposium Computational Technology For Fluid / Thermal / Chemical / Stressed Systems With Industrial Applications* San Diego / La Jolla, California, July 25-29.

Vatandaş, E., Özkol İ., 2004d. Genetik Algoritma ve Dinamik Ağ Yöntemleriyle Kanat Optimizasyonu *Havacılıkta İleri Teknolojiler ve Uygulamaları Sempozyumu (HİTEK)* 9-10 Aralık , Hava Harp Okulu, İstanbul

Vatandaş, E., Özkol İ. and Nas, S., 2004e. Implementation of Genetic Algorithm on The Design of a Transonic Wing by Using Parallel Processing, *ICSP, International Conference Of Signal Processing*, December 15-17, Istanbul, Turkiye.

Vatandaş, E., Özkol İ. and **Hacioglu, A.** 2005a. Combining Vibrational Genetic Algorithm (VGA) and Dynamic Mesh in the Optimization of 3-D Wing Geometries *Finite Element for Flow Problems FEF05 IACM Special Interest Conference supported by ECCOMAS*, April 4-6, Swansea, Wales, UK

Vatandaş, E., Özkol İ., 2005b. Wing shape optimization by using the dynamic mesh and genetic algorithm, *Abstract for Third M.I.T. Conference on Computational Fluid and Solid Mechanics*, Massachusetts Institute of Technology Cambridge, MA 02139 U.S.A., June 14-17.

Vatandaş, E. and Özkol, İ., 2006. Dynamic mesh and heuristic algorithms for the design of a transonic wing *Aircraft Engineering & Aerospace Technology*, Vol.78, No.1, pp. 34-44.

Vatandaş, E., Özkol, İ., 2006a. Combined Parallel Computing, Dynamic Mesh and Heuristic Algorithms in Tapered Wings *Accepted for 2nd AIAA*

Multidisciplinary Design Optimization Specialist Conference, Newport, Rhode Island, USA 1 - 4 May.

Vatandaş, E., Özkol İ. and **Hacioglu, A.** Vibrational Genetic Algorithm (VGA) and Dynamic Mesh in the Optimization of 3-D Wing Geometries *accepted for publication by the Journal of Inverse Problems in Science and Engineering*

Vicini, A. and Quagliarella, D., 1999. Airfoil and Wing Design Through Hybrid Optimization Strategies, *AIAA Journal*, Vol. 37, No. 5.

Yılmaz, E., 2000 A Three Dimensional Parallel and Adaptive Euler Flow Solver for Unstructured Grids*, PhD Thesis,* Middle East Technical University (METU), January, Ankara-Turkiye.

Yilmaz, E., Kavsaoglu, M.S., Akay, H.U. and Akmandor, I.S., 2001. Cell-Vertex Based Parallel and Adaptive Explicit 3D Flow Solution on Unstructured Grids, *The International Journal of CFD*, Vol. 14, pp.271-286

BIOGRAPHY

Ergüven Vatandaş was born in Aydın/Turkiye in 1967. He graduated from the Department of Aeronautical Engineering, Istanbul Technical University in 1990.

After this, he worked in 2nd Air Supply and Maintenance Center, Kayseri for 3 years and in TAI (Turkish Aerospace Industries), Ankara as Government Quality Representative for 3 years.

Later he got Master of Science Degree from the Department of Aeronautical Engineering, Middle East Technical University (METU) and was appointed to Turkish Air Force Academy in 1999.

He presently works for Turkish Air Force Academy, in the Department of Aeronautical Engineering as a lecturer.

He is married and has two daughters.